

# POLITECNICO DI TORINO

**Corso di Laurea Magistrale  
in Ingegneria Energetica e Nucleare**

Tesi di Laurea Magistrale

**Analysis of the state of art on modelling of the consequences of  
CO<sub>2</sub> releases into the atmosphere.  
Application to the Allam-cycle case study.**



**Relatore**

prof. Andrea Carpignano

**Correlatrici**

Prof.ssa Raffaella Gerboni

Dott.ssa Anna Chiara Uggenti

**Candidato**

Cristina Bleve

Anno Accademico 2020-2021

# Summary

<i>List of figures</i> .....	4
<i>List of tables</i> .....	6
<i>Abstract</i> .....	7
<b>1 Introduction</b> .....	8
<b>1.1 Thesis objectives</b> .....	9
<b>1.2 Summary</b> .....	10
<b>1.3 Bibliographic analysis method</b> .....	11
<b>2 CO<sub>2</sub> properties and transport characteristics</b> .....	12
<b>2.1 CO<sub>2</sub> physical-chemical properties</b> .....	12
<b>2.2 Transport of CO<sub>2</sub> by pipelines</b> .....	13
<b>2.3 Joule-Thomson effect</b> .....	14
<b>2.4 The toxicological properties of CO<sub>2</sub></b> .....	15
<b>2.5 CO<sub>2</sub> - impurities</b> .....	15
<b>2.6 The failure rate of CO<sub>2</sub> pipeline</b> .....	16
<b>3 Research programmes</b> .....	18
<b>4 Carbon dioxide release in CCS project</b> .....	21
<b>4.1 Scenarios in a CCS project</b> .....	22
<b>4.2 Planned release (with controlled depressurization)</b> .....	23
<b>4.2.1 Blowdown of plant and equipment</b> .....	23
<b>4.2.2 Pipeline venting</b> .....	23
<b>4.3 Accidental release - Uncontrolled depressurization</b> .....	27
<b>4.3.1 Rapid phase transitions in CO<sub>2</sub></b> .....	28
<b>4.3.2 Transportation pipeline system accidental release scenarios</b> .....	32
<b>5 Modelling of CO<sub>2</sub> release</b> .....	40
<b>5.1 Time dependence of the release</b> .....	40
<b>5.1.1 Transient pipeline depressurization</b> .....	40
<b>5.2 Release characteristics</b> .....	43
<b>5.2.1 Instantaneous or continuous release</b> .....	43
<b>5.2.2 Orientation of the release</b> .....	44
<b>5.2.3 Solid CO<sub>2</sub> particle snow-out (rain-out) and sublimation</b> .....	45
<b>5.2.4 The momentum of the release</b> .....	46
<b>5.2.5 Conservative release assumptions</b> .....	47

5.3	Fracture control model .....	47
6	<i>Modelling of CO<sub>2</sub> dispersion</i> .....	50
6.1	Dense carbon dioxide dispersion phenomena .....	51
6.1.1	Dense gas dispersion .....	51
6.2	Types of dense gas dispersion models .....	52
6.2.1	INTEGRAL MODELS.....	53
6.2.2	CFD MODELS.....	57
6.3	The numerical approach in modelling hazards related to the sublimating bank .....	60
6.4	Effects of impurities in CO <sub>2</sub> release modelling .....	62
7	<i>CO<sub>2</sub> gas dispersion models validation</i> .....	64
7.1	Scale-up issues with CO <sub>2</sub> experiments .....	64
7.2	Evaluation of models against experimental data .....	64
7.3	Validation of models with CO <sub>2</sub> field study observations.....	66
7.4	Meteorological conditions and terrain description.....	70
7.5	CO <sub>2</sub> release in complex terrain and weather .....	71
8	<i>Analysis conclusions</i> .....	73
9	<i>Application to the Allam-cycle case study</i> .....	75
9.1	Description of the Allam-cycle.....	75
9.2	Settings of the Phast environment.....	77
9.2.1	Allam-cycle plant upload .....	77
9.2.2	Materials definition .....	77
9.2.3	Models definition .....	78
9.2.4	Discharge and dispersion parameters.....	81
9.2.5	Weather conditions.....	82
9.3	Study objectives .....	82
9.4	Results.....	84
9.4.1	Analysis of CO <sub>2</sub> solid fraction .....	84
9.4.2	Determination of damage areas between cold temperatures and toxic CO <sub>2</sub> .....	87
9.4.3	Determination of the most critical component.....	88
9.4.4	Comparison of damage areas between CO <sub>2</sub> and CH <sub>4</sub> .....	90
9.5	Case-study conclusions.....	92
10	<i>Thesis conclusions</i> .....	94
	<i>References</i> .....	96

## List of figures

Figure 1. Outline of the main phases of CCS technology: capture, transport and storage of CO <sub>2</sub> [2].	8
Figure 2. Carbon dioxide phase diagram [2].	12
Figure 3. Phase diagram of CO <sub>2</sub> with transport conditions [2].	14
Figure 4. The phase diagram in the case of CO <sub>2</sub> with impurities [4].	15
Figure 5. CO <sub>2</sub> release from a high-pressure pipeline [61].	21
Figure 6. The schematization of CO <sub>2</sub> release from an onshore pipeline [18].	21
Figure 7. Different scenarios for CO <sub>2</sub> release [15].	22
Figure 8. Formation of solid CO <sub>2</sub> /ice around a pressure gauge during leakage of CO <sub>2</sub> [5].	23
Figure 9. CO <sub>2</sub> plume release from a vent.	24
Figure 10. Vertical vent pipe used in experiments of the COOLTRANS research program.	25
Figure 11. Schematic view of two-phase jet release [26].	27
Figure 12. Theoretical pressure/volume graph for CO <sub>2</sub> showing spinodal curve [10].	28
Figure 13. Blast-distance relationship for a pipe rupture [9].	30
Figure 14. (a) Impulse calculations, and (b) pressure measurements from the vented chamber bottom sensor. From 0-500 ms after diaphragm rupture.	31
Figure 15. Comparison of simulations and experimental results from the vented chamber bottom sensor. (a) Impulse histories, and (b - c) pressure histories.	31
Figure 16. Visible cloud development of the dense CO <sub>2</sub> release experiments with the full-bore orifice.	33
Figure 17. View of the crater formed during the instrumented burst.	34
Figure 18. Images of the visible cloud resulting from the rupture of the pipeline, respectively at 10, 30 and 120 s from break [41].	34
Figure 19. Quadrant modelling of an underground pipe release [56].	35
Figure 20. Ductile-brittle transition temperature.	36
Figure 21. Spreading CO <sub>2</sub> cloud and crater and the fractured test section.	37
Figure 22. Crater profile and length measured after the rupture test [55].	37
Figure 23. Upward loss of CO <sub>2</sub> from a pressurized vessel.	44
Figure 24. a) The downward release of CO <sub>2</sub> from the high-pressure vessel with the consequent formation of a dry-ice bank; b) The low concentrations of the gas in the air following the subsequent sublimation of solid CO <sub>2</sub> from the bank surface during 14 days in June [33].	45
Figure 25. Photo of the crater and a broken pipe in the COSHER [5].	46
Figure 26. Definition of pseudo source plane [58].	50
Figure 27. Generalized development of a dense gas cloud [56].	51
Figure 28. Snapshots with particles on vertical planes [38].	60
Figure 29. Pressurized CO <sub>2</sub> release and sublimating bank dynamics with a general time scale.	61
Figure 30. CO <sub>2</sub> volume fraction distribution in space at different heights from the ground with wind velocity equal to 2 m/s.	61
Figure 31. Impact distances for CO <sub>2</sub> and H <sub>2</sub> S for different H <sub>2</sub> S fractions.	63
Figure 32. Discharge modelling (DISC/TVDI/ATEX) and dispersion modelling (UDM).	67
Figure 33. Natural gas-fuelled Allam cycle.	76
Figure 34. CO <sub>2</sub> solid fraction and DISC flow rate.	85
Figure 35. Dispersion predictions with hole size variation.	85
Figure 36. Dispersion prediction with the variation of thermodynamic conditions.	86
Figure 37. Safety distances comparison between cold exposure and CO <sub>2</sub> concentration, pre-AWD results.	88
Figure 38. Cloud Maximum Footprint for Outlet CO <sub>2</sub> recycle pump 200A.	89

Figure 39. Side View comparison between CO<sub>2</sub> and Oxidant..... 90

Figure 40. Comparison between the safety distances for Jet Fire and Fireball Radiation for CH<sub>4</sub> with the concentration of CO<sub>2</sub>. ..... 91

Figure 41. Damage areas comparison between CO<sub>2</sub> concentration (green), Jet Fire radiation (blue) and Fireball radiation (red), with Horizontal impingement, D5 and 70 mm hole. .... 92

Figure 42. Attachment A. .... 102

Figure 43. Attachment B. .... 103

## List of tables

Table 1. Emissions of CO <sub>2</sub> by process or industrial activity as worldwide large stationary CO <sub>2</sub> sources emitting more than 0.1 Mt of CO <sub>2</sub> per year [1].	8
Table 2. Physical properties of Carbon Dioxide [3].	12
Table 3. Indicative compositions of impurities in CO <sub>2</sub> streams [1].	16
Table 4. Failure rate distribution, per year, for modules 1-5 [11].	16
Table 5. Leak frequency vs hole size from EGIG.	17
Table 6. JIPs and RPs programs over years on release and dispersion of CO <sub>2</sub> from pipeline [18].	18
Table 7. Experiments tested depressurization in a broken CO <sub>2</sub> pipeline when events of venting/puncture occur [5].	26
Table 8. Initial conditions, measured properties and calculated properties.	30
Table 9. Experimental works reproduced an orifice leakage via CO <sub>2</sub> pipeline/vessel [5].	38
Table 10. Experiments related to full-bore rupture scenario of CO <sub>2</sub> pipeline [5].	39
Table 11. Types of dispersion models [15].	53
Table 12. Characteristics of the different integral models.	56
Table 13. Characteristics of CFD models.	59
Table 14. Validation overview of integral models for modelling of the release and dispersion of CO <sub>2</sub> [5].	68
Table 15. Validation overview of CFD models for modelling of the release and dispersion of CO <sub>2</sub> [5].	69
Table 16. Weather data [65].	70
Table 17. Terrain description.	71
Table 18. Applicability and calculation models for influences of terrain and weather conditions on the dispersion process and complexity of inputs [15].	72
Table 19. Thermodynamic properties of the Allam-cycle streams.	79
Table 20. Failure frequencies for each hole diameter and component of the Allam-cycle.	80
Table 21. Thresholds for the concentration of CO <sub>2</sub> .	83
Table 22. Fatality thresholds for the temperature of CO <sub>2</sub> .	83
Table 23. Fatality thresholds for CH <sub>4</sub> Thermal Radiation.	83
Table 24. Phast solid fraction predictions with 150 mm orifice diameter.	84
Table 25. Comparison between concentration and temperature thresholds.	87
Table 26. Components safety distances for IDLH, 1% and 50% fatality, with relative Leak Frequency.	89
Table 27. Safety distances comparison between pure CO <sub>2</sub> and Oxidant.	90

## ***Abstract***

As part of the large-scale development of Carbon Capture and Sequestration (CCS) infrastructures, this thesis focuses on the analysis of the state of art on modelling of the consequences related to accidental or controlled releases of CO<sub>2</sub> into the atmosphere, to understand whether the techniques available are able to simulate this phenomenon, and on the application of the knowledge acquired on a real case study. After a description of release characteristics, such as the formation of solid particles of CO<sub>2</sub> and the possible formation of the dry ice bank, specific models were presented with their capability to predict the thermo-fluid dynamic behaviours of CO<sub>2</sub> in a broken pipeline, to define the source term and to predict the near- and far-field dense dispersion of CO<sub>2</sub>.

In the analysis, the integral and CFD models were studied. It was found that among the integral gas dispersion models analyzed, the PHAST and EFFECTS models are the only ones able to simulate the pipeline depressurization, considering the formation of solid CO<sub>2</sub> particles, and the consequent sublimation, with the following discharge and dense dispersion. For CFD models instead, there is not a general model applicable to a wide range of scenarios, but the entire simulation has to be constructed. With them it is possible to represent complex terrain, space, and time-variable meteorological conditions, paying in more computational effort and time compared with integral models. Finally, all the validation work on dense CO<sub>2</sub> models has been summarized, considering the few data available for CO<sub>2</sub> with respect to other dense gases. Particular attention is given to the effects of topography and meteorological conditions on the dispersion phenomenon and to the ability of models to handle them.

The second part of this study focused on the application of one of the models analyzed to a real case study. Phast version 8.23 software was used to study the analysis of the consequences and areas of damage resulting from a possible release of CO<sub>2</sub> in the supercritical, dense or vapour state, in the plant of an Allam-Fetvedt cycle. That is an oxy-combustion thermodynamic cycle that produces electricity and captures CO<sub>2</sub> for sequestration, with supercritical CO<sub>2</sub> as the working fluid. Among the objectives of this study, there was the analysis of how the solid fraction of CO<sub>2</sub> influences the cloud temperature and dispersion, the comparison between the damage areas at certain concentrations of CO<sub>2</sub> and low temperatures, that can be reached during the release and the following dispersion, and the determination of the most critical thermodynamic point within the cycle corresponding to the inlet or outlet of one of the components.

At the end of the study, it was confirmed that the chosen Phast software is suitable for modelling and simulating such phenomena.

# 1 Introduction

Due to the continual increase in the level of greenhouse gases, including CO<sub>2</sub>, in the atmosphere, climate change is an urgent problem that needs to be managed globally. In fact, in 2021, CO<sub>2</sub> has reached 416 ppm of concentration in the atmosphere.

The major point sources of CO<sub>2</sub> are fossil fuels or biomass energy facilities, major CO<sub>2</sub>-emitting industries, natural gas production, synthetic fuel plants and fossil fuel-based hydrogen production plants. Most of the emissions of CO<sub>2</sub> to the atmosphere come from the electricity generation and industrial sector, in the form of flue gas from combustion, in which the CO<sub>2</sub> concentration is typically 4-14 % by volume.

In the table below, from IPCC (2005) [1], are reported the worldwide large stationary CO<sub>2</sub> sources emitting more than 0.1 Mt of CO<sub>2</sub> per year, where the emissions from the transportation sector are not included.

Process	Number of sources	Emissions (MtCO <sub>2</sub> yr <sup>-1</sup> )
<b>Fossil fuels</b>		
Power	4942	10539
Cement production	1175	932
Refineries	638	798
Iron and steel industry	269	646
Petrochemical industry	470	379
Oil and gas processing	Not available	50
Other sources	90	33
<b>Biomass</b>		
Bioethanol and bioenergy	303	91
<b>Total</b>	<b>7887</b>	<b>13466</b>

Table 1. Emissions of CO<sub>2</sub> by process or industrial activity as worldwide large stationary CO<sub>2</sub> sources emitting more than 0.1 Mt of CO<sub>2</sub> per year [1].

The decarbonization of steel and energy production plants starting from fossil fuels, especially coal-fired ones, is one of the main objectives and investments. By 2050 the International Energy Agency (IEA) has included the CCUS technology (Carbon Capture Utilization and Storage) as a strategy to reach the net-zero of emissions, contributing to the 9% globally. Among the benefits of this technology is the economic aspect, as the CCS can be adapted to recently built coal plants [18].

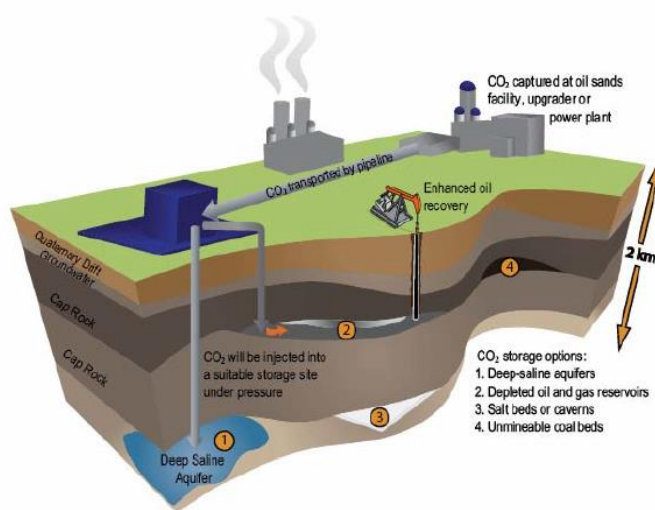


Figure 1. Outline of the main phases of CCS technology: capture, transport and storage of CO<sub>2</sub> [2].

The CCUS is a process that involves the capture and utilization or storage of carbon dioxide (CO<sub>2</sub>) emissions in a deep geological formation. It is emitted from sources such as power plants and other industrial processes and captured through different techniques like pre-combustion, post-combustion, or oxy-fuel process. Then there are two alternatives:

- most commonly it is compressed and transported from the capture source to a storage site by pipelines and/or tankers, and then injected deep underground into various types of geological structures and formations (e.g., depleted oil and gas reservoirs, deep saline aquifers, unmineable coal seams) for long-term storage,
- it can be used to produce chemical intermediates, plastics or fuels or to feed algae to obtain biofuels or carbonates.

In the next few years, CCS projects in Europe and other countries will be developed near/across densely populated areas, requiring an accurate risk assessment, to identify potential environmental, safety and health risks associated with the large-scale development of CCS. Therefore, the safe transportation of carbon dioxide through pipelines is essential [2].

## 1.1 Thesis objectives

This thesis is aimed at the study of the modelling of CO<sub>2</sub> releases into the atmosphere, based on the existing technical literature and on the projects carried out by the international scientific community, to provide information regarding quantitative risk assessment analysis in the context of CCS plants and to apply the knowledge acquired on a real case study of CO<sub>2</sub> release.

The first part is focused on the critical analysis and synthesis of the previous studies on controlled (venting) and accidental (leak) CO<sub>2</sub> releases, with the aim of:

- characterize the release scenarios according to whether these are emergency, planned or accidental, distinguishing between releases above the ground or below the ground with consequent formation of a crater, and considering any effects of overpressure due to rapid phase transition;
- characterize the source term and the phenomenon of CO<sub>2</sub> dispersion;
- produce an indicative prospect of the appropriate models that can be used and of the main parameters to be assumed to model the CO<sub>2</sub> releases, specifically the depressurization models for long pipelines and models for the consequent dispersion;
- understand the main differences between the existing models in terms of source term modelling, surrounding environment and weather conditions modelling, and computational complexity;
- study how the particular properties of CO<sub>2</sub> are managed by the commercial modelling software available;
- carry out a validation analysis of the software for the dispersion of CO<sub>2</sub> as a dense gas.

In the second part, the acquired knowledge was applied to a real case study involving a CO<sub>2</sub> capture plant, with the following objectives:

- set the Phast 8.23 by DNV GL simulation software to model the consequences due to the release of CO<sub>2</sub> into the atmosphere from an Allam-cycle system;
- validate Phast software as a tool for modelling CO<sub>2</sub> releases, paying particular attention to how the solid fraction affects cloud dispersion;
- obtain safety distances based on CO<sub>2</sub> concentration and temperature thresholds, to assign a relative degree of vulnerability;

- compare the results obtained for the various thermodynamic conditions present in the cycle, considering both the effects due to exposure to high concentrations and those of exposure to the low temperatures reached during release;
- compare the damage areas obtained from a release of CO<sub>2</sub> with those of CH<sub>4</sub> and analyze which and under what conditions one prevails over the other.

## 1.2 Summary

The paper is divided and described according to the following structure:

- Chapter 2 Description of the main characteristics of CO<sub>2</sub> and its optimal thermodynamic transport conditions from the capture site to the storage site, paying attention to the Joule-Thompson effect, its toxic properties, the possible presence of impurities and the associated failure rates of the CO<sub>2</sub> pipelines.
- Chapter 3 Classification of all the experimental works carried out, both on a small and large scale, in which controlled release (venting) or accidental (puncture, full-bore rupture and full-scale burst test) phenomena have been observed, and the consequent dispersion of CO<sub>2</sub> in the atmosphere, especially in the dense/supercritical phase.
- Chapter 4 Identification of CO<sub>2</sub> release scenarios for risk assessment in a CCS project through the analysis of the consequences of emergency releases, i.e. with controlled depressurization, and accidental releases, i.e. characterized by uncontrolled depressurization. For the latter, the phenomenon of the rapid phase transition of CO<sub>2</sub> was considered, and all the scenarios of releases from pipelines above the ground, below the ground with crater formation, and from long-running propagating fracture were analyzed.
- Chapter 5 Modelling and characterization of CO<sub>2</sub> releases, defining all the characteristics of the source term, depressurization models for transient releases from pipelines, paying particular attention to the formation of solid particles and the possible rain-out (snow-out), and how the direction of the releases influences the formation or not of the dry ice bank, to be considered as a new source of dispersion. Fracture models were also described that were applied for the CO<sub>2</sub> pipeline depending on whether the fracture is brittle or ductile.
- Chapter 6 Description of the differences between the CO<sub>2</sub> dispersion models, focusing on the differences between the CFD and integral models, highlighting the positive and negative aspects, their ability to calculate the CO<sub>2</sub> source term, including the modelling of the crater through CFD programs. Then modelling of the sublimation of CO<sub>2</sub> from the dry ice bank, and also on how impurities affect the release of CO<sub>2</sub>, specifically the decompression waves and the discharge rate.
- Chapter 7 Comparison and validation of CFD and integral models through experimental campaigns carried out to identify critical points in CO<sub>2</sub> modelling, highlighting their accuracy, scale problems, especially as regards the phenomenon of solid particle size and their behaviour, and also how the complexity of the terrain and weather conditions influence the choice of modelling software.
- Chapter 8 Conclusions relating to the study of the analysis of the state of the art carried out, with particular emphasis on which are the best software to use depending on the scenario considered.
- Chapter 9 Quantitative risk analysis was carried out on the Allam power plant cycle, calculating the safety distances associated with the related vulnerability thresholds using the PHAST software, both in terms of exposure to high concentrations of CO<sub>2</sub> and for exposure to low

temperatures. Particular attention was given to how the solid fraction affects the consequent dispersion of CO<sub>2</sub> and how the software is able to model it.

Chapter 10 Conclusions that report the initial objectives starting from the bibliographic analysis up to the application of the case study, which of these have been achieved and highlight which aspects it is necessary to focus more on in the future.

The paper was carried out as part of an internship in the HSEQ sector of Eni S.p.A.

### **1.3 Bibliographic analysis method**

The study of the CO<sub>2</sub> release modelling techniques has started from an analysis of the general phenomenon, how this happens and in which phases, focusing on the main characteristics of this substance and in particular on those that differentiate it from the releases of most common toxic substances.

Before starting the analysis of the various phases that characterize the dispersion of CO<sub>2</sub>, the work was focused on identifying all the release scenarios that may be present in a CCS project, distinguishing between controlled release and accidental release, and then describing the main features.

Subsequently, the research moved first on the study of every single phase, see the characterization of the term source, characterization of the dispersion of the dense gas in the atmosphere and of the possible formation of dry ice, then on the analysis of all the studies and experiments carried out in precedence regarding modelling the consequences of CO<sub>2</sub> release. Finally, starting from the latter, the scenarios considered, the respective thermodynamic conditions, the software used and the temperature and concentration distributions obtained, were identified, with the final aim of obtaining a synthesis of all the models used for the simulations, the main parameters that influence this choice, and of all the experimental campaigns with which these models have been validated.

## 2 CO<sub>2</sub> properties and transport characteristics

### 2.1 CO<sub>2</sub> physical-chemical properties

Carbon dioxide at atmospheric pressures and temperature is a colourless and odourless gas, which is 1.5 times heavier than air. The CO<sub>2</sub> is composed of two oxygen atoms covalently related to a single carbon atom, for this reason, is chemically inert and is not flammable.

Property	Unit	Value
Molecular weight	g/mol	44.01
Critical pressure	bar	73.8
Critical temperature	°C	31.1
Triple point pressure	bar	5.18
Triple point temperature	°C	-56.6
Aqueous solubility at 25 °C, 1 bar	g/L	1.45
Standard (gas) density	kg/m <sup>3</sup>	1.98
Density at critical point	kg/m <sup>3</sup>	467
Liquid density at 0°C, 70 bar	kg/m <sup>3</sup>	995
Sublimation temperature, 1 bar	°C	-78.5
Solid density at freezing point	kg/m <sup>3</sup>	1562

Table 2. Physical properties of Carbon Dioxide [3].

Among the data shown in the table, noteworthy are those concerning the critical point and the triple point. To summarize its particularities, the phase diagram of carbon dioxide is shown below.

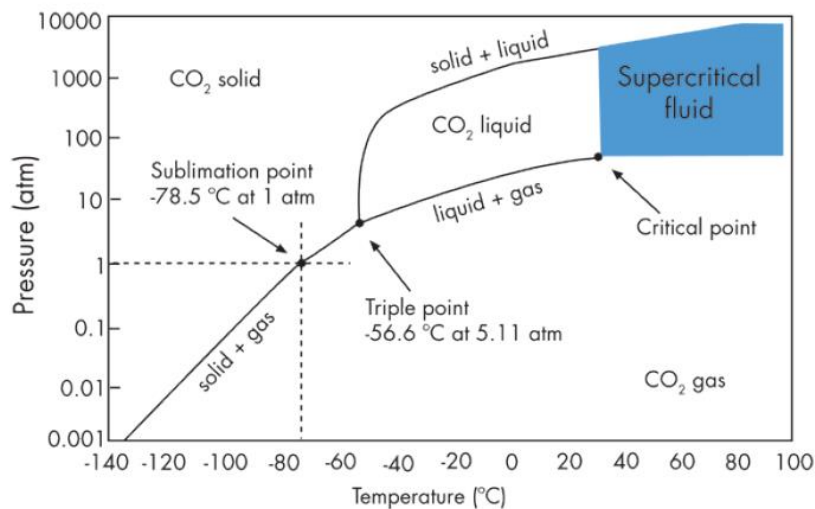


Figure 2. Carbon dioxide phase diagram [2].

The phase diagram of a substance shows the regions of pressure and temperature where its various phases are thermodynamically stable. The lines that separate these different regions are called phase boundaries and represent the place of the points (p, T) of coexistence in the equilibrium of the two adjacent phases. In this way four regions are distinguished: the solid phase region, the liquid phase region, the supercritical region and the gaseous phase region.

For carbon dioxide, it is fundamental to define the supercritical fluid region at pressure and temperature higher than those characterizing the critical point (7.383 MPa; 31.04 °C). In this region it assumes properties intermediate between a liquid and a gas, it has a viscosity similar to that of gas and the density as that of liquid

phase. Moreover, if the carbon dioxide has only the pressure higher than the critical one is defined as the dense phase.

From the phase diagram, it should be noted first of all that the triple point lies at a pressure higher than the atmospheric one, therefore liquid carbon dioxide isn't present at atmospheric pressure, whatever its temperature.

The triple point of CO<sub>2</sub> lies at 0.518 MPa and -56.57 °C and represents the condition of coexistence of solid, liquid and gaseous CO<sub>2</sub>. At this point, the boundary lines between the different phases meet and this condition also identifies the minimum pressure value at which liquid CO<sub>2</sub> can exist.

From Figure 2, it can be noted clearly that at atmospheric pressure the two permissible phases are solid and gaseous: solid carbon dioxide, also called dry ice, directly sublimates when left outdoors under atmospheric pressure. This will be a very important point for subsequent discussion.

Furthermore, at atmospheric pressure, the gas gives rise to a desublimation phenomenon which means a direct passage to the solid phase, if carried out at a temperature lower than the sublimation temperature -78.5 °C and 1 atm. Instead, above this temperature, the deposited solid sublimates directly, moving into the gaseous phase [2].

## 2.2 Transport of CO<sub>2</sub> by pipelines

CO<sub>2</sub> captured for CCS application can be transported either by pipeline or by ships, with the transport by pipeline as the dominant method for transport CO<sub>2</sub>, considering the large quantities that will be produced.

The nature and extent of the pipeline network depend on many factors including the proximity between the source and the storage site, the cost of acquiring network installation rights, the expense of purchasing and installing of the various components and operating and maintenance costs [2].

Already 6500 km of CO<sub>2</sub> pipelines are being operated in North America, Europe, the Middle East, Africa and Australia. But most of these pipelines are in North America and they transport and inject CO<sub>2</sub> for the Enhanced Oil Recovery (EOR) projects [5].

Mostly pure CCS are being developed under a pilot or laboratory scale. The pipelines for the transport of onshore and offshore CO<sub>2</sub> are conceptually constructed in the same way as those for the handling of hydrocarbons. The transport will cover distances of hundreds of kilometres and will pass through different natural environments such as deserts, zones mountainous, highly populated areas, arctic and sub-arctic areas and seas and oceans at depths of up to 2200 m. Considering the number of offshore storage sites identified so far, a large number of pipeline systems could be operated below sea level. However, experience in this field is very limited. All the networks currently operating in the United States are onshore and only a small part of their route passes through populated areas. Most of the onshore network is buried in the ground for most of its length, at a depth of 1-1.2 m, except for the pumping and control stations.

To efficiently transport large quantities of CO<sub>2</sub>, the fluid must be converted into a form with a high density such as the liquid or supercritical phase, because it permits smaller pipeline diameters and larger flow rates [8]. The following figure shows the carbon dioxide temperature as a function of the operating pressure of transport both by pipeline and by ship [2].

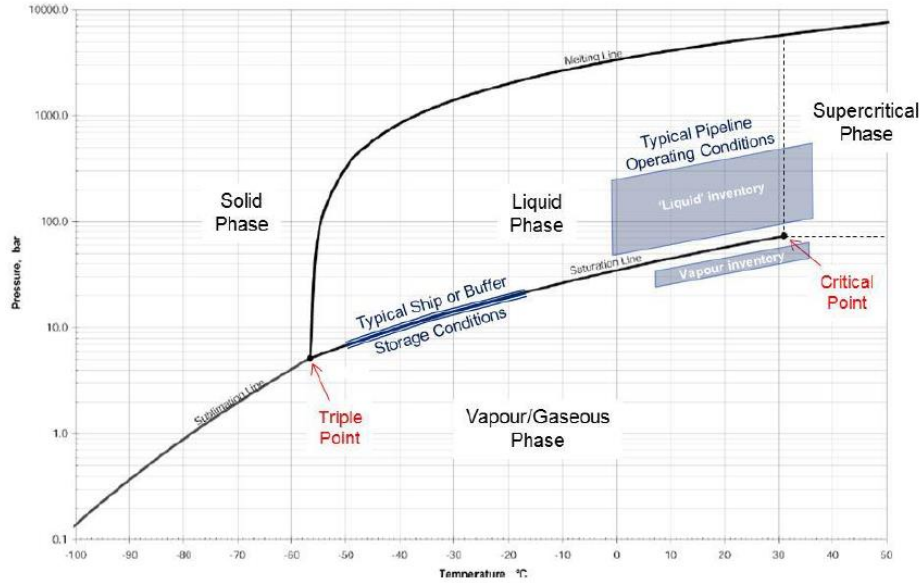


Figure 3. Phase diagram of CO<sub>2</sub> with transport conditions [2].

Hence the most efficient and economical method to move CO<sub>2</sub> by pipeline involves its transport in the supercritical/dense phase. For this reason, CO<sub>2</sub> is generally transported at temperatures and pressures in the range of 12-44 °C and 85-150 bar, respectively [6].

The lower pressure limit is imposed by the need to maintain the dense fluid phase during CO<sub>2</sub> transport while the upper one is driven by economic issues. For the temperature, on the other hand, the lower limit is connected to the winter temperature of the soil and the upper one is guided by the outlet temperature from the upstream compression phase and by the temperature limit to which the coating materials can be subjected. Instead, offshore piping systems can withstand a higher design pressure (even up to 300 bar) both because they affect populated areas in a reduced way and because there is a compensatory effect determined by the external hydrostatic pressure, especially for pipelines located at great depth [7].

It is essential to ensure that the flow of CO<sub>2</sub> within the pipeline remains single-phase, avoiding sudden pressure drops. In fact, in a two-phase flow, there are simultaneously two physically distinct phases (for example liquid and gas or supercritical and gas) which could generate even very serious problems for compressors and transport equipment, significantly increasing the frequency of pipeline rupture.

At pressures very close to that of the critical point, a small variation in the temperature or in the pressure of the fluid leads to a very marked variation in the density of the CO<sub>2</sub> which can lead to a change of phase and velocity of the fluid, resulting in a slug-type stream. Temperature variations are very frequent and are mainly determined by atmospheric and piping conditions [2].

### 2.3 Joule-Thomson effect

As specified above, the supercritical CO<sub>2</sub> has a liquid-like density but behaves like a gas, i.e. it occupies the volume of its container. At high pressure, CO<sub>2</sub> molecules develop attractive forces among each other, reaching a low-energy equilibrium. In case of a leakage from a high-pressure transportation facility, the internal energy is used to overcome these forces during the expansion caused by a pressure drop, thus lowering the temperature.

The Joule-Thomson effect relates the temperature change to the pressure change for real gases:

$$\Delta T = \varphi \Delta P$$

where  $\phi$  is the J-T coefficient. The value of the J-T coefficient for carbon dioxide was found experimentally and it is equal to  $\phi_{\text{CO}_2} = 13 \text{ K MPa}^{-1}$ . The temperature drop caused by the pressure change ( $\sim 10 \text{ MPa}$ ) after leakages from CCS transportation facilities would be around 130 K. When passing from 10 to 0.1 MPa, the molecules of  $\text{CO}_2$  would experience a phase change to solid (dry ice)/vapour phase. Below  $-78.8 \text{ }^\circ\text{C}$ , in the solid state, carbon dioxide (dry ice) has a density of  $1562 \text{ kg m}^{-3}$ . At a temperature slightly higher than the sublimation temperature, gaseous  $\text{CO}_2$  has a density of about  $2.8 \text{ kg m}^{-3}$ , significantly higher than its value at standard conditions of approximately  $1.8 \text{ kg m}^{-3}$ . The simultaneous presence of dry ice and very cold gaseous  $\text{CO}_2$  in the plume, formed after a high-pressure release, would increase the tendency of carbon dioxide to stay near the ground since the sublimation of the solid  $\text{CO}_2$  would contribute to keeping the temperature of the plume low [8].

## 2.4 The toxicological properties of $\text{CO}_2$

In the case of  $\text{CO}_2$  release, in addition to the danger of exposure to low temperatures and of asphyxiation due to the decrease of oxygen in the, there is the hazard that is toxic at certain concentrations. Depending on the inhaled  $\text{CO}_2$  concentrations and the duration of exposure, the toxicological symptoms in people range from headaches, increased respiratory and heart rate, dizziness, muscle twitching, confusion, unconsciousness, coma and death. Breathing air with a  $\text{CO}_2$  concentration of around 5% will within a few minutes cause headache, dizziness, increased blood pressure and uncomfortable and difficult breathing (dyspnea). At  $\text{CO}_2$  concentrations greater than 17 %, loss of controlled and purposeful activity, unconsciousness, convulsions, coma, and death occur within 1 minute of initial inhalation [12].

## 2.5 $\text{CO}_2$ - impurities

Captured  $\text{CO}_2$  may contain impurities like water vapour,  $\text{H}_2\text{S}$ ,  $\text{N}_2$ ,  $\text{CH}_4$ ,  $\text{O}_2$ , Hg, and hydrocarbons, which may require specific handling or treatment depending on the capture processes from coal and gas power plants. The physical properties of  $\text{CO}_2$  are changed by the presence of impurities, affecting the design of the pipeline and its capacity, compressor power, recompression distance and the prevention of fracture propagation.

Figure 4 below illustrates the effect on the critical point in the case of  $\text{CO}_2$  with impurities.

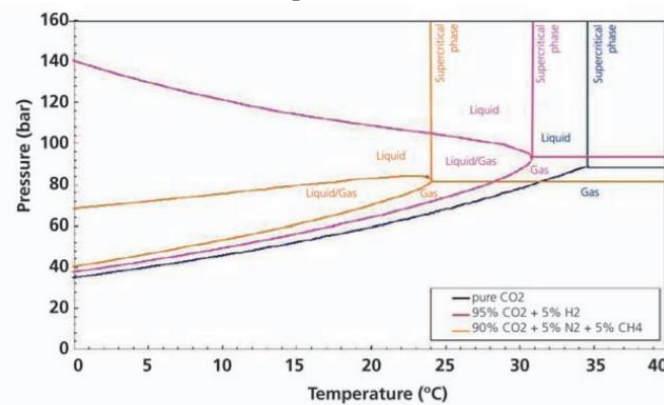


Figure 4. The phase diagram in the case of  $\text{CO}_2$  with impurities [4].

The presence of impurities changes physical properties such as the critical pressure, which may have an impact on the  $\text{CO}_2$ 's flow behaviour. Sequentially this may change the operating regime of the pipeline and higher pressures than used for pure  $\text{CO}_2$  might be required in order to maintain it as supercritical or dense single-phase. Therefore, depending on the impurities present in the  $\text{CO}_2$  stream, they will have a significant effect on hydraulic parameters such as pressure and temperature and also on the density and viscosity of the fluid [4].

The specific quantities of impurities present in the captured carbon dioxide stream are related to the fossil fuel and the plant used. Indicative compositions of impurities in CO<sub>2</sub> streams are presented in the table below for coal and gas-fired power plants using different capture technologies (IPCC 2005) [1].

Component	Impurity Concentration (ppmv)					
	Coal-Fired Power Plant			Gas-Fired Power Plant		
	Post	Pre	Oxy-fuel	Post	Pre	Oxy-fuel
Ar/N <sub>2</sub> /O <sub>2</sub>	0.01	0.03-0.6	3.7	0.01	1.3	4.1
H <sub>2</sub> S	0	0.01-0.6	0	0	<0.01	0
H <sub>2</sub>	0	0.8-2.0	0	0	1	0
SO <sub>2</sub>	<0.01	0	0.5	<0.01	0	<0.01
CO	0	0.03-0.4	0	0	0.04	0
NO	<0.01	0	0.01	<0.01	0	<0.01
CH <sub>4</sub>	0	0.01	0	0	2.0	0

Table 3. Indicative compositions of impurities in CO<sub>2</sub> streams [1].

## 2.6 The failure rate of CO<sub>2</sub> pipeline

To assess the risks from an accidental loss of containment of carbon dioxide, various failure cases for the processes involved will need to be considered.

The release scenarios need to be determined and release and dispersion modelling carried out, to evaluate the consequences, considering that the consequence analysis of any identified threat to the pipeline will require an assessment of the potential likelihood of the occurrence and the physical situation (damage) that occurred.

Depending on the risk evaluation required, the failure cases may need to cover the whole range of possible events from small continuous releases through to line ruptures or catastrophic failure of vessels where large but finite inventories of hazardous material could be released [9].

The principal causes of natural gas/CO<sub>2</sub> pipeline incidents have been classified as relief valve failure, weld/gasket/valve packing failure, corrosion, and outside forces [8]. Both CO<sub>2</sub> and natural gas pipelines are fabricated from the same grades of carbon steel, and both are installed using the same equipment and practices. However, natural gas is lighter than air and explosive in air, whereas CO<sub>2</sub> is non-flammable but toxic (and heavier than air). In this study, we will refer to the toxicity of CO<sub>2</sub> even if not classified as such by the legislation, but for the effects that causes on health, as explained before.

The failure frequency is calculated by dividing the number of incidents by the exposure. The exposure is the length of a pipeline multiplied by its exposed duration and is expressed in kilometres-years [km · yr] [16].

Vendrig et al. (2003) [11] estimate the failure frequency (per km per year) of high-pressurized CO<sub>2</sub> pipeline punctures and ruptures in a generic CCS offshore system using representative leak size, as can be seen in the table below.

Module	Module Description	Small (3-10 mm)	Medium (10-50 mm)	Large (50-150 mm)	Full-bore (>150 mm)
1	CO <sub>2</sub> recovery at source	9.6 x 10 <sup>-2</sup>	5.1 x 10 <sup>-2</sup>	2.0 x 10 <sup>-3</sup>	5.6 x 10 <sup>-3</sup>
2	Converging pipelines	3.5 x 10 <sup>-3</sup>	8.8 x 10 <sup>-4</sup>	1.0 x 10 <sup>-4</sup>	1.5 x 10 <sup>-4</sup>
3	Booster station	3.5 x 10 <sup>-2</sup>	3.8 x 10 <sup>-3</sup>	3.0 x 10 <sup>-4</sup>	8.8 x 10 <sup>-4</sup>
4	Pipelines	1.4 x 10 <sup>-4</sup>	9.5 x 10 <sup>-5</sup>	2.0 x 10 <sup>-5</sup>	8.5 x 10 <sup>-5</sup>
5	Injection plant	1.2 x 10 <sup>-1</sup>	5.3 x 10 <sup>-2</sup>	2.1 x 10 <sup>-3</sup>	5.8 x 10 <sup>-3</sup>

Table 4. Failure rate distribution, per year, for modules 1-5 [11].

According to Gave and Davidson study, where a mile-by-mile comparison was made between pipeline incidents of natural gas transmission, hazardous liquids and CO<sub>2</sub>, a frequency of incident of 0.32 per 1000 km per year was obtained for CO<sub>2</sub> pipelines, whereas for natural gas and other hazardous liquids pipeline a frequency of 0.17 and 0.82, respectively [12].

The EGIG (European Gas Pipeline Incident Pipeline Group) data shows that pinholes (diameter of the defect  $\leq 20$  mm) represent approximately 50% of all incidents, while holes (diameter of the defect  $> 20$  but  $\leq$  of the diameter of the pipeline) approximately 40%, on the other hand, ruptures approximately 10%. The frequency rates, for different hole size ranges, are shown in the following table, although for QRA of a CO<sub>2</sub> pipeline, the data in the table should be considered as a conservative estimate [15].

Category	Hole range [mm]	Frequency [events per 1000 km per year]
Pinhole	$\leq 20$	0.160
Puncture	$> 20$ and $<$ pipe diameter	0.142
Rupture	Pipe diameter or greater	0.05

Table 5. Leak frequency vs hole size from EGIG.

Instead, PHMSA (2010) [13] recorded accidents related to CO<sub>2</sub> pipelines and natural gas pipelines in the period that go from 1990 to 2009 in the USA. This report subdivided the percentage of failure as follow:

- 41.9 % of these accidents were from pipeline leakage (include pinhole and puncture)
- 32.9 % from pipeline ruptures
- 25.2 % from system failures.

The analysis presented in [14] points out that in the past the risk associated with CO<sub>2</sub> pipelines was overestimated, with QRA orders of magnitude higher. They suggest that the likelihood of having significant (potentially lethal) releases of CO<sub>2</sub> from pipelines ranges between  $10^{-6}$  (acceptable) and  $10^{-7}$  (negligible).

### 3 Research programmes

All the experimental work on the release and dispersion of CO<sub>2</sub> into the atmosphere can be classified on a large-scale and small-scale. The objective of these experiments is to analyze both the near-field and the far-field, specifically: the first can be analyzed on a small-scale or a laboratory scale, as its thermodynamic behaviour must be carefully studied; on the contrary, for far-field dispersion, it is more appropriate to perform a large/medium-scale analysis. Considering that the costs of supporting them are significant, especially for large-scale experiments, several joint industrial projects (JIPs) and research projects (RPs) have been developed in Europe and the UK in recent years. A summary table is reported below with relative periods, scale and objectives [18].

JIP/RP Name	Years/Period	Scale	Objectives and Scope
CO2SAFEARREST	2016-2019	Full-Scale	Burst tests research program. Two full-scale tests with buried pipeline (CO <sub>2</sub> -N <sub>2</sub> ), 610 mm.
COSHER	2011-2015	Large-Scale	Obtain data to support the development of models to determine safety zones/consequence distance.
CO2PIPETRANS	2009-2015	Medium-Scale Large-Scale	Fill the knowledge gap identified in the DNV-RP-J202. Results of the project were included in DNV GL-RP-F104 (2017).
COOLTRANS	2011-2015	Large-Scale	Identify and propose solutions to key issues relating to the safe routing, design, construction and operation of onshore CO <sub>2</sub> pipelines in the UK.
CO2PIPEHAZ	2009-2013	Small-Scale Large-Scale	Improve the understanding of the hazards represented by CO <sub>2</sub> releases.
CO2QUEST	2013-2016	Small-Scale Medium-Scale	Study the impact of the quality of CO <sub>2</sub> on storage and transport.
CO2EUROPIPE	2009-2011	N/A	Outline guidance to elements of the European plan to develop large-scale EU CO <sub>2</sub> infrastructure.
CO2RISKMAN	2010-2013	N/A	Development of industry guideline to assist the designer and projects on the emerging CCS industry. Potential hazards associated with handling CCS CO <sub>2</sub> streams are discussed.

Table 6. JIPs and RPs programs over years on release and dispersion of CO<sub>2</sub> from pipeline [18].

#### CO2SAFEARREST

CO2SAFEARREST was a full-scale burst tests research program for carbon dioxide pipelines. The project involved two full-scale burst tests of 610 mm, X65 buried line pipes using a mixture of carbon dioxide and nitrogen. The objective was to evaluate the fracture propagation and arrest characteristics and CO<sub>2</sub> dispersion in the atmosphere.

#### COSHER

Cosher stands for *CO<sub>2</sub> safety, health, environment and risk*. The studies of this project comprised large scale pipeline rupture tests that were performed simulating loss of containment and subsequent dispersion of CO<sub>2</sub> as a result of a rupture caused by third party interference. Two large scale experiments were conducted to provide data under well-defined conditions studying the full-bore rupture of a CO<sub>2</sub> dense phase high-pressure underground pipeline. This is the largest experimental program on CO<sub>2</sub> as far as the authors know.

The rupture release experiments were conducted in different wind speed conditions. During the experiments, a ground crater was formed and the CO<sub>2</sub> was allowed to flow freely from both ends of the ruptured section of the pipeline. The following measurements were made:

- fluid pressure,
- fluid temperature,

- wall temperature of the test facility,
- measurements of the dispersing gas cloud.

### **CO2PIPETRANS**

In detail it is a Joint Industry Project (JIP) led by DNV that involved the following area of research:

- Experimental medium-scale CO<sub>2</sub> release experiments for the development and validation of robust models for dense phase CO<sub>2</sub> depressurization, release, and dispersion. It includes the BP (British Petroleum) and Shell projects, whose experimental work on CO<sub>2</sub> releases was carried out at the Spadeadam site (UK) by GL Noble Deston.
- Full-scale experiments on pipeline rupture, to improve the design theory for fracture arrest.

### **COOLTRANS**

This programme was commissioned by National Grid to offer the technical foundations for the design and operation of CO<sub>2</sub> pipelines in the UK. The programme includes a series of large shock tubes, burst, venting, puncture, rupture and full-scale fracture propagation tests, to give information on CO<sub>2</sub> release from a buried pipeline and its dispersion. Follow the list of participants and the corresponding objective of their research:

- *DNV GL* guided field-scale CO<sub>2</sub> release experiments and give prediction through consequence models used in risk assessments.
- *Nottingham University* developed an equation of state for CO<sub>2</sub> (with and without impurities) through laboratory experiments and conducted field experiments to examine the environmental effects of the release of CO<sub>2</sub>.
- *University College London, University of Leeds and Kingston University* created Computational Fluid Dynamics (CFD) models to model the release rate, near-field and far-field dispersion behaviour of CO<sub>2</sub>.
- *The Health and Safety Laboratory* developed a Model Evaluation Protocol (MEP) and developed some limited tests using the DNV consequence modelling package, PHAST.
- *Atkins* studied the crack-propagation in CO<sub>2</sub> pipelines with the objective to develop and validate corresponding models.

### **CO2PipeHaz**

The CO2PipeHaz project was established by the *European Commission FP7 Energy Programme*, and involved collaboration between University College London, University of Leeds, GEXCON AS, Institut National de l'Environnement et des Risques (INERIS), NCSR, Dalian University of Technology and the Health and Safety Laboratory (HSL).

The project had the aim to obtain predictions of the fluid phase, discharge rate and atmospheric dispersion during accidental releases from pressurized CO<sub>2</sub> pipelines. Small- and large-scale experiments to validate the models were carried out to improve the understanding of the hazards represented by CO<sub>2</sub> releases.

### **CO2Quest**

The CO2Quest project is funded by the *European Commission FP7 Energy Programme*. Coordinated by *University College London*, the CO2QUEST project involves the collaboration of 12 industrial and academic partners in Europe, China and Canada.

The CO2Quest project includes the study of under-expanded CO<sub>2</sub> jets, cloud dispersion characteristics and the formation of dry ice particles in the near-field.

**CO2EUROPIPE**

CO2EUROPIPE is a European project that focuses on the details for the development of large-scale CO<sub>2</sub> infrastructure, also describing the infrastructures for large plants, including those for injection and those for the reuse of pipelines that previously transported natural gas.

**CO2RISKMAN**

The CO2RISKMAN project was initiated by DNV to create a guide for the CCUS sector related to the most common management problems and potential hazards arising from CO<sub>2</sub> flow management. The guide is divided into 4 documents ordered by degree of detail, with also an executive summary. It was developed thanks to the contribution of 17 partners and did not include the implementation of experimental activities, therefore all considerations on risks and safety are relevant in a general way [18].

## 4 Carbon dioxide release in CCS project

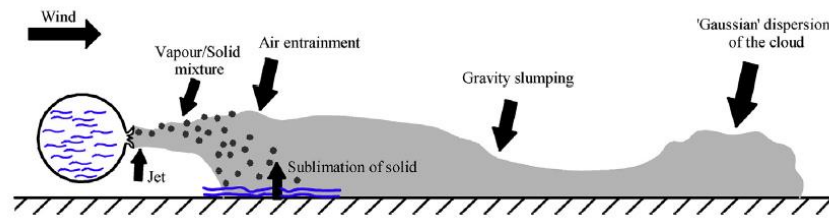


Figure 5. CO<sub>2</sub> release from a high-pressure pipeline [61].

Figure 5 shows a schematic representation of the consequences of releasing CO<sub>2</sub> from a high-pressure pipeline. In most cases, a cold liquid or hot supercritical vapour, due to rapid depressurization, can generate a two-phase flow inside the pipeline. After release, this fluid expands as an under-expanded jet up to ambient pressure, cooling due to the Joule-Thompson effect and generating a jet of vapour mixed with solid particles.

If the release is horizontal, a fraction of the solid particles can fall on the ground and form a dry ice bank, while the remaining part is subjected to the phenomenon of sublimation. It must be considered that even the ice bank can then in turn sublimate due to the heat from the external environment, constituting an additional source of CO<sub>2</sub>.

In the near-field, the dispersion will be dominated by the high momentum of the jet, but with the entrainment of the surrounding air, it will lose it and first, being heavier than air it will tend to slump and travel close to the ground and finally it will become a passive Gaussian cloud.

For the analysis of the release phenomenon and the consequent atmospheric dispersion, it is necessary to use appropriate mathematical models to provide the results necessary for the risk assessment analysis [61].

Therefore, modelling the consequences of released carbon dioxide from pipeline/vessel typically takes place in two stages, as represented in Figure 6:

1. The first stage, near-field release, where the release rate from a given inventory or scenario is calculated (source term), beyond the exit source where the liquid/supercritical CO<sub>2</sub> may flash to vapour while simultaneously cooling, such that solid CO<sub>2</sub> particles are produced;
2. The second stage, far-field release, where the subsequent dispersion of the released carbon dioxide following an operational, emergency or accidental release is calculated, considering that some hazard modelling packages may carry out the two stages together without the need for the user to transfer data.

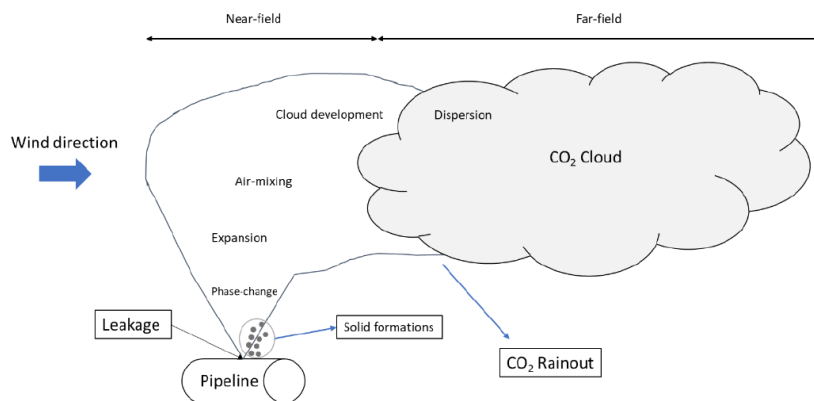


Figure 6. The schematization of CO<sub>2</sub> release from an onshore pipeline [18].

The results of a consequence analysis are generally presented in the form of contours or iso-surfaces of carbon dioxide concentration (in ppm) at values that relate to differing levels of harm to exposed persons.

In general, the predictive models tend to be conservative, but not excessively, since highly conservative models can cause too high constraints on a facility design. Hence, the competent selection and use of the appropriate tools and techniques are key aspects.

The analysis needs to focus first on near-field experiments that highlighted important release aspects. Since near-field modelling can strongly impact the far-field modelling and the definition of safety distances[18].

For release rate calculation, the thermodynamic state of the inventory is a key parameter. The same also for dispersion, where additional parameters need to be taken into consideration, like surrounding buildings, landscape and meteorological conditions.

It is possible to divide the CO<sub>2</sub> release scenarios into two main categories:

- **Planned/emergency release (e.g. venting):** blowdown of the pipeline and/or plant due to a shutdown or problem at one end of a pipeline. It is then important to understand if the carbon dioxide plume can reach down inside or outside of the site boundary, its concentration level, the wind conditions. This is to understand if it is necessary to modify the vent stack, or its location and change the rate of the carbon dioxide release according to the corresponding weather and wind conditions.
- **Accidental release:** if a gas plume could spread offsite by an accidental release from pressurized vessels or pipelines. It is necessary to know the concentrations, the distance that can reach, the weather and wind conditions, and the time that a gas plume persists to calculate the corresponding harm to people [9].

#### 4.1 Scenarios in a CCS project

In order to identify the high consequence events that impose major risks to the project, people and environment, it is necessary to characterize the nature of the CO<sub>2</sub> release, so that appropriate source terms for dispersion modelling may be correctly defined. Identification of suitable pipeline/vessel scenarios is an important part of the analysis and will affect the size of the dispersion results.

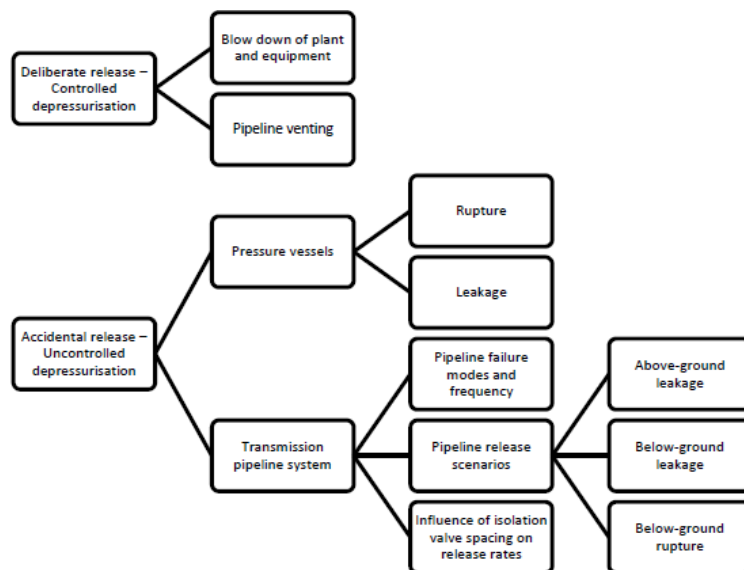


Figure 7. Different scenarios for CO<sub>2</sub> release [15].

The release scenario starts with a loss of containment that can be described by the event tree above. Different release scenarios are possible, depending on whether the release is vented or accidental, full-bore rupture or large/small holes, from a storage tank, pipeline or valve, or from below or above ground.

## 4.2 Planned release (with controlled depressurization)

### 4.2.1 Blowdown of plant and equipment

Planned release of CO<sub>2</sub> from CCS equipment is essential to allow the plant maintenance and manage process upset or emergencies. Therefore, to ensure correct long-term operation of the equipment, it is necessary to carry out periodic blowdown operations, hence the choice of isolation valves is a key aspect. It has to be considered that the carbon dioxide will often be released in the gaseous phase, possibly upstream the export compression, though in some situations blowdown of some inventories can be required directly from the liquid state.

To avoid the formation of dry ice, the blowdown must be carried out slowly, considering that there may be a blockage of the leakage due to the presence of solid, giving the impression that the release has finished, but that in reality, the subsequent heating leads to an uncontrolled release of CO<sub>2</sub>, with dangerous consequences [9].



Figure 8. Formation of solid CO<sub>2</sub>/ice around a pressure gauge during leakage of CO<sub>2</sub> [5].

However, it must be considered that, given the low CO<sub>2</sub> release rates during the blowdown phenomenon, it is difficult for solid particles to form, resulting in a full-gas cloud. If the state of CO<sub>2</sub> inside the pipeline is that of a pressurized liquefied gas, the mass flow rate to the hole can correspond to the maximum one, calculated with the Bernoulli formula if the flow does not flash before the outlet, otherwise, it can be calculated with a reduction factor of 5-10% to the maximum calculated (100% liquid) [15].

### 4.2.2 Pipeline venting

During a maintenance or repair operation, a section of the pipeline needs to be emptied, therefore a vent station must be placed along the line between the isolation valves [9]. Since, during depressurization, the temperature may drop up to 90 °C, it is necessary to control the releases for longer times than with methane gas pipelines, to avoid the formation of dry ice and also consequent embrittlement of the pipes due to low temperatures reached [15].

To have an idea of the required time for venting operations, in the Clausen et al. study [17] it is reported that the duration to empty a 50 km section with a diameter of 600 mm containing 9300 tons of supercritical CO<sub>2</sub> is about 10 hours, for a depressurization from 8 MPa to ambient pressure.

The transient behaviour of CO<sub>2</sub> inside the pipeline strongly influences the generation of noise, the formation of dry ice, and the consequent dispersion, therefore suitably validated pipeline simulation tools are required.

To avoid the presence of solid CO<sub>2</sub> in the system upon complete depressurization the following can be done:

1. Undertake a carefully controlled depressurization during which the inventory pressure is monitored and maintained above the triple point pressure by adjusting the venting rate until all the liquid CO<sub>2</sub> inventory has vaporized. Once the inventory is a single-phase vapour, the pressure can be dropped to ambient without solid CO<sub>2</sub> being formed.
2. Vent the contents of the inventory from the low point(s) in the system to remove the liquid inventory before venting the vapour.
3. Maintain the pressure of the CO<sub>2</sub> inventory above the CO<sub>2</sub> triple point pressure until it is removed, by either introducing another substance (e.g. nitrogen) to the CO<sub>2</sub> or if the system is a pipeline, using a pig with another substance behind the pig so that the CO<sub>2</sub> gets pushed out without contamination [3].

The previous discussion highlights how to avoid the formation of solid particles in the system during release, but in case it does happen, the challenges associated with the design of the vent system itself must also be considered. This system must be able to handle the extreme cold and solid CO<sub>2</sub> formation it will be exposed to and the release point must also be designed and positioned in such a way that people and other sensitive receptors are not exposed to a harmful concentration of CO<sub>2</sub>.

In the study conducted by COOLTRANS, an experimental release was performed from a 25 mm diameter vent into a 914 mm diameter pipe containing dense phase CO<sub>2</sub> [19].

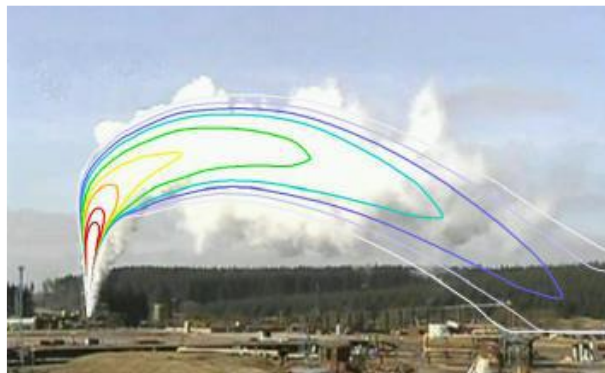


*Figure 9. CO<sub>2</sub> plume release from a vent.*

From Figure 9, it is possible to observe a comparison between the CO<sub>2</sub> cloud and the gas concentration isopleths curves obtained through an integral model. From the simulation made by the software it can be seen how the cloud travels close to the ground, but this is not noticed in reality, as the white colour is given by the condensation of the humidity present in the air. For this reason, the modelling of CO<sub>2</sub> dispersion is also essential for venting stations.

As another example, the COOLTRANS research program conducted a study on the venting of dense phase CO<sub>2</sub> through a 3 m vertical vent pipe with an internal diameter of 24.3 mm (Figure 10). The reservoir conditions of CO<sub>2</sub> were at 15 MPa and a temperature of 7.45 °C. The purpose of the experiment was to measure the release behaviour of CO<sub>2</sub> and the discharge flow rate.

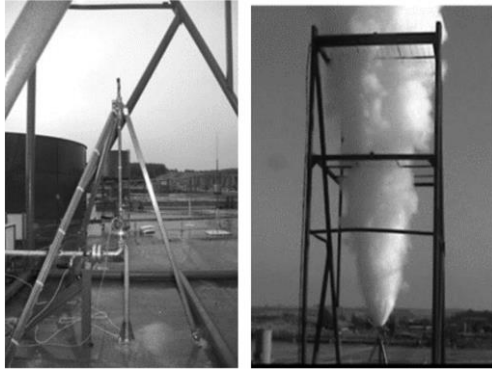


*Figure 10. Vertical vent pipe used in experiments of the COOLTRANS research program.*

Other examples of vent tests performed during the COOLTRANS program are described in the work of Allason et al. [25]. In these upward release experiments, no solid CO<sub>2</sub> rainout was observed and the CO<sub>2</sub> concentrations measured downstream were not dangerous. In general, the dispersion of this type of above-ground CO<sub>2</sub> release can be predicted satisfactorily, if the release conditions are known.

Table 7 below presents a summary of the experimental investigations of CO<sub>2</sub> behaviour in a pipeline/vessel in the event of venting/puncture, taken from the report on the review of the experimental and modelling methods for the release of carbon dioxide [5].

Reservoir conditions		Phase	Component release (%mol)	Length (m)	Diameter (mm)	Thickness (mm)	Aim of the study
Temperature (°C)	Pressure (MPa)						
7.45	15	Dense	100% CO <sub>2</sub>	3	24	5	Release behaviour of CO <sub>2</sub> and the discharge rate
3-15	10	Dense	100% CO <sub>2</sub>	200	50	19	Rapid depressurization of CO <sub>2</sub> pipeline
34	8	Supercritical	99.8% CO <sub>2</sub> , 0.2% air	256	233	20	In-pipe transient pressure and temperature
39	9	Supercritical	99.8% CO <sub>2</sub> , 0.2% air	256	233	20	In-pipe transient pressure and temperature
17	5	Liquid	99.8% CO <sub>2</sub> , 0.2% air	256	233	20	In-pipe transient pressure and temperature
30	7	Liquid	100% CO <sub>2</sub>	3 & 10	6	Unknown	Flow properties of CO <sub>2</sub>
31	8.1	Supercritical	99.14% CO <sub>2</sub> , 0.22% N <sub>2</sub> , 0.63% CH <sub>4</sub> , 42 ppmv H <sub>2</sub> S, 31 ppmv H <sub>2</sub> O	50,000	610	Unknown	Influence of impurities on the decompression process
10	15	Dense	91.03% CO <sub>2</sub> , 1.15% H <sub>2</sub> , 4% N <sub>2</sub> , 1.87% O <sub>2</sub> , 1.95% CH <sub>4</sub>	144	146	11	Influence of impurities on the decompression process
40.5	29	Supercritical	72.6% CO <sub>2</sub> , 27.4% CH <sub>4</sub>	42	38	11	Influence of impurities on the decompression process
20	12	Dense	89.8% CO <sub>2</sub> , 10.2% N <sub>2</sub>	140	10	1	Influence of impurities on the decompression process
20	12	Dense	80% CO <sub>2</sub> , 20% N <sub>2</sub>	140	10	1	Influence of impurities on the decompression process
20	12	Dense	70% CO <sub>2</sub> , 30% N <sub>2</sub>	140	10	1	Influence of impurities on the decompression process
20	8.5	Dense	92-98% CO <sub>2</sub> , 2-8% N <sub>2</sub>	52	4	Unknown	Influence of impurities on the decompression process

Table 7. Experiments tested depressurization in a broken CO<sub>2</sub> pipeline when events of venting/puncture occur [5].

### 4.3 Accidental release - Uncontrolled depressurization

Accidental releases can occur in different process conditions, including both gaseous and liquid inventories, together with the dense/supercritical fluid state, can happen above ground or below, in an isolated area or in densely packed and congested areas.

Gaseous releases from a hole in a vessel or broken pipework have a similar effect to the planned releases, with the following characteristics:

- In general, at the exit plane, they will be sonic releases from pressurized vessels/pipelines and will be choked, remembering that choking occurs if the ratio of the inventory pressure,  $p_v$  to the atmospheric pressure  $p_a$ , is greater than a critical value which depends on the ratio of specific heats,  $\gamma$ , for the gas. For carbon dioxide, the release will be choked if  $p_v/p_a > 1.89$ .
- Wilson's "double exponential" model is commonly used, which is described in the TNO Yellow Book manual on calculating physical effects when modelling releases [26].
- From pressurized gaseous storage, it is less likely to intercept the saturation line than from liquid storage.

Releases from vessels with liquid and some supercritical inventories are significantly more complex. In these cases, as the carbon dioxide enters the atmosphere it makes a transition from the liquid state to a two-phase gas/solid mixture where the solid fraction depends on the upstream conditions. During this transition, the fluid expands in a characteristic "tulip" shape. The solid particles which are formed then sublime back to gas. This phenomenon can be described by the "spray release" model taken from the TNO Yellow Book and explained below [26].

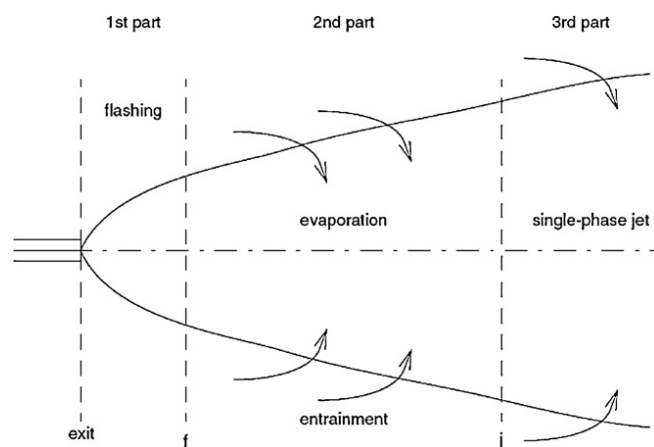


Figure 11. Schematic view of two-phase jet release [26].

A two-phase jet flow is generally composed of three parts. In the specific case of carbon dioxide, the first part (flashing) is the one in which the flow of  $\text{CO}_2$  would get frozen (partially) after expansion, due to the Joule-Thomson effect reaching the ambient pressure at the equilibrium plane. In the second part, molecules would sublime back to the gaseous state due to the heat provided by the resistance air that opposes the high-speed release, while mixing with air takes place. Some of the dry ice particles may not reconvert to the gaseous state, falling on the ground in solid form (rainout). In the third phase, all the molecules composing the flow would be in the gaseous phase and the jet would continue its expansion with more air entrainment.

Another distinct class of accidental release is that from a pipeline. Normally for risk assessment purposes, various leaks sizes can be considered, from full-bore rupture, which represents the worst case in terms of peak flow rate, to puncture rupture.

It is important to highlight that if the case of a gaseous pipeline is relatively straightforward with analytical expressions in common use, the case of a liquid or supercritical pipeline is significantly more complex to calculate [9].

### 4.3.1 Rapid phase transitions in CO<sub>2</sub>

Rapid depressurization and evaporation of pressurized liquefied gas are phenomena of relevance to hazard identification and risk analysis in the process industry. Tank explosions and pipeline ruptures are accidental scenarios that happen infrequently but have the potential to cause fatalities and significant material damage. It is necessary to quantify the damage potential of a sudden CO<sub>2</sub> release that originates from scenarios such as a boiling liquid expanding vapour explosion (BLEVE). A catastrophic vessel/pipeline failure would be expected to not just release a large quantity of CO<sub>2</sub> with subsequent dispersion, but also release overpressure and vessel fragments that may cause injury or fatalities.

In the past years, three incidents of rupture of a CO<sub>2</sub> storage vessel due to accidental over-pressurization have been recorded [9]. The resulting consequences can be the following:

- The cold liquid released can freeze personnel.
- Fragments can be thrown with tremendous force.
- Part of the vessel with CO<sub>2</sub> still expanding can act like a rocket.
- The rapid transition from supercritical to atmospheric pressure can create shock waves that cause damage, fatalities, and injuries.

In chapter 7 of the TNO Yellow Book, there are the standard equations used to describe the localized effects of overpressure and fragmentation of the vessels. However, it must be taken into account that the distance and time for reaching a fatal concentration of CO<sub>2</sub> can be more serious than the effects of overpressure and expulsion of the fragments.

Below is an explanation of the BLEVE phenomenon taken from (Energy Institute, 2013) [10].

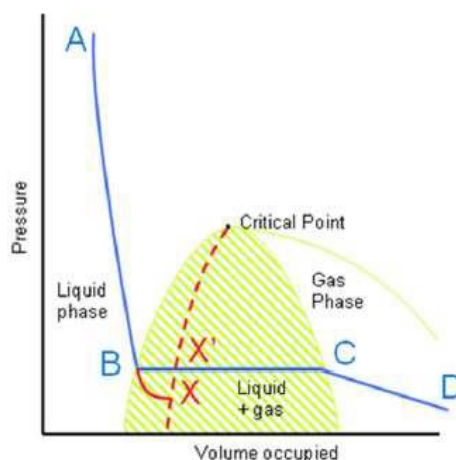


Figure 12. Theoretical pressure/volume graph for CO<sub>2</sub> showing spinodal curve [10].

Consider for example a large pipe of liquid CO<sub>2</sub> which is being depressurized for maintenance. The blue line A-B-C-D in Figure 12 shows the behaviour of the CO<sub>2</sub> at a constant temperature and thermodynamic equilibrium. Along the line A-B, the CO<sub>2</sub> is a liquid, and as the volume, it occupies is expanded the pressure falls rapidly. Eventually, the pressure falls to the vapour pressure of the liquid at the particular temperature at B. The liquid CO<sub>2</sub> then starts to evaporate to become a liquid-gas mixture, and the pressure keeps constant at the vapour pressure. Eventually, it reaches C, where the liquid has been completely converted into gas. The pressure then drops as it is expanded further as a gas (to D).

However, if having reached the vapour pressure line (B-C), the CO<sub>2</sub> pressure falls suddenly, (for example, due to a failure in the containment, or a valve being rapidly opened), the CO<sub>2</sub> can become an unstable liquid along the path B-X, the solid red line. Along this line, the CO<sub>2</sub> is metastable, and could at any time boil to return to the equilibrium horizontal line B-C.

In this case, a sudden and violent disturbance would take place, although it would not become a BLEVE until it reached point X.

X is called the spinodal point: here the slope of the solid red line is zero. The dashed line (spinodal curve) indicates the loci of spinodal points with changing temperatures. Along the spinodal curve, large density changes can take place because pressure can increase without any volume increase. Once the spinodal curve is reached, the CO<sub>2</sub> (which is an equilibrium of liquid and gas) gas will separate into gas and liquid states. This occurs homogeneously throughout the whole of the mass of the CO<sub>2</sub>. The rise in pressure to (X') on the vapour pressure line B-C may be not large, but takes place very quickly, and the pressure shock to the vessel in which the CO<sub>2</sub> is contained is significant, and failure (i.e. BLEVE) is likely to occur.

#### 4.3.1.1 Modelling and examples

The catastrophic ruptures of high-pressure pipelines may result in a physical blast close to the site caused by the expansion ratio of the liquid to gas. The common method to predict the most important effect produced by a BLEVE, i.e. the peak overpressure, consists in determining the total mechanical energy released by the explosion. Then, assuming that a certain percentage of this energy is converted into a pressure wave, the peak overpressure can be estimated by the method of the TNT equivalent mass. With this method, a scaled distance is calculated, and the consequent peak overpressure is obtained from the corresponding graph, comparing the experimentally measured effects of certain masses of TNT charges with the real effects of this explosion, as fully described in [26].

The velocity of the escaping gas from the pipeline is limited to its speed of sound in choked conditions. The actual release velocity just downstream from the rupture is equal to the speed of sound plus the speed of the gas particles driven by the rapid expansion into the ambient air. During this very fast phenomenon, the pressure gradients are unable to form, the energy is dissipated through the formation of a spherical pressure front that expands radially from the break. The dissipation in space of the pressure blast will be approximately linear with distance from the breach and dependent on the energy of the initial shock front.

It must be taken into account that the duration of the pressure blast front is short (hundreds of seconds) and limited in the space surrounding the catastrophic rupture, on the order of meters [45].

Molag and Raben [28] reported in their study 0.3 bar overpressure, as a result of sudden expansion, within 3 m for a pipeline transporting CO<sub>2</sub> at 16.5 bar with 100 % of fatality and 2.5 % of fatality within 5 m.

As an example, the overpressure trend versus the corresponding distances was calculated in the report of Energy Institute [9], using the PHAST's (described in chapter 6) BLEVE model in the case of a full-bore rupture at one end of a 203 mm diameter pipeline at a pressure of 11.7 MPa, as follows:

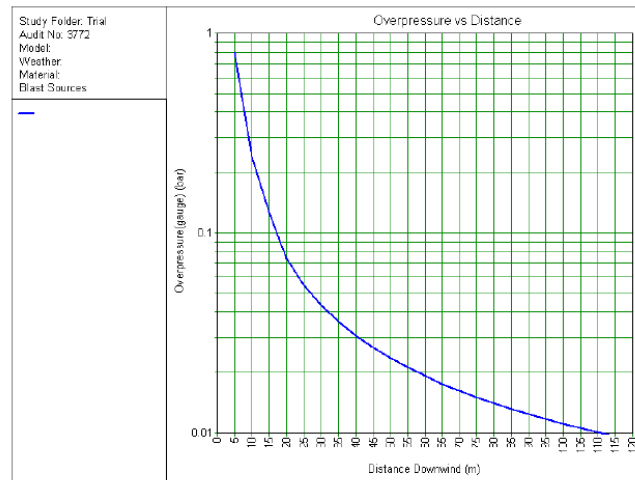


Figure 13. Blast-distance relationship for a pipe rupture [9].

Instead in Hansen et al. study [27], the explosion of pressurized carbon dioxide was observed when released from a high-pressure vessel into an openly vented atmospheric chamber. Small scale experiments were carried out with pure vapour and liquid/vapour mixtures and compared with the simulation, only the vapour release. The goal was to analyze how the vent size and liquid content affect the overpressure peak and impulse response in the atmospheric chamber.

The table shows results reproduced from tests TR1-TR5 and simulation was applied for the vapour case only.

Description	Unit	TR1	TR2	TR3	TR4	TR5	Sim
Initial pressure	MPa	5.5±0.1	5.3±0.1	5.6±0.1	5.6±0.1	5.6±0.1	5.5
Initial temperature	K	292±1	292±1	292±1	292±1	292±1	292
Open vent area	m <sup>2</sup>	0.1	0.01	0.1	0.01	0.01	0
Liquid volume	cm <sup>3</sup>	0	0	130	130	70	0
Vapour volume	cm <sup>3</sup>	190	190	60	60	120	176
Liquid fraction	vol %	0	0	68	68	37	0
Mass of CO <sub>2</sub>	g	36	36	113	113	77	33
Peak overpressure	kPa	15±2	17±2	20±2	15±2	18±2	12
Impulse at 100 ms	kPa·ms	55	149	326	426	206	

Table 8. Initial conditions, measured properties and calculated properties.

The comparison of vapour-phase CO<sub>2</sub> test results with simulations showed good agreement. It was used a CFD numerical code describing single-phase gas dynamics inside a closed chamber, but did not model any phase transitions. Hence, the simulations described only a vapour-only test into an unvented chamber. Nevertheless, the simulations reproduced the incident shock wave, the shock reflections, and the jet release inside the atmospheric chamber. The rapid phase transition did not contribute to the initial shock strength in the current test geometry. 3D simulations of the CO<sub>2</sub> release were performed with the USN in-house CFD code.

Figure 14 shows that the calculated impulse was significantly higher when the high-pressure reservoir contained a large liquid/vapour fraction, as compared to pure vapour.

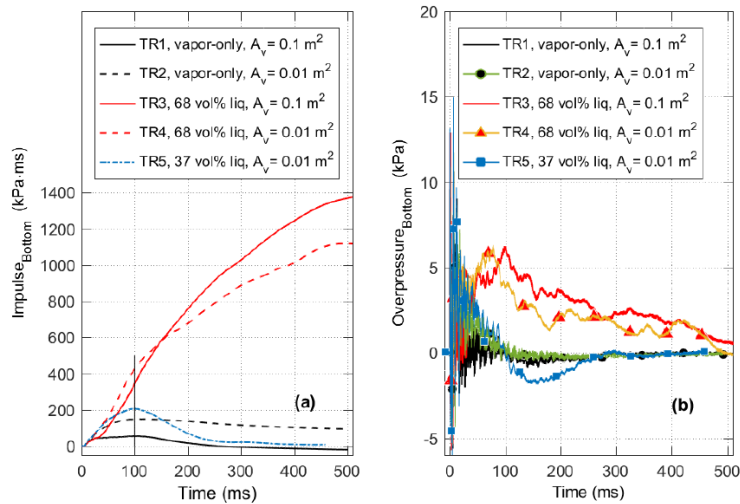


Figure 14. (a) Impulse calculations, and (b) pressure measurements from the vented chamber bottom sensor. From 0-500 ms after diaphragm rupture.

The vent opening from 0.1 to 0.01 m<sup>2</sup> resulted in a slightly higher impulse calculated at 100 ms. The influence of the vent area on the calculated impulse was significant in the vapour-phase tests, but not so clear in the liquid/vapour mixture tests.

The experimental impulse histories and pressure histories in Figure 15 below showed a good qualitative agreement with the simulations. The numerical results reproduced both the incident shock wave and the main shock reflections inside the atmospheric chamber. During the 0-20 ms period, the pressure response in the atmospheric chamber was governed by the rapid expansion of vapour-phase CO<sub>2</sub> from the pre-rupture state to atmospheric pressure.

The measured peak overpressure was in the range of 15-20 kPa. The simulation results produced a calculated peak overpressure of 12 kPa.

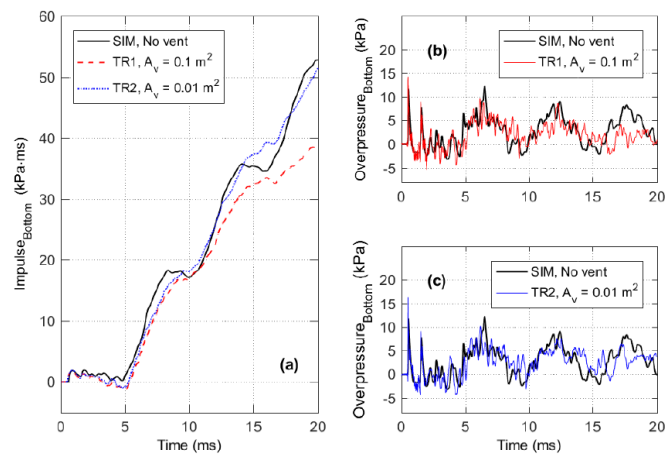


Figure 15. Comparison of simulations and experimental results from the vented chamber bottom sensor. (a) Impulse histories, and (b - c) pressure histories.

### 4.3.2 Transportation pipeline system accidental release scenarios

A CO<sub>2</sub> transportation pipeline will be composed of both above and below ground components. The majority of the pipeline will be buried for protection, but e.g. isolation valves will have to be accessible for maintenance and vent stations will require above-ground valves and pipework. This creates a range of possible scenarios for accidental CO<sub>2</sub> release:

- Above-ground leakage.
- Below-ground leakage/rupture.
- Propagating running fracture leakage.
- Offshore pipeline leakage.

Each of these scenarios is considered below.

#### 4.3.2.1 Leakage from above-ground pipeline infrastructure

In the event of accidental CO<sub>2</sub> leaks from above-ground pipelines, small leaks are detected as they are noisy and visible thanks to the frozen white water vapour. In these situations, there is a risk that the maintenance personnel will approach the leak point as they are drawn from the noise generated, being in danger in the accumulation of CO<sub>2</sub> near the pipeline. For this reason, the staff must be trained and that appropriate safety protocols and monitoring systems are established. On the other hand, the larger releases will be much more visible and just as noisy, to the point of making the surrounding area inaccessible, until the section is isolated and emptied. In both cases, in fairly calm atmospheric conditions or very large enclosed spaces, the cloud is more likely to flow at ground levels, accumulating at some distance from the pipeline [15].

Regarding small releases, Pursell [24] has collected some results from laboratory-scale tests carried out in the Health and Safety Laboratory (UK). The tests were carried out both in the liquid and gas phase of the CO<sub>2</sub>, with release holes from 2 mm to 4 mm and using a vessel with pressurized CO<sub>2</sub> from 40 to 55 bar.

Fan X. et al. [29] reported an experimental study of supercritical CO<sub>2</sub> leakage. The pressure and temperature conditions analyzed varied from 81 to 110 bar and 34.9 °C to 100.9 °C. The authors observed how the mass flow rate was influenced by varying the other parameters. Specifically, the mass flow rate decreases with the increase of upstream temperature and length-diameter ratio and increases with the increase of upstream pressure.

Guo et al. [30] carried out an experimental study both on the near-field characteristics and on the dispersion behaviour of supercritical CO<sub>2</sub> [31], gaseous and dense phase. These tests are present in the CO<sub>2</sub>QUEST project where a large-scale pipeline with an internal diameter of 233 mm and a total length of 258 m was built, for a total of nine tests performed and with hole diameters ranging from 15 mm, to 50 mm and to full-bore rupture. The structure of the under-expanded jet flow was then analyzed, with the related solid phase formation.

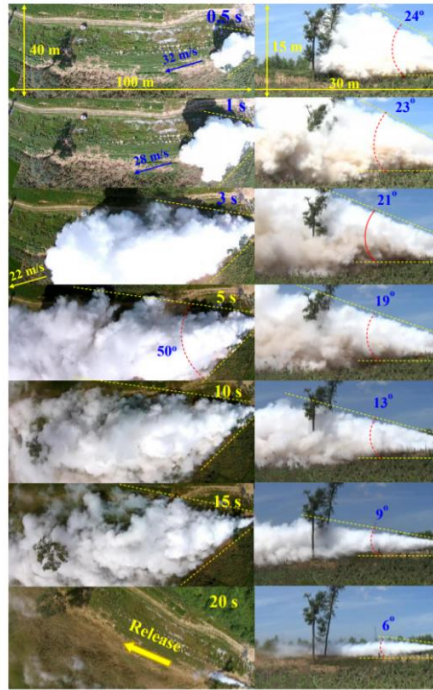


Figure 16. Visible cloud development of the dense CO<sub>2</sub> release experiments with the full-bore orifice.

Considering the consequent sublimation of solid CO<sub>2</sub>, it removes heat from the gaseous phase causing a drop in temperature and affecting the properties and shape of the cloud. Based on the experimental data performed by Guo et al. [30], the development of the visible cloud can be described by dividing it into three phases: a "rapid expansion", a "metastable phase" and a "slow attenuation phase". In all the experiments the concentration of interest for the three hole diameters was set at 50,000 ppm and the distance at which this concentration is reached was calculated.

In the case of full-bore rupture, at the initial dense phase conditions of 9.1 MPa and 21.6 ° C, the maximum safety distance of 160 m was measured. In general, the safety distances measured for the dense phase were much larger than those in the gas phase tests.

All large-scale experimental results obtained from these tests represent the basis for CO<sub>2</sub> dispersion research and can be used to validate discharge, near-field, and far-field models. The distance of 50,000 ppm was used to identify the maximum safety distances for the design, construction and operation of new pipelines. These data are therefore of fundamental importance for carrying out an analysis of the consequences and quantifying the risks associated with CO<sub>2</sub> pipelines.

#### 4.3.2.2 Leakage from buried pipelines and crater formation

Concerning releases from pipelines located underground, the breaking points are easy to detect only in the case of catastrophic ruptures or very large holes, witnessing the lifting of the overlying ground, the formation of a crater, and a subsequent plume of gas.

Instead, the release from small holes would lead to infiltration into the soil (causing in the long term acidification of the soil, lowering of the oxygen level, and death of the vegetation [23]) assumed as a porous medium, following by diffusion the path of least resistance. Subsequently, escaping, in calm atmospheric conditions, could accumulate close to the ground, especially if local depressions are present [22].

Contrary to CO<sub>2</sub> releases from above-ground pipelines or vessels, releases from underground pipelines are more difficult to model and there is no clear consensus on the most suitable approach.

An example, to understand the consequences of release from an underground pipeline is the one reported in the COOLTRANS research program, where full-scale puncture tests were carried out on an underground pipeline at 1.2 m and with an external diameter of 914 mm [25].



Figure 17. View of the crater formed during the instrumented burst.

The puncture experiments have shown that the nature of the surrounding soil can impact the nature of the flow into the atmosphere. The flow from the punctures was observed to stall in the atmosphere above the source and, in low wind speed conditions, a “blanket” was observed to form around and over the source.

Therefore, an influencing parameter on the release of CO<sub>2</sub> from underground pipelines is the type of soil in which it is located. In fact, in the case of clayey soil, a small leak was not able to sweep away the overlying soil, but an underground cavern was created, from which the gas escapes through paths with a diameter of around 100 mm, at a speed of about 40 m/s. Considering a hole of 25 mm at 150 bar, the formation of a crater with a diameter of 3 m was observed in sandy soil, while for clayey soil it was about half. Typically, a crater formed for larger horizontally orientated leaks at which discharge velocities of 40 m/s and 60 m/s were observed with a clear angle from the horizontal plane [25].

Taking as a reference the dimensions of the craters recorded over the years about the methane pipelines in the United Kingdom, these varied for buried pipelines from 1 to 4 m: from 3.3 m to 152 m in length; from 1.7 m to 33 m in width; from 1.7 m to 7.6 m in depth [36].

Among the rupture tests carried out on large-scale underground CO<sub>2</sub> pipelines, there is the one built-in Spadeadam (UK), part of the COSHER JIP research program. In particular, a 219 mm diameter pipeline with dense phase CO<sub>2</sub> was used, at conditions of about 150 bar and 13 °C. A maximum height reached by the cloud of 60 m and a maximum horizontal extension of 400 m was found, for a total of 136 tons of CO<sub>2</sub> released in 204 seconds. The minimum temperature reached was -78 °C, obtained with low wind conditions of 1.9 m/s, conditions also used for the distribution of the concentration of the dispersion cloud [41].



Figure 18. Images of the visible cloud resulting from the rupture of the pipeline, respectively at 10, 30 and 120 s from break [41].

More in general, evaluation of the consequences of a release (medium and large leaks) from an underground pipeline could involve modelling in quadrants as suggested by the International Association of Oil and Gas Producers (IOGP) [56] and presented in the following figure.

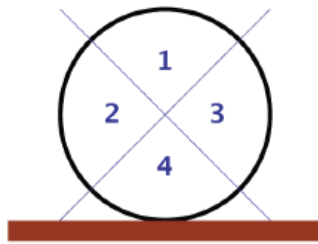


Figure 19. Quadrant modelling of an underground pipe release [56].

- **Quadrant 1** considers a vertical release modelled as occurring in the absence of coverage or at undisturbed speed.
- **Quadrants 2 and 3** involve a horizontal release modelled with an inclination of  $45^\circ$  upwards and with a speed of 70 m/s. However, this assumption is valid for natural gas releases, in the case of  $\text{CO}_2$  the exit speed was evaluated according to a proportionality factor (20 %) to that in the undisturbed case.
- **Quadrant 4** involves vertical downward releases. The modelling involves the assumption that the jet is vertical upwards but with a very low speed to reflect the loss of moment in impact with the ground (about 5 m/s).

Small leaks are only expected to form a crater when a puncture occurs in quadrant 1, which should be modelled.

Most crater modelling proposals are mainly theoretical with limited empirical evidence to support them (including IOGP, Energy Institute, PDVSA). The experimental  $\text{CO}_2$  release studies were used to provide additional information and a method of validation for the theoretical proposals.

#### 4.3.2.3 Leakage from propagating running fractures

Propagating or running fractures are considered the most catastrophic type of pipeline failure given that they result in a massive escape of inventory in a short space of time, mostly under buried conditions. As such it is highly desirable to design pipelines with sufficiently high fracture toughness such that when a defect reaches a critical size, the result is a leak rather than a long-running fracture.

In the case of  $\text{CO}_2$  pipelines, such types of failure will be of particular concern in Europe as large pipeline sections will inevitably be onshore, some passing near or through populated areas. In addition, there is a significant financial incentive in using the existing stock of hydrocarbon pipelines for transporting  $\text{CO}_2$ .

A fracture in a pipeline can propagate in either a ductile or a brittle mode.

Ductile fractures, characterized by the plastic deformation of the pipeline along with the tear, are the more common of the two modes of failure and therefore best understood. These may begin following an initial tear or a puncture in the pipeline, for example, due to third party damage or corrosion. The potential for this initial through-wall defect transforming into a propagating ductile fracture may be assessed using the simple well-established Battelle Two Curve (BTC) methodology.

This methodology involves the comparison of the pipeline decompression and the crack tip velocity curves. The crack will propagate as long as the decompression wave speed in the fluid is slower than the crack tip velocity. The BTC approach was recently extended based on the coupling of the fluid decompression and the crack velocity curves. This enabled the prediction of the variation of the crack length with time and hence the

crack arrest length. Given the almost instantaneous transformation of the initial tear into a ductile fracture running at high velocity (ca. 200-300 m/s), heat transfer effects between the escaping fluid and the pipe wall during the propagation process will be insignificant. As such the transient pressure stress is the only driving force for propagating a ductile fracture.

The propagation mechanism in the case of brittle fractures is somewhat different. A situation may arise in which the pressure inside the pipeline at the time of formation of a puncture or a leak will be insufficient to drive a ductile fracture. However, with the passage of time, the Joule-Thomson expansion induced cooling of the escaping fluid lowering the pipe wall temperature in the proximity of the leak. In the case that the pipe wall temperature reaches its Ductile to Brittle Transition Temperature (DBTT), for most pipeline materials, there will be an almost instantaneous and significant drop in the fracture toughness. In such cases, depending on the initial defect size and geometry, if the prevailing pressure and thermal stresses exceed the critical fracture toughness, a running brittle fracture will occur.

As such the modelling of brittle fractures requires the consideration of both the transient thermal and pressure stresses in the proximity of the initial through-wall defect.

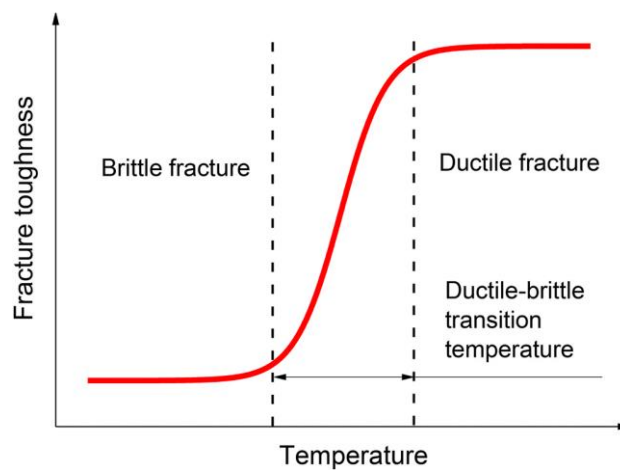


Figure 20. Ductile-brittle transition temperature.

Three factors render CO<sub>2</sub> pipelines especially susceptible to brittle fractures as compared to hydrocarbon pipelines. These include:

- CO<sub>2</sub>'s high saturation pressure and its significant sensitivity to the presence of even small amounts of impurities,
- its "slow" depressurization following a leak especially during the liquid/gas phase transition,
- its high Joule-Thomson expansion induced cooling.

There are economic incentives in using existing natural gas pipelines for transporting CO<sub>2</sub>, but these pipelines are more susceptible to brittle fractures as compared to newer pipeline materials, given their much higher DBTT (cf. -10 °C with -80 °C). Given the relatively short time frames being proposed for CCS introduction, the development of suitable mathematical models for assessing the susceptibility of CO<sub>2</sub> pipelines to brittle fractures is very timely [57].

To analyze the propagation and arrest characteristics of the fracture and the consequent dispersion of CO<sub>2</sub> into the atmosphere, two real-scale burst tests were carried out, as part of the CO<sub>2</sub>SafeArrest project, in 2017 in Spadeadam (UK) [55]. Through the use of explosives, crack propagation was induced, causing the pipeline rupture. For the first burst test, the pipe was buried at a height of 1 m, while for the second trial only half of

the pipeline section was buried. The steel pipeline, with an external diameter of 610 mm and length of 85 m, had a mixture of 91% of CO<sub>2</sub> and N<sub>2</sub> inside at a pressure of about 15 MPa.



Figure 21. Spreading CO<sub>2</sub> cloud and crater and the fractured test section.

As can be seen in the figure below, the measurements of the crater are respectively: 45 m along the direction of the pipe and an average width of 7.4 m, which is 12 times the external diameter of the pipe. The CO<sub>2</sub> cloud also reached an altitude peak of 250 m.

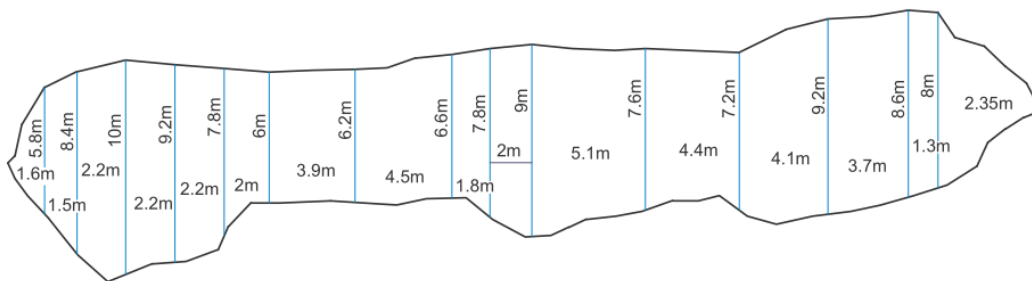


Figure 22. Crater profile and length measured after the rupture test [55].

#### 4.3.2.4 Accidental release from offshore pipelines

For accidental releases which can occur under water from subsea CO<sub>2</sub> pipelines and associated plant, the CO<sub>2</sub> has to rise to the water surface before being dispersed. However, it is expected that within a short distance from the release, gaseous bubbles of CO<sub>2</sub> will have formed which then rise through the column creating a bubble column. The evolution of this bubble column must be tracked using some model to give the size of the release at the sea surface. Therefore, the CO<sub>2</sub> will spread as it rises in the bubble column and the size of the release at the sea surface can be much larger than the area of the hole in the pipeline. Using as an example the North Sea, the pressure and temperature at the sea bed, are respectively 10 bar and 4 °C, therefore the CO<sub>2</sub> will be in the gaseous phase, though the pipeline could contain it liquid or supercritical phase.

Distinguishing between shallow and very deep waters, for the former, the release from the submarine pipeline leads the overlying water cover to be blown away; for the latter, it can be assumed that the release would result in a cloud of gas that rises to the surface, exiting the water with a diameter equal to 20% of the depth of the release, regardless of the flow rate, and with an exit speed that decreases as the area increases [37].

The tables below represent respectively a summary of the experiments conducted to study CO<sub>2</sub> behaviour in a vessel or a pipeline during orifice leakage and during a full-bore rupture as described in [6]. The experimental tests cited so far have paid great attention to the high density of CO<sub>2</sub> and the formation of dry ice in the jet (aspects to be taken into account in the modelling phase), highlighting significant differences with the management of natural gas release [18].

Reservoir conditions		Phase	Component release (%mol)	Orifice size (mm)	Aim of the study
Temperature (°C)	Pressure (MPa)				
10.4	4.5	Gas	100% CO <sub>2</sub>	2	Influence of the changing initial conditions (nozzle diameter) on the T, $\Delta p$ e mass flow rate at the exit plane
11.6	5.5	Liquid	100% CO <sub>2</sub>	2	
-3.5	4.1	Gas	100% CO <sub>2</sub>	4	
2.2	4.9	Liquid	100% CO <sub>2</sub>	4	
20-70	14-15	Dense/ supercritical	100% CO <sub>2</sub>	6.4, 12.7 & 25.4	Discharge flow rate, profiles of temperature and pressure within vessel and pipe
20	12	Dense	100% CO <sub>2</sub>	3.2, 6.4 & 12.7	The relation between the thermodynamic state and the mass release rate inside the vessel
Unknown	15		100% CO <sub>2</sub>	25 & 50	Exit velocities at the exit plane
40	5, 7 & 8	Dense/ supercritical	99.5 % CO <sub>2</sub>	1	Dependence of the process of leakage from initial pressure and release duration from nozzle length
40	9	Supercritical	99.5% CO <sub>2</sub>	1	Thermodynamic and fluid dynamic behaviours of supercritical carbon dioxide
Unknown	5.5 & 6.5		100% CO <sub>2</sub>	0.1, 0.2 & 0.5	
25	5.7	Liquid	100% CO <sub>2</sub>	0.3	Investigation of the influences of superheat on flashing spray properties and on the snow formation
19.85	6	Liquid	100% CO <sub>2</sub>	0.3, 0.5 & 2.5	Jet temperature and solid CO <sub>2</sub> particle size
-8.15	3		100% CO <sub>2</sub>	6	Large scale jet-release behaviour of CO <sub>2</sub>
Unknown	4.5		100% CO <sub>2</sub>	6	
Unknown	3.9		100% CO <sub>2</sub>	6	
Unknown	9.5		100% CO <sub>2</sub>	9	
Unknown	8.5		100% CO <sub>2</sub>	12	
5	7.7	Dense	100% CO <sub>2</sub>	25	
147.2	15.7	Supercritical	100% CO <sub>2</sub>	11.9	
149.5	14.8	Supercritical	100% CO <sub>2</sub>	11.9	
3-15	10	Dense	100% CO <sub>2</sub>	12-50	
35.1	7.6	Supercritical	100 % CO <sub>2</sub>	15	Study of the near-field characteristics and dispersion behaviour of supercritical, gaseous and dense-phase CO <sub>2</sub>
33.4	7.9	Supercritical	100 % CO <sub>2</sub>	50	
17.4	9.2	Dense	99.9 % CO <sub>2</sub>	15	
19.3	9.1	Dense	99.9 % CO <sub>2</sub>	50	
33.8	4.1	Gas	99.9 % CO <sub>2</sub>	15	
33.4	4.0	Gas	99.9 % CO <sub>2</sub>	50	

Table 9. Experimental works reproduced an orifice leakage via CO<sub>2</sub> pipeline/vessel [5].

Reservoir conditions		Phase	Component release (%mol)	Length (m)	Diameter (mm)	Thickness (mm)
Temperature (°C)	Pressure (MPa)					
13	15.1	Dense	100% CO <sub>2</sub>	94	194	13
5	15.3	Dense	100% CO <sub>2</sub>	144	150	0.05
5	13.5	Dense	100% CO <sub>2</sub>	230	152	11
25.2	7	Dense	100% CO <sub>2</sub>	37	40	0.05
36.9	8	Supercritical	100 % CO <sub>2</sub>	258	233	20
32.7	3.6	Gas	99.9 % CO <sub>2</sub>	257	233	20
21.6	9.1	Dense	99.9 % CO <sub>2</sub>	257	233	20
13.1	15	Dense	100% CO <sub>2</sub>	227	219	N/A

*Table 10. Experiments related to full-bore rupture scenario of CO<sub>2</sub> pipeline [5].*

## 5 Modelling of CO<sub>2</sub> release

When CO<sub>2</sub> enters the atmosphere after a pipeline release, accidentally or intentionally, there will be a sudden pressure drop which will cause a transition from the supercritical/dense/liquid state to the gaseous and/or solid-state and consequently a lowering of the temperature, due to the Joule-Thomson effect. In addition, a phase change may occur within the pipeline, causing damage inside and outside the infrastructure.

To determine the safety area around the pipeline, accurate prediction of the discharge rate is very important, especially in the event of an accidental rupture, to determine the minimum safety distances from populated areas, the ideal distance between the isolation valves, and develop emergency plans.

Hence, to have an accurate estimation of downwind CO<sub>2</sub> concentrations following a deliberate or accidental release, the modelling of the source characteristics is the most critical step, considering that the emission calculations can involve two or three-phase releases.

For modelling, the definition of emission characteristics is known as the “source term”. Specifically, the following steps are necessary for the calculation of the release rate:

- 1) Determine the time dependence of CO<sub>2</sub> release;
- 2) select the most suitable source term model for the case;
- 3) collect specific input data and physical properties useful for the term of origin model;
- 4) calculate the emission rate of the source and the conditions at the release orifice/equilibrium plane (where the jet reaches the ambient pressure) in terms of pressure, temperature, and quality of CO<sub>2</sub> (i.e. the proportions of gaseous, liquid and solid CO<sub>2</sub>) [15].

### 5.1 Time dependence of the release

Estimation of the time dependence of the CO<sub>2</sub> release rate depends on the time-dependent pressure within the process vessel or pipeline, as well as the flow of the resulting CO<sub>2</sub> stream. Therefore, the characterization of the time dependence of the pressure inside the pipeline or vessel is a determining factor for the time dependence of the release rate. The state of outflow of the pipe strongly influences the dispersion of CO<sub>2</sub> into the atmosphere. In an emergency/planned situation the controlled depressurization is necessary given the high Joule-Thomson coefficient, in fact during an uncontrolled depressurization will be the formation of solid CO<sub>2</sub>, which could block the pressure relief valves, generate pipeline running fracture, due to the embrittlement of the pipeline, and in the worst case, it can generate Boiling Liquid Expanding Vapour Explosion (BLEVE) by superheating of liquid phase CO<sub>2</sub>.

#### 5.1.1 Transient pipeline depressurization

To give realistic input boundary conditions to dispersion models, it is necessary to have good depressurization models for pipelines and vessels. To have a correct dispersion of the CO<sub>2</sub> cloud, it is necessary to correctly simulate the transient flow rate and the properties of the CO<sub>2</sub> flow during the release taking into account all the phenomena, as the pressure decreases, the CO<sub>2</sub> remaining in the pipeline will change phase from supercritical to liquid/gas and finally gas/solid.

The CO<sub>2</sub>PipeHaz experimental and modelling project focused on the characterization of fluid state transitions caused by the accidental or intentional release of CO<sub>2</sub>. These studies show that taking into consideration a pipeline tens of kilometres long, the vent fluid changes its composition from liquid-vapour to solid-vapour when the system drops to 518 kPa abs, below the triple point. The presence of solid particles affects the escaping jet, increasing the size and density of the CO<sub>2</sub> cloud [40].

In the literature, to describe the depressurization and release phenomenon, there are different models such as the Homogeneous Equilibrium Mixture (HEM) pipe flow model, the Homogeneous Relaxation Mixture (HRM) pipe flow model, and the Two-Fluid Mixture (TFM) pipe flow model.

HEM (Homogeneous equilibrium model) is one of the most widely used models for calculating liquid/vapour or solid/vapour two-phase flow release from failures of pipeline puncture/rupture, this model assumes that the phases are in the same conditions of velocity, temperature and pressure.

To demonstrate the effectiveness of the HEM model, a CFD model was used to predict the formation of solid particles during depressurization and model the resulting multiphase flow assuming a homogeneous equilibrium. Taking the pressure and temperature data during the Full-Bore Rupture (FBR) decompression of a 144 m pipeline and a diameter of 150 mm, with CO<sub>2</sub> at the initial conditions of 5.25 °C and 153.3 bar, the HEM model was validated. Under these conditions, solid CO<sub>2</sub> fractions of up to 35% were obtained at the point of release.

Another model that can be used is the HRM (Homogeneous Relaxation Model), where a thermodynamic imbalance is assumed between the phases of the fluid present during the depressurization in the pipeline, both for pure fluids and for multi-component mixtures. In fact, in the HRM the phase transition is not instantaneous, as in the HEM, but it is modelled using a “relaxation time”. The HRM model was also validated by comparing its estimates with the experiments of a Full-Bore Rupture of a pipeline containing a series of CO<sub>2</sub> rich-mixture. The predictions obtained from the HRM model was compared with the corresponding measurements, resulting in smaller estimation errors than a HEM model.

The last decompression model of the pipeline considered is the TFM (Two-Fluid Model), where, unlike the other two, for each phase of the fluid the conservation equations are solved individually, also modelling the interactions of the fluid/fluid interface with appropriate relationships. As for the other models, a validation was also carried out for the TFM by comparing its predictions with experimentally measured data relating to two CO<sub>2</sub> pipeline puncture decompression tests, with excellent results, also capturing the significant temperature difference between the vapour phase and liquid, observed experimentally [51].

The thermodynamics properties and phase behaviour of CO<sub>2</sub> pure/mixture usually were estimated based on different real-fluid equations of state (EoS) instead of using an ideal one, the following equations are given as examples:

- Span-Wagner (SW) EoS,
- The multicomponent Peng and Robinson (PR) EoS,
- Redlick and Kwong (RK) EoS,
- Soave-Redlick and Kwong (SRK) EoS.
- The multicomponent PVTsim (Calsep) EoS,
- Stiffened-gas (SG) EoS,
- SAFT, PC-SAFT and tPC-PSAFT EoS,
- Patel and Teja (PT) EoS,
- Valderrama modification of the Patel and Teja (VPT) EoS and
- The multicomponent GERG-2008 EoS.

EOS with a more complex structure may give better estimations of some specific properties, but they are usually more difficult to implement due to their complicated calculation procedure, particularly if they are not already included in the original simulation code.

There are currently the following models for the calculation of the source term, incorporated in commercial software, that can consider the CO<sub>2</sub> pipeline depressurization [15]:

- **Pipebreak.** The DNV-GL consequence model PHAST incorporates two time-varying models for long pipelines; GASPIPE for vapour releases and PIPEBREAK for liquid releases (Witlox et al. 2011)[42]. PIPEBREAK is an integral two-phase flow model which can simulate both choked and unchoked flow conditions.  
This consequence model is used to calculate the mass flow rate at the exit plane in the case of solid-liquid-vapour mixture of CO<sub>2</sub> fluid, PIPEBREAK discharge model in Phast package was also extended to allow released CO<sub>2</sub> to occur in solid transient or vapour to solid transient. Validation of the PIPEBREAK discharge model against the experimental data was also carried out. The predicted mass outflow rate was compared with the measurement from BP (British Petroleum) experiments and Shell experiments (CO2PIPETRANS). It was found that the model can predict well the mass release rate within 10% for both the BP and Shell tests [66].
- **Morrow.** The TNO consequence model EFFECTS incorporates two transient depressurization models. The Wilson model is specifically for gas releases from long pipelines as already specified, while the Morrow model was developed for releases of liquefied gas from long pipelines [26]. This integral model can calculate at the exit plane the pressure, temperature, vapour/solid fraction and total mass flow rate. The Morrow model can be applied for many substances, but it has yet to be validated for the CO<sub>2</sub> pipeline.
- **OLGA.** OLGA is widely used in the oil industry. The single-component two-phase module of OLGA, which uses the Span-Wagner equation of state and incorporates the HEM (homogeneous equilibrium) model, is regarded as the most suitable for CO<sub>2</sub> transport although it is unable to account for the presence of impurities.  
To solve this, Esfahanizadeh et al. [43] used the commercial package PVTism (version 18), to predict the transient phase state and thermodynamic properties in a pipeline containing a mixture of CO<sub>2</sub>, methane and water. PVTism uses the Soave-Redlich-Kwong equation of state, which is more accurate than the Span-Wagner EoS. PVTism was used to generate a fluid file as an input to OLGA, which was then used to model a full-bore rupture of a CO<sub>2</sub> pipeline. The calculated fluid release rate, velocity, temperature and solid CO<sub>2</sub> fraction were then used as an input to PHAST, which was used to model the dispersion behaviour of the resulting CO<sub>2</sub> plume.
- **PIPETECH** is a transient multi-component simulation tool developed by Professor Haroun Mahgerefteh at Interglobe Limited, London. PIPETECH has thermodynamics modules that can account for both CO<sub>2</sub> and impurities, uses the Homogeneous Equilibrium Model for two-phase flashing flow, and it has also the ability to model the evolution of pipeline cracks via a coupled fluid-fracture model.  
The CO<sub>2</sub>PipeHaz project found that PIPETECH was able to provide reasonably good simulations of experimental CO<sub>2</sub> release data, with a discrepancy of generally less than 10%. The model accounted for the formation of solid CO<sub>2</sub> particles and predicted the experimentally observed pressure stabilisation near the triple point pressure. The outflow code was usually subsequently integrated with CFD models to simulate releases from CO<sub>2</sub> pipelines in complex terrain.
- **gCCS** is a part of the gPROMS suite of process modelling tools, available from Process Systems Enterprise Ltd. It has been developed for the design of all the major components of a CCS system, containing steady-state and dynamic models for power generation, through capture, compression, transmission to injection. The pipeline simulation model uses gSAFT EoS to calculate the thermodynamic properties of the fluid.

The models mentioned until now were developed with assumptions including one-dimensional, friction, isentropic, and homogeneous equilibrium, or non-equilibrium fluid flow. But it is possible, though very rare, to use the CFD technique to simulate the process in a pipe following failures of a CO<sub>2</sub> pipeline, to describe the influences of non-isentropic on the decompressed CO<sub>2</sub> pipeline.

In view of this, Elshahomi et al. (2015) [32] used the package ANSYS-Fluent (CFD model) to develop the gCCS decompression model for the depressurization process of a CO<sub>2</sub> mixture flow in a broken pipeline. The gCCS model can solve the transient flows with an accurate EoS through user-defined functions (UDFs) and in three-dimensional geometries.

Particularly, this model can perform well the pressure and temperature drops as well as the transient phase during depressurization in the pipe. The model can also predict the curves of decompression wave speed in CO<sub>2</sub> mixtures, which can be used to estimate fracture propagation in the pipelines [5].

## 5.2 Release characteristics

The “source term” represents the physical and chemical properties of the escaping CO<sub>2</sub> stream, which in turn are determined according to:

- the evolution in time, “instantaneous” or “continuous”
- the orientation of the release (vertical, horizontal etc.)
- solid CO<sub>2</sub> particle snow-out (rain-out) and sublimation
- the momentum of the release
- the state of the release, single-phase or multi-phase.

### 5.2.1 Instantaneous or continuous release

The complexity of the model depends on its dependence on time or not, considering that in reality, all accidental releases are time-varying. There are many models capable of including this transient behaviour, i.e. accepting in input time-varying source terms properties such as mass emission rate, temperature, density etc. But there are also simplified models which require to define only if a release is instantaneous or continuous, in a finite time of duration “ $t_d$ ”.

For an instantaneous release, this occurs over a limited period, generally of a few seconds and resembles a “puff”, while for continuous release it is assumed that the emission rate is continuous over time and the cloud resembles a “plume”. The differentiation between these two characteristics can be based on considering a distance  $X$  between the release point and the receptor that acquires the concentration and a wind speed  $u$ .

From the point of view of the concentration time-series seen at a specific receptor at a distance  $X$ , a source that is instantaneous over a time period  $t_d$  will produce a puff-like time series at that location if:

$$t_d \ll X/u$$

The time required for the released CO<sub>2</sub> to reach a downwind distance,  $X/u$ , is compared to the actual emission duration  $t_d$ . If the emission duration is longer than the time it takes for the CO<sub>2</sub> to reach a downwind distance of interest, the release may be considered continuous. Otherwise, the release should be modelled as being instantaneous. The distinction between a puff-like or plume-like cloud shape and concentration time series at a given location thus depends on  $t_d$ ,  $X$ , and  $u$  [15].

### 5.2.2 Orientation of the release

Another important feature of the release is its orientation, especially in the near-field, i.e.  $x < 100$  m. The direction of the jet relative to the horizontal is an important modelling variable, influencing how the release develops after its expansion at ambient pressure.

Furthermore, recent experimental and modelling methods have indicated that the phase change of  $\text{CO}_2$  is relevant only for the near-field, while it is negligible at ground level when the downwind distance exceeds 100 m [21].

#### [1] Upward Leak



*Figure 23. Upward loss of  $\text{CO}_2$  from a pressurized vessel.*

During an upward release, the  $\text{CO}_2$  decompresses rapidly, leading to the formation of dry-ice particles and the subsequent condensation of the water from the entrainment air due to the lowering of the temperature, giving a characteristic white colour as can be seen from the figure above. The jet that comes out quickly heats up due to the friction with the surrounding air, giving enough energy to sublimate all the dry-ice particles into gas and avoiding the formation of a  $\text{CO}_2$  dry-ice bank on the ground [45].

#### [2] Downward Leak

For an above-ground pipeline, the leak can be downward-directed. As the jet imposes on the ground, a  $\text{CO}_2$  dry ice bank is formed, as illustrated in Figure 24, in the case of a vertical downward release from a pressurized vessel. After the spill, dry ice can sublimate, but given the low sublimation rate of gaseous  $\text{CO}_2$ , around  $2.5 \text{ gm}^{-2}\text{s}^{-1}$ , this does not present a risk to surrounding people, unless wind speeds are too low [33].

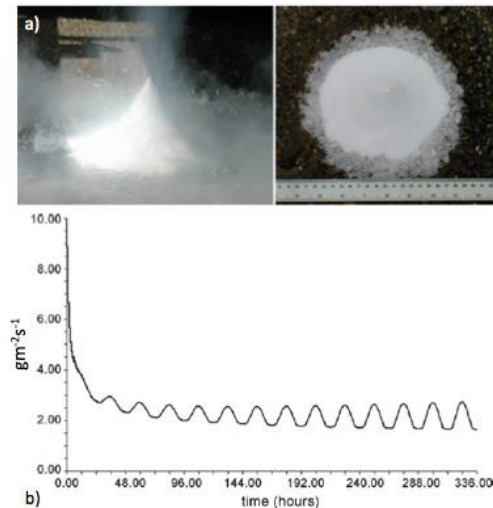


Figure 24. a) The downward release of CO<sub>2</sub> from the high-pressure vessel with the consequent formation of a dry-ice bank; b) The low concentrations of the gas in the air following the subsequent sublimation of solid CO<sub>2</sub> from the bank surface during 14 days in June [33].

### [3] Horizontal Leak

The worst-case for the surrounding people to consider is that of a horizontal CO<sub>2</sub> leak. In this case, if there is a release, for example from a pressurized vessel or even from a pipeline, the cloud will develop primarily horizontally, posing a very high risk for the surrounding area. The amount of CO<sub>2</sub> present in the cloud can also vary, as the dry ice particles present could exit the cloud and fall to the ground, generating a new small source of CO<sub>2</sub>. However, given the difficulty in defining how much dry ice separates, conservatively it is usually assumed that this phenomenon does not occur, in this way the CO<sub>2</sub> cloud will have a greater concentration [45].

The solid fraction of CO<sub>2</sub> present in the horizontal jet affects its dispersion, leading to higher maximum concentrations near the source. Furthermore, the smaller the vapour fraction the larger the CO<sub>2</sub> cloud itself and the further the cloud is propagated into a downwind direction. This can be explained by the effect given by gravity, as the density of the cloud increases as the solid mass fraction increases [46].

### 5.2.3 Solid CO<sub>2</sub> particle snow-out (rain-out) and sublimation

In particular cases as downward release, the solid CO<sub>2</sub> particles formed in the jet will rain out forming a dry ice bank on the ground, which will subsequently sublime, and a consequent vapour cloud will be formed that disperses. The driving force for the sublimation of the dry ice is the heat transport from the subsoil, solar radiation and the wind blowing over the dry ice bank.

The rainout of solid CO<sub>2</sub> particles was confirmed in a small-scale release test from the Sutton-Bonington Campus at the University of Nottingham [33]. In this study, a test was performed with the release of liquid CO<sub>2</sub> from a supply tank with initial conditions of -15 °C and 2.3 MPa through a downward pointing drain valve, as shown in Figure 24 above. Mazzoldi et al. [33] developed a mathematical model to account for the sublimation rate of a dry ice bank formed from this downward vertical release of liquid CO<sub>2</sub>. The model describes the energy balance at the surface of dry ice bank on the ground, including short-wave radiation flux, long-wave radiation flux, sensible and latent heat flux, and heat flux from the ground. The simulation results of the sublimation rate were not validated against the experimental data.

In another study [34] a model for the analytical study of thermal and fluid-dynamic behaviour of a dry ice particle falling to the ground is presented. The model, based on the numerical solution of the equations of motion, the equation of convective mass and heat transfer, describes the kinematic and thermal mechanism affecting a dry ice particle generated in a pressurized release of carbon dioxide starting from the post-expansion conditions.

This analytical model proves that the effects related to solar radiation and relative humidity are negligible, in other words, they don't affect considerably the quick process of sublimation of dry ice particles. Also, the ambient temperature has not an important role in the behaviour of thermal and fluid dynamics since the phenomena involved are extremely fast. On the contrary, the particle size and the air friction, related to the particle velocity, are not negligible when assessing flight particle sublimation. It was verified that, under Italian average weather conditions, the threshold particle diameter that discriminates a deposition on the ground coincides respectively with 150  $\mu\text{m}$  in the case of slanting downwards releases, 120  $\mu\text{m}$  for direct downwards releases and 650 - 700  $\mu\text{m}$  for horizontal releases. So, these variables, in addition to the direction of the release and the local wind flow field, can discern the event of soil deposition of dry ice from releases with only atmospheric dispersion.

In experiments to study the two-phase flow of solid and vapour  $\text{CO}_2$  large-scale releases conducted from COOLTRANS research programme, CO2PipeHaz project and CO2PIPETRANS project, the rain out of the solid  $\text{CO}_2$  particles was not observed.

Also, in an experiment conducted by the COSHER Joint Industry Project, it was observed that, after a rupture of an underground pipeline, no dry ice bank was formed under those experimental conditions. As shown in the figure below, the break however caused a crater, with very cold stones, covered with a white thin coating that melts to water [5].



*Figure 25. Photo of the crater and a broken pipe in the COSHER [5].*

#### **5.2.4 The momentum of the release**

The momentum of the  $\text{CO}_2$  release is also an important factor to consider. A high-velocity jet will entrain ambient air more rapidly and thus may lead to different dispersion behaviour than a slow release.

One direct effect of the release speed is the shorter downwind distance reached by dangerous concentrations of the gas if compared with undisturbed releases, due to the high initial dispersion (jet-mixing effect). This means that in some cases, a consideration of a low momentum of the release may result in an excessive conservative assumption [44].

In particular, the cases, for high-pressure leakage, where a low momentum release could be expected are the following:

- horizontal releases from buried pipelines: these are expected to result in low momentum releases after impinging surrounding walls;
- a complete line rupture (guillotine-type failure): opposing releases are assumed to exert sufficient pressure upon one another to reduce significantly their momentum;
- presence of obstacles in front of the leak (e.g., buildings, trees), impingement releases;
- extremely quick sublimation of solid CO<sub>2</sub> formed after a downward leakage [44].

In the case of small releases with low momentum and large releases with high momentum, it is necessary to consider the different effects that the wind speed causes.

- For small releases with low momentum, a high wind speed favours dispersion, as it improves mixing and transport.
- For large horizontal releases with high momentum, the wind pushes the cloud even further downstream, which is initially accumulated on the ground and dominated by the source moment, increasing the distances reached as the wind speed increases. In this case, the effect of the wind speed on the dispersion is limited, as it is much lower than the discharge speed [61].

### **5.2.5 Conservative release assumptions**

Considering a conservative assumption, “worst-case scenario”, like a full-bore rupture, it is possible to simplify the model by adopting the maximum discharge rate, instead of the time-varying flow rate, underlining that in the quantitative risk assessment it is always necessary to consider the frequency of occurrence of a certain event.

In general, when modelling the release from the long CO<sub>2</sub> pipelines is possible to approximate (in a suitable modelling software package) the discharge rate as a function of time with the average release rate over 20 seconds. Also, this assumption gives a conservative set of results. To be more precise and less conservative, a time-varying method has to be adopted, in case of a rapid variation in the CO<sub>2</sub> flow rate [10].

Further conservative assumptions can be made by considering as a scenario the CO<sub>2</sub> release by a full-bore horizontal rupture at ground level on flat terrain and with no solid formation on the ground.

Moreover, we have to highlight that in the reference [55] it was discovered that the consequence distances predicted in the case of a full-bore rupture assuming horizontal release are far from conservative if compared with a vertical release due to a full-scale pipeline fracture. This may be due to the lower release rate from a full-bore rupture compared to the explosive release rate due to a full-scale fracture, hence a study is necessary in order to control fracture propagation in high-pressure pipelines.

## **5.3 Fracture control model**

Pipeline fractures can be caused by the presence of CO<sub>2</sub> release, so it is critical to assess the conditions for fracture propagation. This is because a full-scale fracture scenario can lead to higher release rates even than a full-bore release. Research on the fracture propagation of high-pressure pipelines has been ongoing for many years.

Therefore, in order to evaluate the possibility of fracture propagation and to prevent unstable fractures along the CO<sub>2</sub> pipelines, a controlled study is needed. Mahgerefteh et al. [57] developed and applied a fully coupled fluid-structure interaction model to simulate the propagation of brittle fractures in the pipeline with CO<sub>2</sub> in dense and gas phases. In this study, the following parameters were tested: the influence of the dense phase, the thickness of the pipe wall, the ductile-brittle transition temperature (DBTT), the crack geometry, the flow temperature, the impurities present and the flow isolation; to understand how they influence the propagation behaviour of the brittle fracture. All the simulations carried out had the purpose of establishing the suitability of the pipelines currently used for the transport of CO<sub>2</sub>, to understand whether or not they are subject to brittle fracture propagation.

The model accounts for all the important processes governing the fracture propagation process including fluid/wall heat transfer effects, the resulting localized thermal and pressure stresses in the pipe wall as well as the initial defect geometry. Real fluid behaviour is considered using the modified Peng Robinson equation of state for CO<sub>2</sub>.

The application of this fracture model to hypothetical but realistic failure scenarios, using British Gas LX/1 pipeline materials, reveals significant, and to some extent, unexpected findings had been found as follows:

- 1) gas-phase CO<sub>2</sub> pipelines are more susceptible to undergoing a propagating brittle fracture as compared to dense phase CO<sub>2</sub> pipelines, despite the lower operating pressures in the former case;
- 2) a buried CO<sub>2</sub> pipeline is more susceptible to brittle fracture propagation as compared to an above-ground pipeline due to the eventual secondary cooling of the pipe wall by the surrounding soil in contact with it;
- 3) isolation of the feed flow to the pipeline following a leak promotes brittle fracture propagation;
- 4) an increase in the pipe wall thickness increases the pipeline's resistance to brittle fracture failure;
- 5) the initial through-wall defect geometry in the pipeline has a profound impact on the pipeline's propensity to brittle fracture failure;
- 6) within the ranges tested, CO<sub>2</sub> stream impurities representative of the main capture technologies does not have an appreciable impact on the pipeline's resistance in undergoing brittle fracture failure.

Finally, it should be noted that in contrast to ductile fractures, brittle fracture propagation is a time-dependent phenomenon. It will only occur if the depressurization duration is sufficiently long such that at the time when the pipe wall temperature in the vicinity of the defect drops below the DBTT, the thermal and pressure stresses exceed the pipe wall fracture toughness.

Instead regarding the ductile fracture propagation, as part of the COOLTRANS research program, two full-scale fracture propagation tests were conducted using dense phase CO<sub>2</sub>-rich mixtures. It was found that the standard method used to predict the toughness required to arrest a running ductile fracture in natural gas pipelines was inadequate to account for the experimental data, in fact, the predicted toughness would need to be increased by a factor of 1.5 to 2.4.

Instead, as part of the CO<sub>2</sub>PipeHaz project, the issue of the effect of small concentrations of impurities on the required arrest toughness was studied, which developed and validated a Dynamic Boundary Fracture Model (DBFM) to calculate CO<sub>2</sub> pipeline decompression and fracture propagation velocity. The DBFM considers all the important fluid-structure interactions taking place during fracture propagation, including unsteady real fluid flow, heat transfer, friction, and progressive variation of the crack tip pressure loading. The Modified Peng-Robinson equation of state is used, which can account for the presence of fluid impurities.

The results of simulation studies with DBFM suggest that, for pure CO<sub>2</sub>, the fracture length is very short in the temperature range 0-20 °C, but increases a lot at 30 °C. This model has been incorporated into the commercial software package PIPETECH. However, the DBFM has been validated only against experimental release data for natural gas containing impurities, but not CO<sub>2</sub> containing impurities. Therefore, the utility of PIPETECH to estimate the required fracture toughness of CO<sub>2</sub> pipelines remains unclear.

Further work on the effect of impurities on ductile fracture propagation is also part of the CO2Quest project. Among the objectives of CO2Quest is to develop and validate fluid/structure fracture models for ductile and brittle fracture propagation in CO<sub>2</sub> pipelines, to identify the type of impurities and operating conditions that have the most critical impact on a pipeline's resistance to withstanding long-running fractures, considering various candidate pipeline steels [15].

## 6 Modelling of CO<sub>2</sub> dispersion

The main features of carbon dioxide dispersion are [9]:

- It is denser than air so that it will tend to slump, especially at low wind speeds.
- It is often cold at its release point (accentuating its dense nature).
- In releases from the dense/supercritical state, it expands rapidly as a spray release and carries solid particles.

Some of these aspects are shared with other gases, with the only different aspect in the solid particles carried by the plume. It must be noted that releases from CCS plants, particularly pipelines, will be at high pressure, therefore in supercritical or dense phase.

Several general methodologies can be employed for dispersion calculations for carbon dioxide and other gases. The parameters that need to be considered in choosing a methodology include:

- if surrounding plant and/or terrain are considered or not,
- wind speed and direction relative to the release,
- meteorological conditions,
- length scales of interest.

An ideal dispersion model calculates all the characteristics of a source-term, without the need to enter them manually or to incorporate them through a source-term calculation model, as other dispersion models would require. In most cases, in order to model a dispersion phenomenon it is necessary to assume a pseudo source plane like in the following figure:

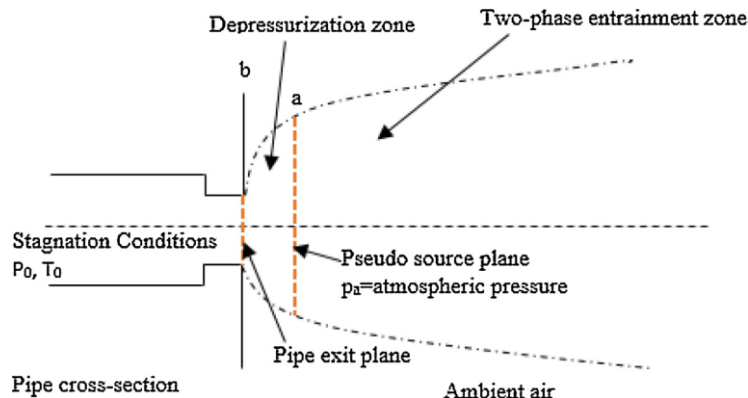


Figure 26. Definition of pseudo source plane [58].

Beyond the exit plane, the fluid expands and the resulting under-expanded jet structure with very high momentum is divided into two regions: a depressurization zone and a two-phase entrainment zone.

The inlet to a CFD/integral dispersion model can be taken to be at the end of the depressurization zone where the pressure in the jet has reduced to atmospheric pressure. As assumptions can be used that there is no entrainment of air into the jet and that friction and heat transfer are neglected in the depressurization zone. Also, conservation principles can be used to find the jet properties at the end of the depressurization zone, in detail conservation of momentum flux, conservation of energy and conservation of mass [58].

It must be highlighted that with this simplified mathematical calculation, it is not possible to know the distance at which the equilibrium phase is reached. This distance could only be found with very specific experimental campaigns or with very detailed CFD simulations that investigate the near-field area. Simulation of this scenario is very complicated because wave structures and Mach discs should be reproduced.

One possible approach could be the one that an integral software, as PHAST, uses, where a Homogeneous Equilibrium Model (HEM) is adopted to model the expansion from the orifice plane to the equilibrium plane, and therefore, calculated equivalent source is applied directly at the source exit, neglecting that distance: consequently, results at short distance are affected by this assumption and they are not accurate [62]. To define the size of the pseudo-source, i.e., the size of its expanded diameter at ambient pressure, it is possible, for example, to consider an effective diameter for liquid releases up to 30% larger than the diameter of the hole considered [18].

## 6.1 Dense carbon dioxide dispersion phenomena

### 6.1.1 Dense gas dispersion

By definition, the dispersion of a dense gas corresponds to gases whose density is greater than that of atmospheric air, as in the case of CO<sub>2</sub>, which therefore has negative buoyancy. The cloud of dense gas, dispersing, drags air and is diluted thus also decreasing its density and passing from a dispersion of dense gas to a passive dispersion, that is, of gases with neutral/positive buoyancy.

During its dispersion, dense gas could be represented through four main phases [56]:

- The initial phase, where there is the turbulent jet.
- The gravity spreading phase, where both buoyancy and the external mean flow are the dominant forces.
- The nearly-passive phase, where external ambient turbulence also becomes a significant force.
- The passive phase, where the motion of the cloud is entirely controlled by the external ambient turbulence and the external mean flow.

The following figure shows how this phenomenon evolves for a horizontal release at ground level.

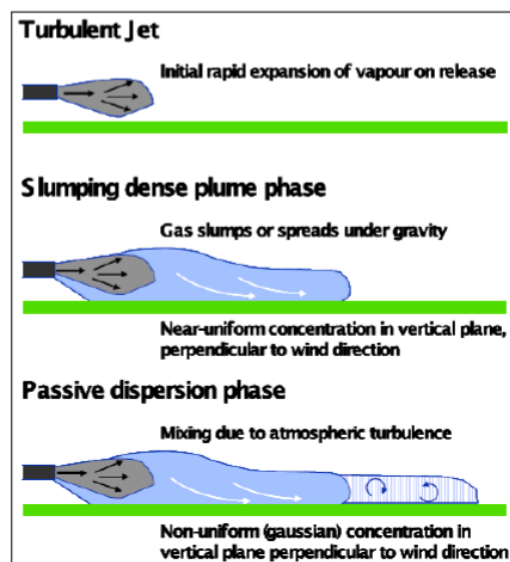


Figure 27. Generalized development of a dense gas cloud [56].

A parameter capable of giving information whether the dispersion of a cloud is dense or not is the Richardson number, which by definition measures the relationship between buoyancy and turbulent stress. In fact large Richardson number means that gravitational potential energy dominates turbulence, so the dispersion cannot

be adequately modelled using the standard Gaussian models, which instead can be used when it is small, where turbulent energy is dominating.

The cloud Richardson number  $Ri^*$  for a ground-based slumping cloud could be expressed as [20]:

$$Ri^* = (g * \frac{(\rho_c - \rho_a)}{\rho_a}) \frac{h}{u^{*2}}$$

Where:

- $g$  is the acceleration of gravity;
- $h$  is the local cloud depth;
- $\rho_c$  is local cloud density;
- $\rho_a$  is ambient density and
- $u^*$  is the ambient friction velocity (equal to about 5% to 10% of the wind speed at a height of 10 m).

Even with an upward vertical release, dense dispersion can occur, if the  $Ri^*$  is large enough, taking the plume width and not the height as the reference direction. If this happens at some point the plume will no longer move upward but will drop downward-moving downwind [15].

The transition from dense gas to passive dispersion occurs when the velocity of lateral enlargement of the cloud, due to atmospheric turbulence, overtakes that due to gravity.

The distance from the source at which there is a transition from dense to neutral gas dispersion with neutral or positive buoyancy, where ambient turbulence dominates, will depend upon the size of the release and the wind speed. This transition, in the position of the source or any distance downwind, is assumed to occur for values of  $Ri^*$  greater than 50.

With a neutral dispersion, it is appropriate to model the gas cloud dispersion using a standard Gaussian atmospheric dispersion model, where the principal mechanism of diffusion is turbulence, which has traditionally been represented as a stochastic process. A stochastic process evolves in time according to probabilistic equations, the behaviour of the system is determined by one or more time-dependent random variables [44].

## 6.2 Types of dense gas dispersion models

Several dense gas dispersion models are currently available and they can be classified through the following four categories:

- Empirical correlations
- Integral models
- Lagrangian puff and particle dispersion models
- CFD models.

The available models for each category are summarized in the table below:

Model Category	Model Name
Empirical correlations	“Workbook on the dispersion of dense gases”, Britter et al [54] is the main reference.
Integral	HGSYSTEM SAFER/TRACE
	SLAB GASTAR
	DEGADIS PHAST
	ALOHA EFFECTS

<b>Lagrangian</b>	QUIC	ArRisk
	SCIPUFF	CHARM
	CALPUFF	
<b>CFD</b>	FLUENT	FLACS
	OpenFOAM	ANSYS-CFX
	PANACHE	

Table 11. Types of dispersion models [15].

In this study, particular attention is given to the integral and CFD models, hereafter described.

### 6.2.1 INTEGRAL MODELS

Many atmospheric dispersion models for environmental analysis are conducted with Gaussian plume models. The Atmospheric Dispersion Modelling Liaison Committee, which is an independent organization that advises on matters of atmospheric dispersion modelling, has developed a simple Gaussian plume model which has been widely used.

Gaussian plume models have several limitations, which are:

- the minimum wind speed for applicability is generally taken as 1 m/s;
- zero wind speed cannot be calculated;
- any vertical component of the wind, which might be generated by upwash or downwash over buildings, structures and terrain, cannot be included;
- they are only applicable when the release source is sufficiently distant from surrounding buildings;
- any momentum in the released plume is accounted for by specifying an “equivalent height” of release;
- no transient calculations.

Simple Gaussian plume models are not expected to be appropriate for the majority of atmospheric dispersion calculations of CO<sub>2</sub> in CCS projects since it behaves as a dense gas, they will only be applicable at concentrations of carbon dioxide at which the hazard is negligible. A possible exception may be if the carbon dioxide contains significant quantities of more toxic material such as hydrogen sulfide [9].

Instead, there are more advanced integral models available than the simple Gaussian plume models, which can deal with heavy gas dispersion. These model the cloud as having a dense central core and Gaussian edges at the sides and in the vertical direction. The mass properties of a dense gas cloud, including for example the plume radius, velocity, centreline concentrations, are described using ordinary differential equations. This modelling is done up to the point where the cloud density becomes neutral. From here on it can be modelled through standard Gaussian dispersion models having become a passive cloud.

These advanced integral models still have some disadvantages concerning carbon dioxide dispersion:

- Some cannot be used with very low wind speeds.
- They cannot deal with cases where the plume interacts with itself, for example where a jet is directed into the wind so that the gas blows back around the jet, even if in most cases it is assumed that the wind is in the same direction as the release, which gives conservative cloud sizes.
- The effect of interaction with buildings and/or plant cannot be accounted for except in a very general way which accounts for the cloud travelling over certain types of terrain, e.g. woodland, farmland, or urban low-rise housing.
- Another limitation of many integral models is that they do not include carbon dioxide as a material that can be modelled automatically, so scenarios cannot be attempted without manual intervention which requires some additional knowledge on the behaviour of carbon dioxide when released [15].

The primary advantages of integral models are that they are quick to set up and run, they work well in appropriate scenarios and the main codes are well-validated and accepted by regulators [9].

Many of the integral models present in the literature are described below [15].

- **HGSYSTEM** is a suite of programs designed by Shell Research Ltd and select industry groups, to assess the release of gases, liquids, and two-phase mixtures from a variety of sources and the subsequent dispersion of heavier-than-air and neutrally buoyant gases. The suite of HGSYSTEM model components may be used separately or consecutively to describe a release from a source, near-field dispersion, and far-field dispersion. HGSYSTEM also includes models for initial two-phase jet releases and for instantaneous puff releases. The HGSYSTEM does not have an inbuilt Graphical User Interface (GUI) and must be run using a command prompt window and a text editor to modify the input files. The modular nature of HGSYSTEM, the versatility of the system, and the lack of a GUI increase model complexity, requiring more substantial training in the model.

HEGADAS represents the dense gas dispersion module of HGSYSTEM.

FRED (Fire Release Explosion Dispersion) is an integral model developed from Shell, that incorporates HGSYSTEM and it is used to be sold as a commercial package. It adopts a semi-empirical jet model for the first part of the release and a similarity model for the dense gas dispersion. FRED assumes the homogeneous equilibrium model (HEM) between the CO<sub>2</sub> phases [18].

- The **SLAB** model was developed by the Lawrence Livermore National Laboratory of the United States to simulate the atmospheric transport and dispersion of dense gases. The code for SLAB is freely available for download from the US EPA (Environmental Protection Agency) website. The SLAB model is an atmospheric dispersion model for denser-than-air releases which includes a ground-level evaporating pool, an elevated horizontal jet, a stack or elevated vertical jet, an instantaneous volume source. Except for the vaporizing pool source, which is assumed to be all vapour, the remaining sources may be either pure vapour or a mixture of vapour and liquid droplets. The US Department of Energy also used SLAB in their CO<sub>2</sub> pipeline risk assessment methodology [4].

SLAB (with a GUI) is also available in the EFFECTS commercial packages.

SLAB is relatively easy to use, particularly with a GUI, though specific training in the model design and input-output parameters is required.

- The **Dense Gas Dispersion (DEGADIS)** model was originally developed for the United States Coast Guard and the Gas Research Institute to simulate the atmospheric dispersion of dense gases following LNG spills. Algorithms for simulating two-phase jet releases were added in the 1990s. The code for DEGADIS is freely available for download from the US EPA website. A simplified version of DEGADIS is used as the dense gas model in ALOHA.

DEGADIS model predicts downwind vapour concentrations for explosion hazards, developed specifically to model heavier-than-air gaseous releases. DEGADIS can model continuous and short duration ground-level releases, vertical jets and vaporizing liquid release [4].

- **ALOHA (Areal Locations of Hazardous Atmospheres)** was developed by the United States Environmental Protection Agency and National Oceanic and Atmospheric Administration to simulate airborne releases of hazardous chemicals. ALOHA users may choose between several specified release options, including a gas leak from a ruptured pipe. Based on the selected scenario, the program will calculate the release rate as a function of time. ALOHA is freely available as part of the CAMEO (Computer-Aided Management of Emergency Systems) suite of software applications. The model includes a database of chemical parameters for several chemicals, including CO<sub>2</sub> and default options for source

emissions. The ALOHA GUI has been specifically designed for simplicity of use in the emergency response environment.

A disadvantage of ALOHA is that it can simulate the release of toxic chemicals only in the horizontal direction.

- The **SAFER Systems TRACE (Toxic Release Analysis of Chemical Emissions)** module is a dispersion modelling tool that can simulate a wide range of accidental toxic gas releases, including those associated with dense gas releases. The program is menu-driven and contains several separate modules to estimate the release and dispersion of chemicals. SAFER TRACE is designed for speed and ease of use, though specific training in the model design and input-output parameters is required.
- **GASTAR** is a dense gas dispersion model developed by Cambridge Environmental Research Consultants (CERC 2009) in association with the HSE. Rex Britter was the primary developer of GASTAR and the original author of the technical documentation. GASTAR can model the dispersion of dense gases from many accidents and emergency response scenarios. However, GASTAR is unable to calculate the source terms for all these scenarios, so they must be provided by the user.  
The application has a Windows-friendly GUI, simplifying input data entry and providing a flexible examination of output. Although GASTAR is also supplied with a database of material properties for common toxic and flammable substances, CO<sub>2</sub> is not included in the database and the physical properties of CO<sub>2</sub> must be added by the user. GASTAR is designed to be as straightforward as possible, though specific training in the model design and input-output parameters is required.
- **Process Hazard Analysis Screening Tool (PHAST)** is a consequence analysis program for modelling accidental releases of hazardous materials.  
PHAST is available commercially from DNV-GL, a non-governmental organization that establishes and maintains technical standards and supports this activity by undertaking in house and sponsored research. The PHAST software is capable of assessing release rates from accidents and modelling subsequent dense gas dispersion. The PHAST GUI allows for a wide range of tabular and graphical output. PHAST is designed to be quick to set up and run and to require relatively limited training.  
For release and dispersion of CO<sub>2</sub>, sensitivity analysis was performed using a Gaussian emulator that was constructed from 100 PHAST simulations. The parameters varied include the reservoir temperature and pressure (range within 100 and 150 bar), orifice size, wind speed, humidity, surface roughness and height of the release. The emulator was used to identify the input parameters that had a dominant effect on the dispersion distance of the CO<sub>2</sub> cloud. The results from the analysis showed that for the range of conditions tested, the orifice diameter had a far greater impact than any of the other parameters varied. The second largest effect was from the release height. There were interactions between these two model input parameters: when the release was close to the ground, a large orifice produced a much longer plume than when the release was higher, due to the limited entrainment of air near the ground [64].
- **EFFECTS** is a consequence analysis program for modelling hazards from accidental releases of hazardous materials. EFFECTS is available commercially from Netherlands Organization for Applied Scientific Research (TNO), which is an independent non-profit organization. EFFECTS incorporates the SLAB dense gas dispersion model. EFFECTS is capable of assessing release rates from accidents and modelling subsequent dense gas dispersion, with the methods and calculations published in the “coloured books” of TNO. Heavy gas dispersion models are available for rapid gas release, pool evaporation, horizontal or vertical jet. The GUI allows for a wide range of tabular and graphical output as PHAST.

An overview of their features is presented in Table 12.

Model name	Producer	GUI	Release duration	Available source types	Include CO <sub>2</sub> as material	Multiphase release
<b>SLAB</b>	Lawrence Livermore National Laboratory of the United States	Yes	C,I,T	Ground-level area (liquid pool evaporation); ground-level and elevated, horizontal and vertical jets	Yes	Limited (equivalent gas density)
<b>DEGADIS</b>	United States Coast Guard and the Gas Research	No	C,I,T	Ground-level area and vertical jets	Yes	Limited
<b>HGSYSTEM</b>	Shell	No	C,T	Area, ground-level jet (no initial momentum for jet releases, which may result in errors near the release point)	Yes	Yes
<b>ALOHA</b>	The United States Environmental Protection Agency and National Oceanic and Atmospheric Administration	Yes	C,I,T	Ground-level area, ground-level jet (no initial momentum for jet releases, which may result in errors near the release point)	Yes	Limited
<b>SAFER/TRACE</b>		Yes	C,I,T	Area and jet, ground-level and elevated	Yes	Yes
<b>GASTAR</b>	Cambridge Environmental Research Consultants (CERC 2009)	Yes	C,I,T	Area, ground-level and elevated jet in any direction including horizontal and vertical	No	Yes
<b>PHAST</b>	DNV-GL	Yes	C,I,T	Area, ground-level and elevated jets in multiple directions including horizontal and vertical	Yes	Yes
<b>EFFECTS</b>	Netherlands Organization for Applied Scientific Research (TNO)	Yes	C,I,T	Ground-level area (liquid pool evaporation); ground-level and elevated, horizontal and vertical jets	Yes	Yes

Table 12. Characteristics of the different integral models.

Where C stands for “continuous”, I for “instantaneous” and T for “transient”.

### 6.2.1.1 Integral models comparison in calculating CO<sub>2</sub> source terms

During a release, the CO<sub>2</sub> expands at ambient pressure as an under-expanded jet forming a mixture of solid particles and gas, rather than, more commonly, a mixture of gas-liquid particles. For this reason, one of the most important factors in choosing the most suitable dispersion model is its ability to handle CO<sub>2</sub> specific source terms, although most models that include source emission modules, such as FRED, can simulate the releases of CO<sub>2</sub>, using the same formulas of other pressurized liquefied gases, excluding the effects of solid particles. Furthermore, for an accurate model of the source term, a characterization of the initial CO<sub>2</sub> flow as mono or multiphase, continuous or instantaneous, stationary or variable in time, constant or decreasing pressure is necessary. In the case of a pipeline, a model suitable for transient depressurization is also needed to provide the correct input to the dispersion model.

Among the models analyzed, only two models of dense gas dispersion take into account the depressurization/flashing, the sublimation of the CO<sub>2</sub> solids in the jet and therefore the consequent cooling of the cloud, the dispersion as dense gas and its subsequent passive dispersion downstream. Specifically, these are the DNV-GL PHAST and TNO EFFECTS models, which include the following modules to simulate the depressurization of pipelines:

- The DNV-GL consequence model PHAST incorporates PIPEBREAK for time-varying liquid releases from the long pipeline and TVDI/DISC for release from vessel/short pipelines, respectively time-varying and steady-state discharge model.
- The TNO consequence model EFFECTS incorporates the MORROW model for releases of liquefied gas from long pipelines.

The versions that allow to characterize this CO<sub>2</sub> behaviour are PHAST from version 6.6 on and EFFECTS 10. In detail, PHAST 6.6, with respect to older version 6.54, accounts for effects of solid formation downstream the orifice and the subsequent sublimation, therefore considering the solid transition for the post-expansion state in the discharge model as well as for the thermodynamic calculations by the dispersion model (UDM). For the dispersion equations, to characterize the mixing of solid/vapour CO<sub>2</sub> with air, the model always assumes the homogeneous equilibrium model without solid deposition (no rainout), i.e. snow-out of carbon dioxide.

This assumption is justified since for most scenarios the rainout is not expected to occur (or conservative predictions are given if rainout is ignored). Furthermore, PHAST 6.6 does not account for the effects of solid formation upstream of the release orifice, but it does apply appropriate warnings in case this should happen. The latter assumption is justified since for most scenarios the hazardous distance will be governed by the flow rate before the onset of solid effects upstream of the orifice [9].

To improve the understanding of the phenomena when CO<sub>2</sub> is released from dense/supercritical phase to atmospheric conditions, both DNV-GL and TNO have participated in several research programs such as CO2PipeTrans, CO2PipeHaz and COOLTRANS.

Models such as SLAB, DEGADIS and ALOHA require instead an external input, as they are not able to simulate this discharge phenomenon and to model the two-phase jet, they define an initial equivalent gas density of the entire CO<sub>2</sub> cloud (gas or solid), but always without considering the phenomenon of the sublimation of the solid particles of CO<sub>2</sub> into vapour, which will affect the density and temperature of the cloud. These models require more effort to achieve a fairly similar result, as they have to merge and interface the various modules.

Therefore, commercial packages such as PHAST from versions 6.6/6.7 onwards and EFFECTS 10 allow to simulate many types of source terms and the formation of solid CO<sub>2</sub> particles [15]. But it is necessary to consider that, for EFFECTS, no validation data have been reported so far, if compared with data available for PHAST or FRED model. Both have been compared with large-scale CO<sub>2</sub> release experiments resulting in a good performance. The disadvantage in using FRED is that having been designed to simulate the risks of hydrocarbons, it does not consider the solid particles, but rather the liquid-vapour line is considered up to ambient pressure, by treating the solid particles as liquid and obtaining however good results.

## 6.2.2 CFD MODELS

CFD models overcome many of the limitations of integral models but on the other hand, they are not suitable for carrying out wide-ranging and rapid project screening analysis.

CFD codes are based on the solution of mass, momentum and energy conservation equations (Navier-Stokes equations) to provide full 3D flow maps in an identified volume. Additional transport equations can be included to calculate the effects of turbulence, using the models for turbulence generation and dissipation as k- $\epsilon$  or k-l, and model the transport of different gas species (CO<sub>2</sub>, CH<sub>4</sub> etc.), pollutants or particulates. Calculated flows may be steady or transient, there are no limiting wind speeds, and momentum of releases and buoyancy are included explicitly. Physical obstructions such as buildings, structures and terrain which modify the flow and subsequent dispersion can be included in the models.

There are several disadvantages still to overcome with CFD:

- In comparison with integral models, CFD modelling is generally substantially more expensive and time-consuming.
- The use of CFD modelling requires significant specialized expertise.
- CFD solvers need separated calculation for equivalent source.
- The codes are general purpose and are not specialized to dispersion so that there is more work required by the analyst, setting up source terms and atmospheric profiles, etc.
- High sensitivity to user-selected input conditions.
- CFD solvers are not designed to deal with the atmospheric boundary layer so that the profiles typically change slowly through an empty terrain [9].

One of the major advantages of simulation with CFD models is that with these it is possible to explicitly represent scenarios with complex terrains, and meteorological conditions varying in space and time.

In the following, five CFD models are described [15]:

- **FLUENT** is a general-purpose CFD platform that can simulate the physics of dense gas releases and dispersion, as well as a wide variety of other physical phenomena. The model is not explicitly set up to simulate releases of dense gases. To simulate such a release requires extensive modeller effort and expertise to prepare the scenario. The modeller must set up the parameters of the source itself and set up an atmospheric parameterization scheme using user-defined functions. The modeller must build the 3D domain using computer-aided design (CAD) software and mesh the modelling domain into a grid of discrete fluid cells. The modeller must also make a set of decisions regarding the use of physical models, numerical solver schemes, and solver convergence criteria. FLUENT CFD software is distributed by ANSYS.
- **OpenFOAM** is an open-source CFD toolbox that contains an extensive set of modules to solve complex fluid flow problems. Since OpenFOAM is a general-purpose CFD model, it is not pre-configured to simulate the release, atmospheric transport and dispersion of dense gases, therefore an experienced modeller is necessary.
- **Fluidyn-PANACHE** is a commercial package of software modules for modelling atmospheric flows, developed by Fluidyn/Transoft in collaboration with the French Ministry and Environmental Agency. It is a self-contained, fully 3D CFD software package designed to simulate atmospheric flow and pollutant dispersion in complex environments, i.e. with topography, buildings, land covers and usages. Fluidyn-PANACHE has been designed for use by environmental or industrial safety engineers with limited knowledge in CFD simulation. It is claimed to be easy to use even if the topography is very complex, with a user-friendly GUI.
- The **FLACS** (FLame ACceleration Simulator) is a commercial CFD model, available from GexCon in Norway. FLACS was developed to simulate the dispersion of gas leaks and subsequent explosions in offshore oil and gas platforms. FLACS uses a distributed porosity approach for parameterizing buildings and other obstacles, which serves to significantly (by factors of 10 to 100) reduce the run time needed for the code.

- **ANSYS-CFX** software is a general-purpose commercial fluid dynamics program that has been applied to solve wide ranging fluid flow problems for over 20 years. The software is claimed to include an abundant choice of physical models to capture virtually any type of phenomena related to fluid flow. The flow solver and associated physical models are integrated with a user-friendly GUI, with extensive capabilities for customization and automation.

An overview of their features is presented in Table 13.

Model name	Producers	Available release profiles	Available source types	Multiphase release
<b>FLUENT</b>	ANSYS	C,I,T	User “builds” the source, model capable of representing any built source configuration.	Yes
<b>OpenFOAM</b>	OpenFOAM Foundation and OpenCFD Ltd			
<b>PANACHE</b>	Fluidyn/Transoft with the French Ministry and Environmental Agency.			
<b>FLACS</b>	GexCon			
<b>ANSYS-CFX</b>				

Table 13. Characteristics of CFD models.

### 6.2.2.1 CFD models for calculation of CO<sub>2</sub> source terms

Through a CFD model, it is possible to build very complicated source configurations, also having the possibility to create a 3D map of the source. Despite this, it remains a complex method and there is no generic model for its use, but each scenario is built specifically for the case being treated.

An example is that of the University College London (UCL) and the University of Leeds (COOLTRANS project), which have developed a model for the jet release of CO<sub>2</sub> and dispersion in the near-field, with the aim of predicting the speed and the dilution of the CO<sub>2</sub> flow that comes out of the ground resulting from the puncture [39] or rupture [38] of an underground pipeline. In the Wareing et al. [38] study the source term was represented by the rupture of a 96 km underground pipeline with a diameter of 0.61 m. In this simulation, the aim was to calculate the integrated mass and the fluxed momentum out of the crater. These in turn were used as a source for the second simulation of CO<sub>2</sub> dispersion in the far-field. In addition, sensitivity studies were carried out, varying the size of the fracture length to 24 m and 72 m, positioning the pipeline at a greater depth, with a shallower crater, with misaligned pipes, and a crater in sandy soil. The amount of CO<sub>2</sub> deposited in the crater was also estimated through a "particle tracking" algorithm. Figure 28 shows a representation obtained numerically of the trend of flow dispersing into dry air.

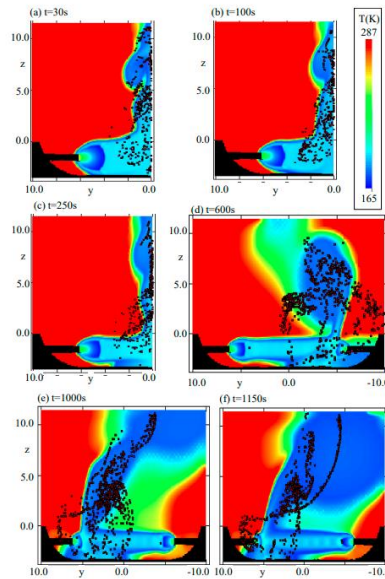


Figure 28. Snapshots with particles on vertical planes [38].

The last example reported here is that of Woolley et al. [53], in which CFD models have been used for the simulation of the near-field dispersion of a multi-phase CO<sub>2</sub> release, in low wind conditions. For this purpose, the system was modelled using a second-order upwind finite volume solution scheme and a k- $\epsilon$  model for turbulence. The properties of the gas phase were calculated with EoS by Peng-Robinson, those of the dense phase and the saturation pressure with EoS by Span and Wagner. Finally, an HRM was implemented to consider vapourization delay during decompression. After the source modelling process, the study focused on modelling the far-field dispersion using CFDs (FLACS and ANSYS-CFX). In this, both the deposition of particles and the interaction of these with the surrounding environment have been considered, while collisions between particles have been neglected. The CO<sub>2</sub> stream at the exit of the crater was considered as two-phase gas-solid, even managing to include the contribution of a realistic dispersion ground. The result led to a comparison between the two CFX and ANSYS models. With the first, the particles were assumed to be "small", 20  $\mu\text{m}$  in diameter, and the rain-out effect was completely absent, as they underwent complete sublimation. In the second, however, the particles were considered to be 300  $\mu\text{m}$  in diameter, the phenomenon of the creation of a dry ice bank due to the rain-out occurred. The integration of output from the near-field model as input for the far-field model, in order to obtain a higher level of accuracy, will also require some adjustment of the most relevant thermodynamic properties. The disadvantages of this approach are the high computational effort as well as the complexity of the thermodynamic calculations involved.

Finally, CO2PipeHaz has also developed an advanced version of PIPETECH to model CO<sub>2</sub> releases, with the aim of integrating it with CFDs to simulate CO<sub>2</sub> releases in complex environments. The recommendation is to use it in all points where there are high risks of ruptures and also to use simplified versions for initial identification of the critical parts, as these are faster to perform [15].

### 6.3 The numerical approach in modelling hazards related to the sublimating bank

In a scenario with the formation of a dry ice bank, the comparison between the incidence on carbon dioxide concentration of the pressurized jet and the carbon dioxide released from the dry ice bank leads to the conclusion that the incidence of the latter is minimal when the time horizon of the analysis is limited only to the time evolution of the release, as represented in the figure below.

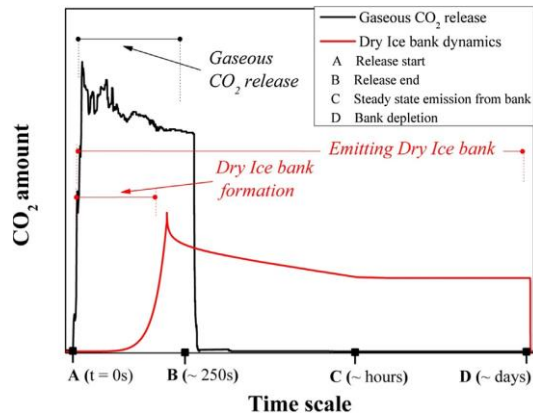


Figure 29. Pressurized CO<sub>2</sub> release and sublimating bank dynamics with a general time scale.

Mocellin et al. [59] modelled, with a CFD program, the atmospheric dispersion of carbon dioxide from a dry ice bank (in the case of a pressurized release, guillotine rupture, of CO<sub>2</sub> from a buried pipeline), studying the influence of atmospheric conditions and the presence of a high-speed pressurized jet.

Under Italian average weather conditions, the dispersion of carbon dioxide from dry ice bank generates volume fraction peaks of about 11 % v/v (1200 ppm) that are dangerous in case of prolonged stays near the sublimating bank.

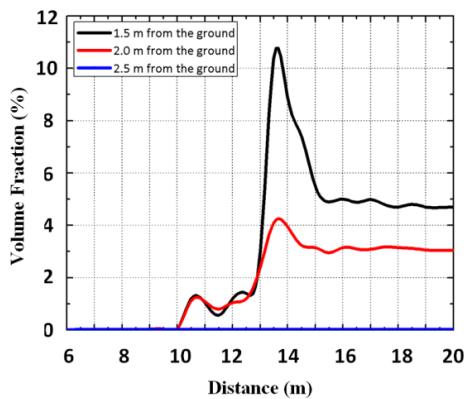


Figure 30. CO<sub>2</sub> volume fraction distribution in space at different heights from the ground with wind velocity equal to 2 m/s.

It must be highlighted that release from the guillotine rupture produces a mass release that lasts usually in a few minutes depending on the position of shut-off valves. On the contrary, the formation of a dry ice bank and its sublimation follow extremely slower dynamic mechanisms. So, when assessing CCS failure risks, the determination of events' timeline is of crucial importance. Considering this aspect, the sublimation from the bank becomes the predominant source of risk only when the pressurized release goes down and its effects last for hours and days. Unless special measures are taken, even a brief exposure may cause danger, especially to operators locally involved in recovery operations and maintenance.

In another work of Vianello et al. [60], three different predictive modelling approaches to consequences related to the sublimating bank have been tested. Starting from the most simplified approaches represented by algebraic and ODEs equations solved by ALOHA and PHAST to the more complicated and resource-demanding CFD approach, the latter gives the most detailed description of the system, especially near the hazard source. A comparison in the predicted results shows a certain degree of similarity among the different approaches. The order of magnitude of safety distances is conserved moving to different models except for the lateral dispersion that is not always comparable. The investigated simplified approaches are not able to describe phenomena near the sublimating bank, where detailed information should instead be available to face hazards.

On the contrary, the CFD modelling gives a full characterization of the CO<sub>2</sub> dispersion also showing the significant stratification that takes place as a result of the dense CO<sub>2</sub> gas behaviour. The computational burden is strictly linked to the degree of detail required and the CFD is thus the more demanding in this sense. So, while the CFD modelling provides better results with respect to the immediate surroundings, it requires longer setup and run times making it not compatible with a rapid response to an emergency.

Overall, these studies emphasize that the quantities of CO<sub>2</sub> released from the dry ice bank are in general much smaller than the quantities from a direct release of a pressurized jet.

## 6.4 Effects of impurities in CO<sub>2</sub> release modelling

Considering that liquid phase and in particular supercritical phase CO<sub>2</sub> is an efficient solvent, in CCS applications, and particularly during transport of CO<sub>2</sub> by pipeline, CO<sub>2</sub> streams will not be 100% pure CO<sub>2</sub>. Substances such as hydrogen sulphide (H<sub>2</sub>S), carbon monoxide (CO), sulfur dioxide (SO<sub>2</sub>), oxygen and other impurities may become mixed or in solution with the CO<sub>2</sub>. When there is a substantial reduction in pressure of liquid or supercritical CO<sub>2</sub>, for example during a leak, it will change state to gas-phase essentially losing its solvency capacity, thus liberating any chemicals which were previously held in suspension. It should thus be considered that the release of any hazardous substances during a release of CO<sub>2</sub> could pose a threat to humans or the surrounding environment [3].

Elshahomi et al. (2015) [32] simulated the two tests conducted to investigate the impact of impurities on phase change of CO<sub>2</sub> and the decompression wave speed in two shock tubes, to validate the CFD-FLUENT 14.5 integrating with an accurate GERG-2008 equation of state for CO<sub>2</sub> mixture.

The 2D CFD decompression model simulations were validated by comparison with the results of two different shock tube tests. The first test was implemented at the TransCanada pipeline test facility in Didsbury, Alberta, Canada, while the second test was conducted at GL Noble Denton's Spadeadam Test Site in Canada by National Grid. The CFD simulations were carried out for two mixtures: a binary mixture (CO<sub>2</sub> and CH<sub>4</sub>) and a five-component mixture (CO<sub>2</sub>, H<sub>2</sub>, N<sub>2</sub>, O<sub>2</sub>, CH<sub>4</sub>). The predicted results were found to be consistent with respect to the available experimental results, in fact, the CFD model successfully tracked the rapid pressure drop.

It was also indicated that the maximum influence on the decompression wave speed (changing the pressure plateau level) that could affect the fracture propagation requirements for CO<sub>2</sub> pipeline came from H<sub>2</sub> in comparisons with other impurities performed such as CO, O<sub>2</sub> and N<sub>2</sub>.

Liu et al. (2015) [61] has instead sensitively simulated a full-bore rupture of the CO<sub>2</sub> mixture pipeline. This study focused on the investigation of the effect of impurities in CO<sub>2</sub> release modelling. Binary CO<sub>2</sub> mixtures with various fractions of the following impurities, N<sub>2</sub>, O<sub>2</sub>, CH<sub>4</sub>, H<sub>2</sub> and Ar, were analyzed and the predicted source strength from full-bore rupture of pipelines carrying these binary mixtures was estimated for three values of the stagnation pressure (10 MPa, 15 MPa and 20 MPa) with the stagnation temperature equal to 20 °C for all cases.

To do such simulation, the integrated CFD model developed and validated by Elshahomi et al. (2015) [32] above was used to investigate the impact of impurities on the discharge rate.

The general trend is that a higher fraction of impurity yields a higher discharge rate and among the considered impurities the hydrogen gives the maximum impact. This is mainly because of the higher speed of sound with a higher fraction of impurity in the mixture.

In this study, particular attention was given also to the effect of hydrogen sulphide (H<sub>2</sub>S), the H<sub>2</sub>S may present a greater hazard than the CO<sub>2</sub> itself as it is a much more toxic substance than carbon dioxide.

The dispersion of a CO<sub>2</sub> mixture contained in a pipeline, with 9000 ppm of H<sub>2</sub>S, of the Weyburn Enhanced Oil Recovery (EOR) project in Saskatchewan, was therefore investigated. The threshold value of the fraction of

H<sub>2</sub>S was found to be 0.4%. If the fraction of H<sub>2</sub>S is less than 0.4% at the source, after rupture the 200 ppm H<sub>2</sub>S envelope will be contained within the 50,000 ppm CO<sub>2</sub> envelope, as explained in the figure below.

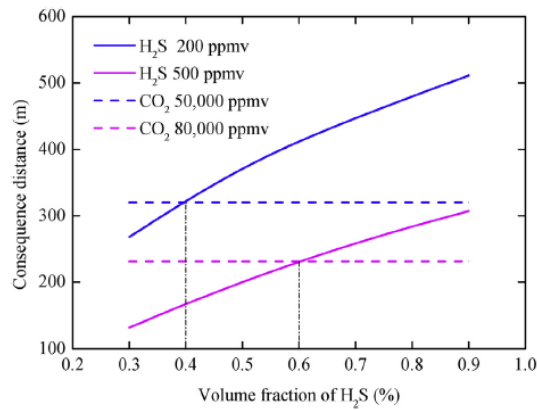


Figure 31. Impact distances for CO<sub>2</sub> and H<sub>2</sub>S for different H<sub>2</sub>S fractions.

But overall, the impact of the toxic impurities on the CO<sub>2</sub> mixture in CCS depressurization, release and dispersion was not enough experimentally investigated. Hence further laboratory- and large-scale experimental data are required to investigate and support validation of models predicting the impact of the toxic impurities on the CO<sub>2</sub> mixture release.

## 7 *CO<sub>2</sub> gas dispersion models validation*

For the validation of the dense gas models, far-field data were used in most cases, thus neglecting the source term and the near-field zone, but relatively few were performed directly on CO<sub>2</sub>. Considering both integral and CFD models, it is relevant that these are compared and validated, to identify the critical points in the case of CO<sub>2</sub> modelling. Generally, the validation of integral models has priority, as these are more commonly used in a risk assessment, but also the comparison with CFD models is important, for the simulation of more critical scenarios [18].

### 7.1 Scale-up issues with CO<sub>2</sub> experiments

In general, for many types of releases of hazardous substances, there are uncertainties in relation to the scale-up as many experimental data are usually obtained smaller than those of the “worst-case” accidental scenarios. We must then consider the issue of safety linked to the simulation of a full-scale “worst case” scenario, as it would involve having large quantities released. To get an idea, a full-bore rupture of a CO<sub>2</sub> pipeline with a diameter of 1 m, with shut-off valves positioned every 30 km, would release a quantity of CO<sub>2</sub> equal to 1000 tons, it is an experiment in fact which would not be approved by government authorities.

Among the most common examples of CO<sub>2</sub> experiments are the Kit Fox experiments, carried out to obtain data on dense gas dispersion in 1995. These experiments consist of 52 trials at the Nevada Test Site, where short-duration CO<sub>2</sub> gas releases were made at ground level over a rough surface during neutral to stable conditions and the terrain roughness is reproduced in the experimental field with the installations of rectangular sections of plywood to approximate the buildings and other obstacles at a chemical processing facility. Here CO<sub>2</sub> is released in small quantities at a rate of 1 to 4 kg/s from a 2.25 m<sup>2</sup> area source in the midst of many 2.4 m tall billboards, and it was regarded as a 1/10 scale simulation of HF releases in chemical processing plants, thus being a surrogate for two-phase HF cloud. Wind tunnels or water channels also use the same method but with a scaling distance of 1/100 or 1/200 and chemical surrogates to properly represent the density of the chemical of interest.

It has to be considered that in general the studies regarding the release and dispersion of CO<sub>2</sub> are limited. Recent large-scale studies include the one carried out by BP (British Petroleum) and Shell on dense phase CO<sub>2</sub> releases at Spadeadam. These data will help model validations, but they were of short duration, less than two minutes and with limited pressure and temperature conditions with a maximum diameter of 25 mm. When in reality the CCS CO<sub>2</sub> pipelines could be even larger than 610 mm and have an isolable inventory of tens of thousands of tons, so there is a need to understand and be able to model large and long-lasting releases. Therefore, the data obtained from these experimental campaigns are not sufficient, but further validation experiments are required to fill the scale-up knowledge gaps.

For model validation, it is necessary to assume that the basic principles of chemistry and physics apply across scales reasonably, such as the Richardson number, an important dimensionless parameter. Although some phenomena are not scaled well, such as the size and behaviour of solid particles that form during the flashing process, which can vary as the hole increases, the duration of the release, the initial tulip shape and the phase change that could occur in a vessel or connecting pipe. Even if not quite correct, for such cases the phenomena are simulated through small-medium releases that can be controlled and confined, then applying the scientific relationships obtained to realistic large-scale releases [15] [12].

### 7.2 Evaluation of models against experimental data

During the phenomenon of dispersion into the atmosphere, a gas is subjected to turbulence which adds randomness to this process. In order to consider this phenomenon, the estimation and accuracy of the modelling of the far-field dispersion are evaluated in statistical terms and not on a single experiment. This comparison,

therefore, involves evaluating temperatures and concentrations based on an average, variance and frequency of occurrence, rather than with the direct use of instantaneous values.

There are several sets of dispersion model evaluation against experimental data methodologies and software available. The use of maximum concentration for the model evaluation exercise is standard for evaluations of dispersion models and field experiments in open terrain.

The following equations define the statistical performance measures:

1. Fractional Mean Bias (FB):

$$FB = \frac{(\bar{C}_o - \bar{C}_p)}{0.5(\bar{C}_o + \bar{C}_p)}$$

2. Geometric mean bias (MG):

$$MG = \exp(\overline{\ln C_o} - \overline{\ln C_p})$$

3. Normalised mean square error (NMSE):

$$NMSE = \frac{\overline{(C_o - C_p)^2}}{\bar{C}_o \bar{C}_p}$$

4. Geometric variance (VG):

$$VG = \exp[\overline{(\ln C_o - \ln C_p)^2}]$$

5. FAC2 = fraction of data that satisfy  $0.5 \leq \frac{C_p}{C_o} \leq 2.0$

Where:

- $C_o$ : observation of concentration from an experiment (highest value recorded)
- $C_p$ : model predictions of concentration (highest value predicted)
- $\bar{C}$  : average over the dataset

A perfect model would have MG, VG and FAC2 = 1; FB and NMSE = 0. Because of the influence of random atmospheric processes these values are not attainable, and the minimum performance measures for a model to be defined as ‘‘acceptable’’, based on extensive experience with model evaluations, are as follows:

- The fraction of predictions within a factor of two from observations is about 50% (i.e., FAC2 > 0.5);
- the mean bias is within  $\pm 30\%$  of the mean ( $-0.3 < FB < 0.3$  or  $0.7 < MG < 1.3$ );
- the random scatter is about a factor of two of the mean (NMSE < 4 or VG < 1.6) [35].

### 7.3 Validation of models with CO<sub>2</sub> field study observations

During many experimental campaigns, view pictures of the release are recorded: it shall be noted that the visible cloud in a test site is not the carbon dioxide plume that appears in software results. The visible cloud during an accidental CO<sub>2</sub> release is the area in which air humidity condensates in small droplets that are suspended in the stream. Such condensation occurs because CO<sub>2</sub> expansion causes a sudden decrease of temperature, due to the positive and high Joule-Thomson coefficient of the substance [62]. The visible and simulated clouds are therefore not directly comparable, despite being related to each other and the presence of carbon dioxide.

The field-scale CO<sub>2</sub> release experiments that can be used to validate far-field dense gas dispersion models are of limited number. The most widely-used for model evaluations is the Kit Fox field experiment. Among these, a study compared HGSYSTEM predictions with the Kit Fox CO<sub>2</sub> arc-maximum data obtaining a mean relative bias of less than about 50 %. Also, Mazzoldi et al. [35] evaluated the Fluidyn PANACHE CFD model and ALOHA 5.4 performances with the Kit Fox data. In this study, it was found that the default k- $\epsilon$  turbulence model led to an under-prediction of the maximum arc-wise concentrations. They, therefore, used the k-l turbulence model for the Kit Fox tests in stable atmospheric conditions. The authors noted also that for CO<sub>2</sub>, the application of threat zones modelled with Gaussian methods like ALOHA to population densities was over-conservative. The use of Fluidyn PANACHE model was also demonstrated in simulated releases from a CO<sub>2</sub> pipeline, for both punctures [44] and full-bore rupture [45].

The McQuaid wind tunnel tests using CO<sub>2</sub> as a dense gas were carried out in three locations as part of the same study of the Kit Fox field experiments. Those data have been used to improve the vertical entrainment formulation used in many dense gas models (e.g. DEGADIS/HEGADAS).

The Kit Fox and McQuaid experiments all involved line or area sources and are not directly relevant to near-field modelling of two-phase jet releases associated with CO<sub>2</sub> pipeline ruptures.

Dixon et al. [48] compared the integral model FRED (that incorporates HGSYSTEM) with two CFD models (OpenFOAM and ANSYS-CFX) and experimental data. The horizontal releases tests conducted by Shell at Spadeadam (UK) test facility were considered (orifice diameter up to 25.4 mm). The concentration and plume width predicted from the FRED model produced a slightly better agreement with the data than both CFD models. Despite the prediction of solid particles, the FRED model overall reproduced well the hazard distances. Also, the simulations with OpenFOAM and CFX models for CO<sub>2</sub> dispersion, assuming homogeneous equilibrium between solid particles and the surrounding vapour, have provided reasonable agreement with small-scale experiments using the k- $\epsilon$  turbulence model.

Simulation results from the integral model PHAST and two different CFD models (ANSYS-CFX and FLACS) have been compared to data experiments conducted by INERIS [49]. The integral model PHAST adopted produced similar results to the ANSYS-CFX model, particularly the centreline temperatures were under-predicted by up to 20 °C, while an over-prediction of the centreline concentrations by up to 8% v/v has been registered.

OpenFOAM has been used to simulate dense gas dispersion and validated against wind tunnel data for both high and low turbulence conditions.

An OpenFOAM model of far-field CO<sub>2</sub> dispersion (CO<sub>2</sub>FOAM) was developed as part of the COOLTRANS project [63]. The model incorporated the homogeneous relaxation method for fully compressible two-phase flow, treatment of the transient atmospheric boundary conditions and time-varying inlet source conditions.

The model was validated against several experimental releases and the predictions showed “promising” agreement with the available experimental data. It is observed that in most cases, the predicted peak CO<sub>2</sub> concentrations were higher than the measured values.

Witlox et al. [66] performed a validation of the experimental data from CO2PIPETRANS JIP with the consequence-modelling package included in PHAST 6.7. The results from the tests performed by BP and Shell have been considered for high-pressure releases. A total of nine tests from BP and eight tests from Shell have been considered for the validation procedure. Several orifice diameters from 6.3 mm to 25.62 mm are reported for the validation; the minimum release duration of 40 s was registered for the biggest orifice (25.62 mm), while a maximum release duration >700 s for the 6.3 mm orifice diameter.

Different models available in PHAST have been used for the simulation of steady-state liquid release (DISC model), time-varying releases (TVDI model) both with the submodel ATEX (for atmospheric expansion) and the consequent dispersion (UDM model, with THRM module) as represented in Figure 32. To have a more precise concentrations prediction, conservation of momentum was considered for the expansion from the orifice to the equilibrium plane.

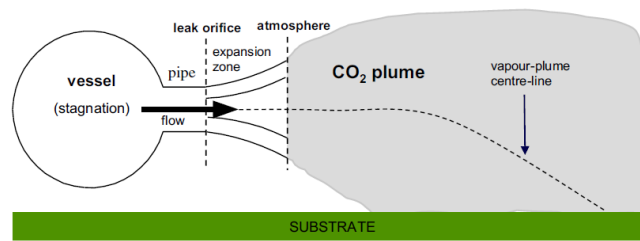


Figure 32. Discharge modelling (DISC/TVDI/ATEX) and dispersion modelling (UDM).

The global accuracy of PHAST in the near-field was not affected by wind direction deviation, while the far-field accuracy has been impacted. Compared to British Petrol (BP) data, in the near-field, the averaged concentration output from PHAST seems to match with good accuracy. A larger effect of averaging was observed downstream (at 20 m and 40 m) with more deviation compared to experimental data. Generally, the estimation provided by PHAST resulted conservative in terms of averaged concentrations. Shell experiments results were generally under-predicted by PHAST. However, better accuracy for the steady-state has been registered if compared with BP experimental data. For time-varying releases, the Peng-Robinson EoS produces the most accurate results, especially for the flow rate predictions since the equation provides accurate density values.

According to the results, the PHAST discharge and dispersion models predicted the release rates and concentrations accurately.

The EFFECTS model was used in some works like in [50] to estimate the dispersion from a CO<sub>2</sub> pipeline. EFFECTS models are sensitive to the initial pressure, temperature, composition and orifice size. Such a model seems well suited to modelling CO<sub>2</sub> releases, considering its ability to model CO<sub>2</sub> with its particular properties and the different models included. However, not many publicly available validation studies of this model have been found for CO<sub>2</sub> release

During CO2SafeArrest JIP, full-scale burst tests of the CO<sub>2</sub> pipeline were performed in 2017-2018. Xiong Liu et al. [55] described the numerical and experimental investigation of the dispersion of CO<sub>2</sub> in the atmosphere following its release after the burst tests. ANSYS Fluent was used for CFD simulation of the release, the species transport model was employed to predict the fraction of each species and the turbulence was modelled with the k- $\omega$  SST model. The authors highlight that the wind direction, as well as the pipe orientation, can affect the calculated consequence distance, especially for high-speed wind conditions. The major consequence distance (more than 1500 m) calculated for the 50,000 ppm envelope was reached from an 800 mm (ID) at a wind speed of 10 m/s [18].

As summary, the accuracy and validation of the integral and CFD modelling methods for the release and dispersion of pure CO<sub>2</sub> are presented in Table 14 and Table 15 below [5].

Model Name	Specifications	Stage	Accuracy	Validations
<b>HEGADAS</b>	HEGADAS 3.0 & 3+	Far-field release	Overall 0.92 of the model predictions were within a factor of two (FAC2) of observation.	Kit Fox
<b>DEGADIS</b>		N/A	N/A	Kit Fox
<b>SLAB</b>		N/A	N/A	Kit Fox
<b>HGSYSTEM</b>	HGSYSTEM	N/A	Little mean bias when evaluated with the full data set.	Kit Fox
	HGSYSTEM	N/A	N/A	McQuaid wind tunnel data
	FRED	N/A	N/A	COOLTRANS
	FRED	Near-field release	N/A	CO2PIPETRANS
	FRED	Far-field release	Plume widths were slightly better predicted by FRED than the two CFD codes.	CO2PIPETRANS
<b>ALOHA</b>	ALOHA 5.4	Far-field release	Overall 0.76 of the model predictions were within FAC2 of observation.	Kit Fox
<b>SAFER/TRACE</b>				Kit Fox
<b>GASTAR</b>			No validation information against CO <sub>2</sub> found.	
<b>PHAST</b>	PHAST	N/A	N/A	Kit Fox and McQuaid experimental datasets
	PHAST 6.7	Far-field release	Predicted concentrations from various far-field dispersion models were in reasonable agreement with the measurements within over-prediction of FAC2.	CO2PipeHaz
	PHAST 6.7 & 7.01 DISC-TVDI	Discharge rate	Discharge flow rate was accurately predicted using Phast PR EoS, instead of using Phast default EoS. The prediction of the Phast PR EoS was within about 10% compared to experiment. Concentrations were found to be predicted accurately (well within FAC2).	CO2PIPETRANS
	PHAST 6.7 & 7.01-UDM	Far-field release		
<b>EFFECTS</b>				Kit Fox

Table 14. Validation overview of integral models for modelling of the release and dispersion of CO<sub>2</sub> [5].

Model Name	Specifications	Stage	Accuracy	Validations
<b>FLACS</b>	FLACS	Far-field release	Overall 0.94 of the model predictions were within a factor of two (FAC2) of observation.	Kit Fox
	FLACS	Far-field release	Predicted concentrations from various far-field dispersion models were in reasonable agreement with the measurements within over-prediction of FAC2.	CO2PipeHaz
<b>CFX</b>	CFX	Far-field release	Had a good agreement with experiment.	BP project
	CFX 12.1	Far-field release	Overall 0.77 of the model predictions were within FAC2 of observations.	Kit Fox
	CFX 13.0	Far-field release	Had a good agreement with experiment.	CO2PIPETRANS
	CFX 14.0		Predicted concentrations from various far-field dispersion models were in reasonable agreement with the measurements within over-prediction of FAC2.	CO2PipeHaz
<b>PANACHE</b>	PANACHE 3.4.3	Near-field release	Overall 0.89 of the model predictions were within a factor of two (FAC2) of observation.	Kit Fox
<b>OPENFOAM</b>	OPENFOAM	Far-field Release	Had a good agreement with experiment.	CO2PIPETRANS
	OPENFOAM	Far-field release	Suitable for consequence modelling of the far-field dispersions of CO <sub>2</sub> releases in vertical and horizontal directions.	COOLTRANS
<b>FLUENT</b>	FLUENT 14.0	Near-field release Discharge rate	Accurately predicted the CO <sub>2</sub> droplet size distribution from point of release, as well as the size of solid particle formed from horizontal rapid expansion of liquid CO <sub>2</sub> through a nozzle.	RESS experiment
	FLUENT 14.0	Near-field release Far-field release	Discharge rates predicted by FLUENT had a good agreement with experiment. However, PHAST could predict slightly better discharge rate than FLUENT.	CO2PIPETRANS

Table 15. Validation overview of CFD models for modelling of the release and dispersion of CO<sub>2</sub> [5].

## 7.4 Meteorological conditions and terrain description

Usually, in a dispersion simulation, at least two weather categories shall be selected, based on the actual conditions of the area (e.g. wind rose and wind speed distribution) and representative of day and night conditions.

Commonly weather data to be used in consequence analysis can follow what reported below:

Condition	Ambient Temperature (°C)	Relative Humidity (%)	Solar radiation (kW/m <sup>2</sup> )	Wind Speed (m/s)
Day	Mean summer day value	Mean summer day value	Mean summer day value	5
Night	Mean winter night value	Mean winter night value	0	2

Table 16. Weather data [65].

Unless characterized data on weather conditions are available for the area being analyzed, Pasquill Stability Class D (neutral) should be chosen representative of day conditions (most probable) and Pasquill Stability Class F (stable) should be chosen representative of night conditions (conservative assumption) [65].

According to literature, meteorological conditions have an important influence on the risk of a release of CO<sub>2</sub>. The F2 (Pasquill stability class: F, wind speed: 2 m/s) conditions are considered the most problematic as the stable atmospheric conditions hinder dispersion and result in increased CO<sub>2</sub> concentrations further downwind. Instead, for vertical releases, the D stability class is worse than the F stability class due to “the complex interaction of stability class and elevated plumes”.

Mazzoldi et al. [44] considered the D5 and F2 weather classes for an approximately horizontal release in their study. They calculated the maximum downwind distances to the concentration limits (15,000 and 100,000 ppm) while varying weather class and release velocity (0 m/s vs. 49 m/s). The results show that the F2 weather class is the worst situation for the release without velocity and the D5 is the worst case for the release with velocity. Overall, the maximum distance from the pipeline to the 100,000 ppm contour was found for the release without velocity under F2 weather conditions.

Also, TetraTech [47] mentions D5 and F2 classes as the worst for horizontal releases, which could lead to the maximum concentrations reached. In a sensitivity study conducted by Koornneef [46], to analyze the uncertainties relating to the risk assessment for pipeline CO<sub>2</sub> releases, the impact of weather conditions on dispersion was also assessed, varying the speed of the wind and atmospheric stability classes. From the analysis, it was obtained that condition F2 represents the one for which the greatest distances are reached. Furthermore, it has been obtained that for vertical releases dangerous concentrations are reached only under stable and neutral atmospheric conditions, i.e., F2 and D5.

The dispersion of the cloud may not be predictable for winds of the order of 0.5-1 m/s, as due to gravity, it will be pushed downwards, moving more at ground level, with the risk of accumulating in areas of the low pressure or between topographical obstacles. In the CFD study [53], it was highlighted that the integration of the near- and far-field dispersion CFD models can predict the release and the subsequent dispersion of CO<sub>2</sub> under very low wind conditions (the wind speed may be set up to zero), which causes that CO<sub>2</sub> released will not disperse well and it may be trapped between obstacles. While most of the integral models (Phast, ALOHA, DEGADIS, etc.) cannot perform such conditions [5].

Furthermore, for dispersion calculations purposes, it is necessary to consider a simplified terrain description, most models use a “surface roughness length” as an input to the integral program. This value shall be selected depending on the actual surface type where dispersion will be assessed. Typical values are [65]:

Terrain description	Roughness (m)
Open sea, Fetch at least 5 km	0.0002
Mud flats, snow; no vegetation, no obstacles	0.005
Open flat terrain; grass, few isolated obstacles	0.03
Low crops; occasional large obstacles	0.10
High crops; scattered obstacles	0.25
Parkland, bushes; numerous obstacles	0.5
Regular large obstacle coverage (suburb, forest)	1.0

Table 17. Terrain description.

## 7.5 CO<sub>2</sub> release in complex terrain and weather

As already mentioned, PHAST, FRED and EFFECTS, as other integral models, are designed to simulate the dispersion of dense gas on flat terrain, unlike CFD models, with which more complex scenarios can be considered. Despite this, however, studies show that when the effects due to a non-flat ground around the source are considered, the consequence is a greater dispersion, therefore the risk area is reduced, because, considering the far-field, the influence of the topography on the dispersion of the cloud causes it to mix more quickly, both vertically and laterally. The result is that the consideration of flat terrain is a conservative assumption and represents a worst-case scenario, as announced by the chemical industries and regulatory agencies.

However, this assumption is not always verified, since, in the near-field, higher concentrations could occur locally in case of high surface roughness. Especially, in the case of small releases in low wind conditions, the plume of the cloud could fall downwards, dispersing between buildings, roads, inhabited centres, or stagnating between natural valleys or around hills. For large releases, on the other hand, the cloud will be very large compared to what is around it, travelling unhindered even in low-speed wind conditions.

The study of Liu B. et al. [52], carried out with ANSYS FLUENT simulations, was aimed at understanding the dispersion of the cloud on flat terrain with a hill and on a simplified model of an inhabited centre. The results led to two main conclusions: the CFD model underestimates the concentration of CO<sub>2</sub> in the near-field around the source, albeit slightly, but it simulates well the behaviour of the dispersion since for the case with hills the cloud has dispersed around it stagnating in the lower areas, while for the urban case most of the CO<sub>2</sub> was trapped in the streets downwind of the source with less significant lateral spread. In conclusion, the use of CFD models is preferred to a Gaussian method, as compared in [35], when it is fundamental the assessment of the risk in the cases mentioned, especially when they occur near vehicles, operators, inhabited centres.

In the study conducted in [15], it is explained how the Gaussian model and CFD differ mainly in their ability to consider complex terrain, buildings and complex weather conditions. Among the integral models, there is ALOHA, in which it is only possible to set a constant wind speed and a meteorological class uses a single wind speed and atmospheric stability class to represent meteorological conditions over an entire simulation, or SAFER/TRACE which can exploit spatial-varying wind fields. On the other hand, in the case of CFD models, there are no built-in atmospheric simulation systems, but the wind fields must be calculated using fundamental equations. Consequently, the accuracy is uncertain and the computational, time effort and the need for expert personnel also increase.

Table 18 shows all the comparisons previously made, divided by categories and their abilities to account for the range of source considerations, complex terrain, variable atmospheric conditions and complexity of inputs, as reported by Sherpa [15].

Model category	Model Name	Free?	Ability to represent a range of source configurations	Ability to account for obstacles and complex terrain	Ability to account for complex meteorology	Accounts for wind variability in space	Meteorological considerations	Complexity on inputs	Applied for CO <sub>2</sub> release
<b>Integral</b>	SLAB	Yes	Medium	No	Low	No	Uses P-G	Medium	Yes
	DEGADIS	Yes	Low	No	Low	No	Uses P-G	Medium to High	Yes
	HGSYSTEM	Yes	High	Low	Low	No	Uses P-G	Medium to High	Yes
	ALOHA	Yes	Low	No	Low	No	Uses P-G	Low	Yes
	SAFER/TRACE	No	High	No	Low	Limited	User may enter wind speed and P-G	Medium	Yes
	GASTAR	No	High	Medium	Medium	Limited	User may enter wind speed and P-G	Medium	No
	PHAST	No	High	No	Low	No	Uses P-G	Medium	Yes
	EFFECTS	No	High	No	Low	No	Uses P-G	Medium	Yes
<b>CFD</b>	FLUENT PANACHE FLACS ANSYS-CFX	No	High	High	High	Capable	Atmospheric simulation based on the solution of Navier-Stokes equations of motion, state, and thermodynamics	High	Yes
	OpenFOAM	Yes	High	High	High			High	Yes

Table 18. Applicability and calculation models for influences of terrain and weather conditions on the dispersion process and complexity of inputs [15].

## 8 *Analysis conclusions*

This report presents an overview of the current experimental and modelling methods for the depressurization, release, and dispersion of CO<sub>2</sub> from high-pressure pipelines. It was found that a large number of studies and published literature have examined such phenomena following the venting, puncture, or rupture of CO<sub>2</sub> pipelines/vessels. Many data have been analyzed from big projects to understand the release behaviours of high-pressure CO<sub>2</sub> and to validate the models developed for the assessment of safety distances of CO<sub>2</sub> pipelines. The following projects were identified: COOLTRANS, CO2PIPETRANS, CO2PipeHaz, COSHER, CO2SafeArrest, CO2Europipe, CO2RISKMAN, and CO2Quest. These data are necessary for the consequent validation of the discharge and dispersion models to give as much information as possible for the risk analysis to be carried out, especially, for high-pressure CO<sub>2</sub> pipelines, and more generally for CO<sub>2</sub> capture and storage systems (CCS).

Different release scenarios are possible, depending on whether the release is vented or accidental, major or minor, from a storage tank, a pipeline, or a valve, and from below or above ground.

All the models that allow the modelling of the depressurization of the pipeline, able to characterize the source term, have been summarized, and those that characterize the dispersion of a dense gas such as CO<sub>2</sub> were then analyzed, with particular attention to integral models and CFD models.

Major attention is given to the integral PHAST model, which is able to model the release phase until the expansion to atmospheric pressure and the dispersion of CO<sub>2</sub>, by employing the HE (Homogeneous Equilibrium) model, the Peng-Robinson and other equations of state. It gives good results compared to the experimental data from many projects. It is also highlighted that the Phast model, together with EFFECTS (but considering that no validation data have been reported so far), is the only integral models that can account for the impact of solid CO<sub>2</sub> particles on the release and dispersion of CO<sub>2</sub> since they consider the phenomenon of particles sublimation in the jet. Also, the integral model FRED has been analyzed and it was found to be among the most validated, together with Phast, for the release of CO<sub>2</sub> in dense gas, but does not consider the formation of solid particles in the jet.

The ability of dispersion models to account for complex terrain, variable atmospheric conditions and complexity of inputs was summarized as in the report analyzed by Sherpa.

It was found that the complex three-dimensional CFD models could accurately predict the CO<sub>2</sub> dispersion with the presence of complex terrain and variable meteorological conditions. However, one of the limitations of the CFD models is the long computational time which may be a few weeks for a single simulation, whereas the integral dispersion models need a shorter time to run the calculations. Overall, the CFD models are the best option when huge obstacles or major realistic terrain effects need to be addressed on the dispersion of CO<sub>2</sub>.

It was highlighted that the integration of the near-and far-field dispersion CFD models can predict the release and subsequent dispersion of CO<sub>2</sub> under low wind conditions (the wind speed may be set up to zero), which causes that the CO<sub>2</sub> released will not disperse well and it may be trapped between obstacles. While most integral dispersion models (Phast, ALOHA, FRED, etc.) cannot perform such conditions. Among the best CFD modelling programs with the presence of complex terrain or hills, there is the ANSYS software. On the other hand, the FLACS software with a Cartesian mesh reduces the number of cells required for far-field simulations, so it should be preferred in the event that an accurate description of the near-field behaviour is not required. Terrain effects may be predominant in CO<sub>2</sub> dispersion due to its high density, especially near depressions or large differences in heights in terrain near a pipeline, in such cases, CFD modelling programs should be preferred rather than integral models.

Even if it was stated that generally flat-terrain simulation can be considered as the “worst-case” scenario, because the topography tends to be dispersive causing enhanced vertical and lateral mixing, in the far-field, it can be regarded as conservative to ignore the buildings.

Also, the impact of impurities on the CO<sub>2</sub> depressurization was investigated and modelled against some small- and large-scale experiments. The depressurization tests of CO<sub>2</sub> containing impurities were conducted to

understand the impact of impurities on phase change of CO<sub>2</sub> and decompression wave speed in two shock tubes. It was found that a higher fraction of impurities in the CO<sub>2</sub> mixture can result in a higher discharge rate and that H<sub>2</sub>S may cause a larger hazard than CO<sub>2</sub> itself.

Further development and validation of models that predict the release and dispersion of CO<sub>2</sub> mixture are required to fully understand the design, operation, and safety of CO<sub>2</sub> pipelines.

## 9 Application to the Allam-cycle case study

In this study, an analysis of the consequences of the accidental release of CO<sub>2</sub> from an Allam-cycle system was carried out and the safety distances are calculated according to vulnerability thresholds. Phast software (produced by DNV GL), version 8.23, is used to modelling the consequences for the release of CO<sub>2</sub> in different phase states, vapour, dense, and supercritical, for all the considered scenarios. The aim of these simulations is to obtain the distribution of concentration and temperature for all the accidental scenarios, with some simplifying assumptions, to confirm that Phast is suitable for simulating CO<sub>2</sub> releases in the atmosphere.

Proper set-up for the software is obtained from the analysis of literature carried out in this thesis, specifically from the already mentioned reference work “Phast validation of discharge and atmospheric dispersion for pressurized carbon dioxide releases” [66] measurements from BP (British Petroleum) experiments and Shell experiments (CO2PIPETRANS), from the Eni project work on modelling of the risk associated with CCS technology [62], and from Phast technical documentation released with the software directly by DNV GL.

This study was divided into the following sub-chapters:

- Subchapter 9.1 Description of the Allam cycle, including the components and processes that characterize it, the fluids present and the respective thermodynamic conditions.
- Subchapter 9.2 Description of the settings adopted in the Phast simulation environment to conduct the analysis through the definition of all scenarios, including the definition of release and dispersion parameters, materials, and weather conditions.
- Subchapter 9.3 Definition of the objectives to be achieved through the analysis.
- Subchapter 9.4 Description of all the results obtained, specifically: analysis of the solid fraction, comparison between the effects due to low temperatures and CO<sub>2</sub> inhalation, identification of the most critical thermodynamic conditions, and comparison between the damage areas obtained from a release of CH<sub>4</sub> and CO<sub>2</sub>.
- Subchapter 9.5 Conclusions relating to the results obtained.

### 9.1 Description of the Allam-cycle

The oxyfuel combustion process with supercritical CO<sub>2</sub> (sCO<sub>2</sub>) as the working fluid, is one of the available carbon capture technologies that can be applied to both coal and gas-fired power plants.

Here oxygen is used in place of air for the combustion system, removing NO<sub>x</sub> emissions. In this way, it is needed cryogenic O<sub>2</sub> production, in the Air Separation Unit (ASU), with a consequent energy penalty. The Allam-Fetvedt cycle (hereafter, Allam cycle) includes this technology, where the high degree of heat recuperation and the high temperature/pressure operations are more than enough to compensate the load required by the ASU.

Therefore, the Allam cycle is an oxy-fuel thermodynamic power cycle that produces electricity and captures CO<sub>2</sub> for sequestration, with a schematic representation in Figure 33 below. It can be observed that this cycle operates with a single turbine that has an inlet pressure of 303 bar and a low-pressure ratio equal to 10. A pressurized natural gas reacts with a hot oxidant flow containing a mixture of CO<sub>2</sub> and nominally pure oxygen (coming from the co-located ASU) and with a hot CO<sub>2</sub> diluent recycle stream. The combustor operates at a pressure of 303 bar and the temperature of the exhaust stream is 1150 °C. This flue gas (that is a mixture of CO<sub>2</sub> and H<sub>2</sub>O) then is expanded through a turbine to approximately 30 bar with a temperature of 745 °C, driving an electrical power generator and the main auxiliaries. After the turbine, the exhaust flow enters a recuperating heat exchanger (Main Heat Exchanger, MHE) to transfer heat to both, the high-pressure CO<sub>2</sub> recycle stream (which is needed to moderate the turbine inlet temperature TIT, replacing the moderator effect brought by N<sub>2</sub> and also to cool down the turbine blade), and the oxidant flow, before mentioned.

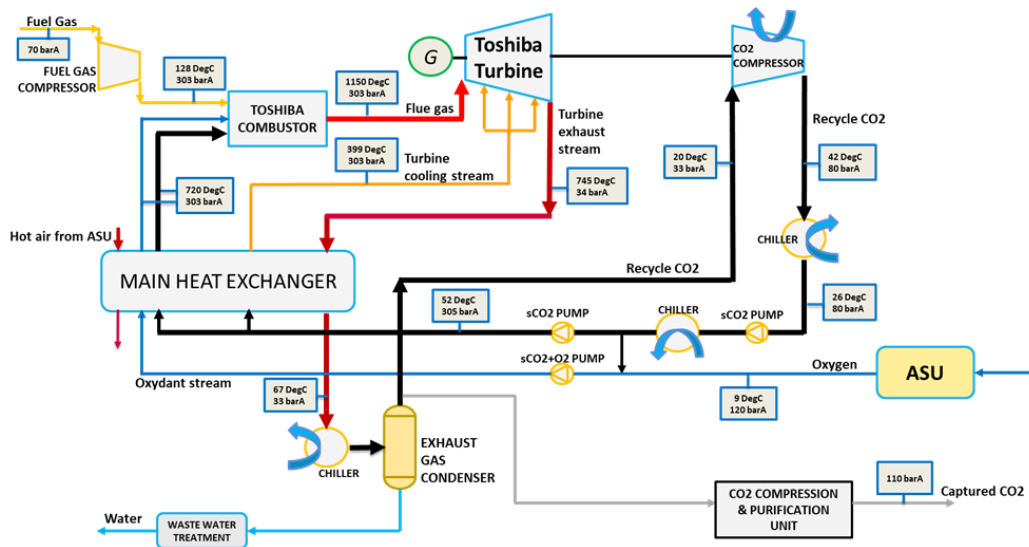


Figure 33. Natural gas-fueled Allam cycle.

After the MHE it is necessary to remove H<sub>2</sub>O from the turbine exhaust stream before it enters the compressors. The condensation of water begins in the last section of the Main Heat Exchanger and then it passes through the Turbine Exhaust Condenser. From there, the exhaust passes to a static mixer, where it is produced additional condensate and finally this two-phase stream (exhaust and condensate) enters the Turbine Exhaust Coalescing Water Separator. All the processes until mentioned and hereafter can be seen more specifically in Attachment A.

After the separator, to maintain mass balance within this semi-closed cycle, 5 % of the CO<sub>2</sub> recycle stream is exported, at a flow rate of 106276-108680 kg/h and 28.9 bar. Before leaving the system, the CO<sub>2</sub> flow enters the purification and compression unit, for abatement of H<sub>2</sub>O and O<sub>2</sub> obtainable in different ways, like molecular sieve drying, glycol drying, cupric drying, cupric oxide absorbing, autocatalytic combustion and auto liquefaction. Net CO<sub>2</sub> export from Allam Cycle after Coalescing Filters separation has a pressure of 110 bar and the following composition: 98.4 % of CO<sub>2</sub>, 0.13 % of H<sub>2</sub>O, 0.57 % of O<sub>2</sub>, and 0.90 % of Ar.

Returning to the Allam cycle, after the separator, the majority of the CO<sub>2</sub> flow is recirculated, and it is sent to the 3 stages intercooler compressor where it reaches the pressure of 80 bar and the temperature of 42 °C. After the compression, the flow is cooled, pumped to 305 bar and it feeds to the combustor via the recuperator heat exchanger. But before entering the main pump, a portion of the recycled CO<sub>2</sub> is mixed with oxygen to form an oxidant flow, which is pumped as well in a dedicated pump and fed separately to the heat exchanger and turbine. More specifically the CO<sub>2</sub> stream is split into three streams as described below:

- 59% of the main CO<sub>2</sub> flow is split again into two streams: the recycle stream to the combustor (48%) and the turbine blade cooling stream (11%), which is fed between the space of the inner casing and outer casing of the turbine to cool it and prevent the metal from reaching its metallurgical limits.
- The remaining part (41 %) is mixed with pure oxygen from Air Separation Unit resulting in an oxidant stream, which is then pumped in a separate pumping stage up to 305 bar and heated in.

Therefore, all these recycle flows enter the main process heat exchanger, reheating themselves against the hot turbine exhaust before returning to the combustor at temperatures exceeding 700 °C. But the only heat from the exhaust is insufficient because there is a very significant imbalance between the heat liberated by the low-pressure turbine exhaust and the heat required to raise the temperature of the high-pressure recycle stream. This imbalance is due to the very large difference in the specific heat of CO<sub>2</sub> in the 300 bar recycle stream

compared to the 30 bar turbine exhaust stream at the low-temperature end of the recuperating heat exchanger. To overcome this, the heat is given by the hot air stream in output from the ASU air compressors and the CO<sub>2</sub> recycle compressor.

Finally, it is needed to be specified that an open-loop evaporative cooling tower provides heat rejection from the process lube oil coolers, generator coolers, CO<sub>2</sub> recycle compressor intercooler, aftercooler, Air Separation Unit, and other loads [67] [68].

All the components of the cycle mentioned until now are shown in the plot plan top view of the system in Attachment B.

## 9.2 Settings of the Phast environment

In order to model the consequences of CO<sub>2</sub> release in this power cycle, it is necessary to set up the Phast environment. To conduct the simulation of a specific scenario, a sequence of steps is required to prepare the simulation environment and build all the accidental events. The steps for the environment setup are the following:

- Allam-cycle plant upload
- Materials definition
- Model definition
- Discharge and dispersion parameters
- Weather conditions

### 9.2.1 Allam-cycle plant upload

A .bmp file representing the Allam-cycle system (Attachment B), was used for the analysis. After loading the file through the "Map" tab, the plant will be visible in the "GIS Input" section, where it will be necessary to define the real scale of the plant, as shown in the bottom right angle of the plant image, giving a reference measure into the graph. The setting regarding the type of soil for dispersion was left with the default value for the "Land" type, instead, the setting regarding the type of building was not used in this simulation as only outdoor simulations were carried out for the calculation of the concentrations of interest.

### 9.2.2 Materials definition

The next step is to define, in the "Material" tab, which are the materials of the flows that pass through the cycle, whose release and subsequent dispersion must be modelled.

Once the material has been selected, it is then necessary to choose with which equation the thermodynamic properties of the treated substance are calculated. There are many equations of state used in the literature, but the most frequently used, because they combine their relative simplicity with their good degree of accuracy, are the cubic equations of state, namely Peng-Robinson (PR), Redlich-Kwong (RK) and Soave-Redlich-Kwong (SRK). In this simulation, the equation of state Phast MC, proposed by the software, has been chosen to model the substances [62], where the set of properties and methods are based on SRK EoS where applicable.

The materials that have been defined are presented below:

- Carbon Dioxide: it was considered as a pure component, as it represents 97.25% of the total recirculating mass. Furthermore, among the properties, it is necessary to set the flag “toxic substance”, because usually the software does not recognize it as such.
- Oxidant: a new component has been created as a mixture of CO<sub>2</sub> and O<sub>2</sub>, as described in sub-chapter 9.1, 41% of the main recycled CO<sub>2</sub> stream goes to mix with the O<sub>2</sub> stream before it enters the Main Heat Exchanger. The O<sub>2</sub> flux was also considered as a pure element, with a purity grade of 99.5%. To create the mixture, the respective molar fractions or mass fractions of the two substances must be entered into the software. In this case, the mass flow rates were taken into consideration, using for oxygen the flow rate equal to 159301 kg/h and for CO<sub>2</sub> the flow rate equal to 846617 kg/h. The last one was calculated by considering that, when the flow of CO<sub>2</sub> comes out of the separator, only 5% is exported from the plant, as mentioned in the description of the cycle, so the recycling flow rate is equal to the remaining 95%, with a flow rate of 2064001 kg/h. Anyway, it is necessary to consider that only 41% of it mixes with O<sub>2</sub> to form the oxidant flow, thus obtaining a CO<sub>2</sub> flow rate of 846617 kg/h.
- Exhaust: also in this case a new mixture has been created for the exhaust fumes that come out of the combustion chamber. It is a mixture consisting of 50% CO<sub>2</sub> and 50% H<sub>2</sub>O without other impurities, considering the purity of the CH<sub>4</sub> fuel used.
- Methane: it was considered as a pure component.

### 9.2.3 Models definition

After having defined the substances to be modelled in this analysis, which constitutes the Allam-cycle, it is possible to proceed with the definition of all the scenarios. Within the “Study” section of the “Models” tab, it is possible to specify which cases are taken into consideration, choosing between “Pressure vessel”, “Atmospheric storage tank”, “Standalones”, “Long pipeline”, and “Warehouse”. For this study only “Pressure vessel” release models were considered. After the model has been selected, the software asks to place it on the map, representing it as a “dot”, therefore all the dots were placed at the inlet/outlet of the relative component in the plant. For each of these scenarios, the following parameters have been set:

- operating conditions of “temperature” and “pressure” of the stream;
- “material” inside the vessel;
- “material to track” only if it is selected a mixture for the “material” field, specifying the CO<sub>2</sub>, whose concentration will be tracked in the dispersion calculations;
- “mass” equal to 1000 kg, ideally considered infinite;
- representative modelling of the mixture, choosing the default “PC Modelling”.

The Pseudo Component approach for modelling mixtures is chosen to model the mixture streams, as it is the approach to be used to model mixtures that contain CO<sub>2</sub>. In this way, the thermodynamic behaviour and the properties of a mixture resemble that of a pure component assuming that the composition of the mixture does not change during the different stages of the discharge and dispersion modelling and whose properties are calculated using simple averaging equations.

The other option implemented in the last Phast versions is the MC multi-component modelling releases of mixtures, which is based on the more rigorous calculation of mixture properties and phase equilibria. For the treated cases, using CO<sub>2</sub> as a substance in the mixture, the MC model cannot be applied, giving the following warning: “Solid formation is likely at 0 m, but not handled. Results will be inaccurate, and case may fail due

to convergence or thermodynamic problems. For modelling CO<sub>2</sub> cases is it recommended you use the PC Vessel/Pipe model”.

Therefore in this simulations are inserted all the entry and exit points of the components, summarized in Table 19 below, extracting the thermodynamic properties, pressure and temperature, from Figure 33 and the names of the components from the Attachments A and B. Particular attention must be given to the conditions of exit of the exhaust gases from the combustor CGT-100, specifically at a temperature of 1150 °C. It was not possible to insert this value in the software as it has a limit regarding the maximum temperature it can model, equal to 926.85 °C. For this reason, the maximum possible value has been entered.

Stream	Component name	Temperature (°C)	Pressure (bar)	Phase
Inlet CO <sub>2</sub> compressor	<b>(C-200)</b>	20	33	Gaseous
Outlet CO <sub>2</sub> compressor	<b>(C-200)</b>	42	80	Supercritical
Inlet CO <sub>2</sub> aftercooler	<b>(E-201)</b>	42	80	Supercritical
Outlet CO <sub>2</sub> aftercooler	<b>(E-201)</b>	26	80	Dense
Inlet CO <sub>2</sub> pump	<b>(P-400)</b>	26	80	Dense
Outlet recycle CO <sub>2</sub> pump	<b>(P-200)</b>	52	305	Supercritical
Inlet recycle CO <sub>2</sub> HEX	<b>(E-103R)</b>	52	305	Supercritical
Outlet recycle CO <sub>2</sub> HEX	<b>(E-101C)</b>	720	303	Supercritical
Outlet turbine cooling CO <sub>2</sub> HEX	<b>(E-102R)</b>	399	303	Supercritical
Inlet turbine cooling CO <sub>2</sub> turbine	<b>(CGT-100)</b>	399	303	Supercritical
Outlet CO <sub>2</sub> separator	<b>(FT-100)</b>	20	33	Gaseous
Inlet CO <sub>2</sub> combustor	<b>(CGT-100)</b>	720	303	Supercritical
Inlet oxidant combustor	<b>(CGT-100)</b>	720	303	Supercritical
Outlet exhaust combustor	<b>(CGT-100)</b>	926.85	303	Supercritical
Outlet exhaust turbine	<b>(CGT-100)</b>	745	34	Gaseous
Inlet exhaust HEX	<b>(T-102)</b>	745	34	Gaseous
Outlet exhaust HEX	<b>(T-103)</b>	67	33	Gaseous
Export CO <sub>2</sub>	<b>(T-100A)</b>	32	110	Supercritical
Outlet CH <sub>4</sub> compressor	<b>(C-001)</b>	128	303	Gaseous

Table 19. Thermodynamic properties of the Allam-cycle streams.

For each point of interest, it is then possible to choose between different types of release scenarios. Specifically, between “catastrophic rupture”, “leak”, “fixed duration release”, “short pipe”, “time-varying leak”, “time-varying short pipe release”, “user-defined source”. For this study, the steady-state leak scenario from a pressurized vessel is adopted. Simulations were performed with orifices of predetermined diameter, respectively of:

- Small release: 7 mm (from 1 mm to 10 mm)
- Medium release: 22 mm (from 10 to 50 mm)
- Large release: 70 mm (from 50 to 150 mm)
- Full bore rupture: 150 mm (>150 mm)

The hole diameters were chosen to represent the various failure classes.

For each "Leak" it is important to consider the height of the release point from the ground and the direction of the release. To ensure that all cases with the worst consequences are considered, a release point height of 2 m was set, very similar to the height of a standing person, as a conservative assumption. For each release, it is also possible to choose between different directions, including “horizontal”, “vertical”, “angled from horizontal”, “down-impinging from the ground”, “horizontal impingement” and “angled from horizontal

impingement". For all the simulations, two release directions were chosen "horizontal" and "horizontal with impingement", since, in the analysis of the consequences, they are the directions that give the greatest damage areas, or the greatest distances reached, for certain concentrations of interest. In the case of "horizontal impingement", where the impingement with the equipment is considered, the condition leads to longer dispersion distances than the others, as it is characterized by a lower release momentum and therefore by lower entrainment with the surrounding air and a subsequent hindered dispersion.

### 9.2.3.1 Equipment leak frequencies

In this case study, it was then necessary to associate the equipment leak frequencies with the analysis of the consequences, to calculate the risk considering both the physical effects and the probability that such events occur, depending on the hole class, for each component. Although in a quantitative risk analysis it is necessary to calculate all the frequencies associated with the sequences representing the accidental scenarios, starting from the initiating event.

The values of the leak frequencies were taken from IOGP Process Release Frequencies, Risk Assessment Data Directory [69]. This datasheet presents frequencies of releases from many processes equipment types that are intended to be applied to process equipment on the topsides of offshore installations and onshore facilities handling hydrocarbons, but they apply also to other substances releases.

In this version all sets of data are given as a single category, that is the combination of the full releases (when the flow is through the defined hole beginning at the normal operating pressure and continuing until controlled by emergency shut-down and blowdown or inventory exhaustion) and the limited releases (when the system pressure is not zero, but the quantity released is much less than from a full release, this may be because the release is isolated locally by human intervention or by a limit in the flow from the system inventory).

The values in this database are based on the analysis of the UK HSE's Hydrocarbon Release Database (HCRD), from October 1992 until March 2006. In this version, data have also been uploaded up to December 2015.

For this study, it was chosen to take the data of the failure frequencies, relating to the entire period 1992-2015, for each class of hole and each component.

Component name	Component code	Failure frequency for each Hole diameter [ $y^{-1}$ ]			
		7 mm	22 mm	70 mm	150 mm
Centrifugal compressor	C200	1.6E-03	7.2E-04	1.6E-04	1.1E-04
Centrifugal compressor	C001	1.6E-03	7.2E-04	1.6E-04	1.1E-04
Shell&tube aftercooler Heat exchanger - tube side	E201	2.9E-04	1.8E-04	6.1E-05	7.7E-05
Shell&tube heat exchanger - shell side	T102, T103	6.0E-04	3.0E-04	7.4E-05	6.1E-05
Centrifugal pump	P400	1.4E-03	3.0E-04	3.0E-05	8.9E-06
Centrifugal pump	P200	1.4E-03	3.0E-04	3.0E-05	8.9E-06
Shell&tube heat exchanger tube side	E103R, E101C, E102R, E101D	2.9E-04	1.8E-04	6.1E-05	7.7E-05
Combustor and turbine	CGT100	2.4E-03	7.9E-04	1.3E-04	2.1E-04
Process (pressure) vessel separator	FT100	2.6E-04	1.4E-04	3.8E-05	3.6E-05

Table 20. Failure frequencies for each hole diameter and component of the Allam-cycle.

## 9.2.4 Discharge and dispersion parameters

Once all the scenarios have been set, the parameters regarding the release and the consequent dispersion must be defined, and it is possible to do this through the "Parameters" section of Phast.

Considering the CO<sub>2</sub> flow pressures present in the Allam cycle, the critical ratio, between the pressure inside the storage and the atmospheric pressure, is always exceeded, as it is equal to 1.83. For this reason, in the case of tank leaks, the phenomenon known as "choked-flow" can be observed. This means that considering an isentropic expansion from the storage conditions to the conditions on the exit orifice, the speed of the CO<sub>2</sub> jet reaches that of the sound on the plane of the hole and therefore also the maximum flow rate (critical flow). The term "choked" derives from the fact that, even if the downstream pressure decreases, it is not possible to accelerate the flow even more.

In Phast for stationary releases, this phenomenon is modelled through the DISC (Discharge) model. Subsequently, the under-expanded jet expands and reaches the ambient pressure, at a plane called the "equilibrium plane". This phenomenon in Phast instead is modelled through the ATEX (Atmospheric Expansion) model. From here on, the entrainment with the surrounding air is considered, which favours the dispersion. For the atmospheric expansion of continuous releases, in the "Discharge parameters" section, several methods are available, including:

- "Closest to initial conditions", in which the program considers an isentropic expansion and conservation of the moment, taking as results those that give the smallest change in conditions during the expansion.
- "Conservation of momentum".
- "DNV GL recommended", which can switch between the two previous models, using the conservation of the moment method, for situations in which the rain-out does not occur, and closest to initial conditions method, for the other situations.

Considering the CO<sub>2</sub>, as already explained in the previous chapters, Phast is not able to model the rain-out phenomenon, that is the fall of solid particles on the ground which can constitute a new source of dispersion. Therefore, for the analysis, the complete sublimation of the solid particles in the jet is considered, and the method chosen to model this expansion phenomenon is the "conservation of momentum".

This model can be described as follows: for a two-phase flow, a homogeneous equilibrium between the phases is assumed, that is thermal and mechanical equilibrium, for which the maximum velocity at the equilibrium plane is bound to the vapour sound velocity. These equilibrium conditions, therefore, serve to set the source term for the consequent modelling of the dispersion. By indicating the exit plane of the hole as "f" and the equilibrium plane as "e", the problem is solved using the following equations:

$$m_f = m_0$$
$$m_f u_f = m_0 u_0 + (P_0 - P_f) A_0$$
$$m_f \left[ h_f + \frac{u_f^2}{2} \right] = m_0 \left[ h_0 + \frac{u_0^2}{2} \right]$$

where  $m_f$  and  $m_0$  are the mass flow rates (kg/s),  $u_f$  and  $u_0$  are velocities (m/s),  $A_0$  is the hole area (m<sup>2</sup>),  $h_f$  and  $h_0$  are the specific enthalpies (J/kg),  $P_0$  and  $P_f$  are pressures (Pa).

Another option enabled in the "Discharge parameters" section was the "Allow phase change (equilibrium) upstream of the orifice". This option describes how to treat flashing or condensation upstream of the orifice. With this option enabled, at the exit plane, the liquid/solid fraction is calculated assuming a homogeneous equilibrium, which means that is at the same temperature of the stream and that droplets or solid particles are transported with the same velocity of the main stream. The Phast software is not able to model the presence of

solid particles before exiting the hole, especially in the case of a pipeline, but with this option enabled, a warning will be shown if there are any.

In the "Dispersion parameters" section, on the other hand, the parameters concerning the behaviour of the cloud are set, after the expansion at ambient pressure has taken place, with different models for the first stages of the near-field release, where the turbulence is quite high, and for far-field release, where entrainment with air is dominated by atmospheric turbulence. These phenomena are described in Phast through the UDM model (Unified Dispersion Model) with the THRM (Thermodynamic Module), to include the thermodynamic logic for mixing of air with the pollutant. The THRM has been updated to include the modelling of the solid effects of CO<sub>2</sub> and in this case, the no rain-out of the particles is assumed, setting the "Droplet evaporation thermodynamics model" option has been set to "No rain-out, equilibrium". All the other parameters in the "Dispersion" section have been left by default.

Instead, from the "General parameters" section, it is possible to access the setting of the maximum release duration and the height of interest, which have been set to 3600 s and 2 m respectively (equal to the height of the release hole, useful for the representation of the clouds concentrations of interest).

### 9.2.5 Weather conditions

Phast software allows describing wind profile, terrain, and atmospheric conditions. In this study, the atmospheric conditions of the site were taken from the project [67] and are equal to:

- Air temperature = 21.89 °C
- Relative humidity = 64 %

These conditions are applied to the chosen weather Pasquill Stability classes D5 and F2, which represent:

- F, stable - night with moderate clouds and light/moderate wind
- D, neutral - little sun and high wind or overcast/windy night

as commonly adopted for risk assessment analysis. In Phast, the wind speeds of 5 m/s and 2 m/s are considered constant during the simulation.

## 9.3 Study objectives

In this study, an analysis of the consequences and vulnerabilities related to the release of CO<sub>2</sub> was carried out and applied to the Allam cycle, to confirm that the Phast software is suitable for modelling CO<sub>2</sub> releases, collecting data for risk assessment in the Carbon Capture and Sequestration sector.

One objective was the evaluation of the solid fraction on the equilibrium plane, in order to understand how it influences the dispersion of the toxic substance in the atmosphere, with the respective distances and temperatures reached. Initially, taking into consideration the thermodynamic condition that determines the higher formation of the solid fraction of CO<sub>2</sub>, a sensitivity analysis was carried out by varying the diameter of the release hole, thus obtaining the trends of solid fraction, temperature, the height of the centreline, concentration in the function of the downwind distance, in order to detect with which hole the most critical situation is reached. Subsequently, once the diameter of the hole was determined, all the conditions in which the solid fraction is present at ambient pressure were compared and the appropriate evaluations were obtained.

Furthermore, another objective of the analysis was to detect the most critical component, or rather the most critical thermodynamic release conditions, for which the maximum safety distances are reached at certain concentrations, and also associated with the relative leak frequencies for each component.

For this analysis, the data obtained from the simulations for the hole at 22 mm were taken, for both weather conditions and horizontal release, with and without impingement. The 22 mm hole was chosen as it represents an intermediate scenario since as the hole increases, the release rate increases as well and the consequent minimum safety distance is reached, while at the same time the failure frequency decreases. These distances were obtained by taking the maximum values from the graph of the Max Footprint, corresponding to the centreline, at the respective concentrations of interest. The Max Footprint graph shows the shape of the contours of the maximum concentration reached during the dispersion, for up to four concentrations inside the cloud, measured at a given height and calculated using a given averaging time. In this case, for CO<sub>2</sub> toxic material, the averaging time has been set in the dispersion parameter section equal to 600s.

The choice of the concentrations to be considered and the respective exposure time was made with the aim of obtaining the damage area according to the IDLH (Immediately Dangerous to Life Or Health) value, a concentration equal to 4% which if inhaled for more than 30 minutes can lead to fainting, and to the probability of death equal to 1% of fatality and 50% fatality, using the UK HSE SLOT (Specified Level of Toxicity) and SLOD (Significant Likelihood of Death) curves with concentrations of 8% and 11% [3]. To reach these fatality thresholds, different exposure times were considered, and the corresponding safety distances are calculated. The main thresholds are summarized in the table below.

	<b>IDLH</b>	<b>1 % fatality</b>	<b>50 % fatality</b>	
Concentration of CO <sub>2</sub>	4 %	8 %	10 %	11 %
Equivalent in ppm	40000	80000	10000	110000
Duration of exposure [min]	30	5	10	5

Table 21. Thresholds for the concentration of CO<sub>2</sub>.

In addition, the safety distances were compared to have 1% and 50% fatality, with the same exposure time, caused by both low-temperature exposures at -26 °C, -34 °C, and -40 °C, and inhalation of the toxic CO<sub>2</sub> substance, respectively at a concentration of 8%, 10% and 11%. Below are the critical temperature values for 1% and 50% fatality with the respective times of exposure [70].

	<b>1 % fatality</b>		<b>50 % fatality</b>	
Temperature [°C]	- 26	- 40	- 34	
Duration of exposure [min]	5	10	5	

Table 22. Fatality thresholds for the temperature of CO<sub>2</sub>.

Finally, once the most critical component has been determined, a further comparison was made between the releases of CO<sub>2</sub> and those of CH<sub>4</sub>. Also, for the release of CH<sub>4</sub> the various diameters of the holes, the directions of the release and the meteorological conditions were considered. The safety distances for methane were obtained in relation to the fatality criteria for thermal radiation, considering both the damage area obtained with the Jet Fire and with the Fireball, as they are the quantities that are usually used for methane risk analysis. The downwind distances obtained by the simulation were compared with those of toxic effects of CO<sub>2</sub> (11% and 5 min), at almost the same exposure time [71].

	<b>50 % fatality</b>
Thermal radiation [kWm <sup>-2</sup> ]	4.0
Duration of exposure [min]	4

Table 23. Fatality thresholds for CH<sub>4</sub> Thermal Radiation.

## 9.4 Results

Before examining the results obtained from the simulations, it is necessary to underline that, starting from version 8 of Phast, a more rigorous method has been introduced, capable of producing smooth, consistent, and time-dependent dispersion profiles. This method is called Along Wind Diffusion (AWD), in which core dispersion calculations are obtained through “release observers”, rather than through “release segments”, where an observer can be imagined as a "particle-sized sensor" being released to the centreline of the cloud at a given time and is then carried along with it. This method was subjected to an extensive validation which included both the comparison of the results with the analytical solutions and with the large-scale experiments, obtaining excellent agreement. Among the benefits of this method there are generally low concentrations in the medium- and far-field, obtaining a more realistic dispersion in the far- and near-field [72].

In the analysis of the results given by Phast, however, it is necessary to differentiate between those before Along Wind Diffusion and post Along Wind Diffusion. Specifically, all the dispersion table results present in the “Report” section of the software, including for example c/line vapour temperature, c/line cloud density, c/line concentration etc., are original results data before-AWD. Instead, the post-AWD results can be taken directly from the graphs that can be obtained during the simulations, including maximum concentration vs downwind distance, concentration vs time, footprint, max footprint and side view graph.

### 9.4.1 Analysis of CO<sub>2</sub> solid fraction

For each simulation carried out, the respective reports can be obtained, regarding both the discharge and dispersion results (pre-AWD). Among the discharge results the data are subdivided between:

- Orifice exit data (before atmospheric expansion): pressure, temperature, solid/liquid mass fraction, discharge coefficient, the velocity at vena contracta;
- Equilibrium plane data (after atmospheric expansion): solid/liquid mass fraction, droplet diameter, expanded diameter, and velocity.

Considering all the thermodynamic conditions containing CO<sub>2</sub> in the flow, the table below shows those for which a percentage of solid fraction was detected on the equilibrium plane, where the equilibrium expansion, therefore, generates jet conditions at the sublimation point of 1 bar and -78.5 °C, such as to create a mixture of vapour and solid. In all other conditions, however, with the stagnation temperature much higher than the critical temperature of 31 °C of CO<sub>2</sub>, during the expansion they will give conditions of pure vapour on the equilibrium plane.

Component name	T [°C]	P [bar]	Mass flow rate [kg/s]	Orifice plane Liquid Fraction	Equilibrium plane Solid Fraction
Inlet CO <sub>2</sub> compressor C200 Outlet CO <sub>2</sub> separator FT100	20	33	167	1.30E-07	0.06
Outlet CO <sub>2</sub> compressor C200 Inlet CO <sub>2</sub> aftercooler E201	42	80	463	1.50E-01	0.12
Inlet CO <sub>2</sub> pump P400 Outlet CO <sub>2</sub> aftercooler E201	26	80	942	1	0.28
Outlet CO <sub>2</sub> recycle pump P200A Inlet recycle CO <sub>2</sub> HEX E103R	52	305	2262	1	0.30
Outlet Exhaust HEX T103	67	33	137	0	0.03
CO <sub>2</sub> Export	32	110	1243	1	0.28

Table 24. Phast solid fraction predictions with 150 mm orifice diameter.

Among these conditions, the one with the greatest post-expansion solid fraction was chosen, i.e. the case of the CO<sub>2</sub> flow output conditions from the P200A pump and the entry to the Main Heat Exchanger E103R, to carry out a sensitivity analysis of the properties of the cloud centreline following:

- C/Line vapour temperature
- C/Line solid fraction
- C/Line concentration
- C/Line height

These were analyzed as a function of the Downwind Distance, varying the size of the hole from 7 mm to 150 mm and choosing as the release scenario "Horizontal Impingement" with weather conditions "F2". These trends are shown in the graphs below and are based on the data taken from the dispersion report, before along wind diffusion.

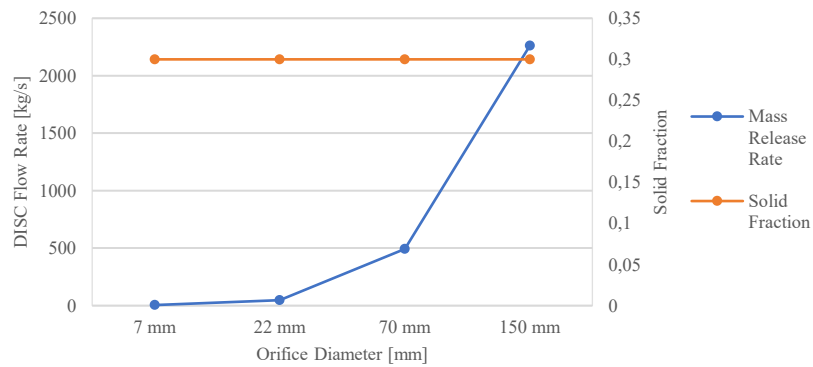


Figure 34. CO<sub>2</sub> solid fraction and DISC flow rate.

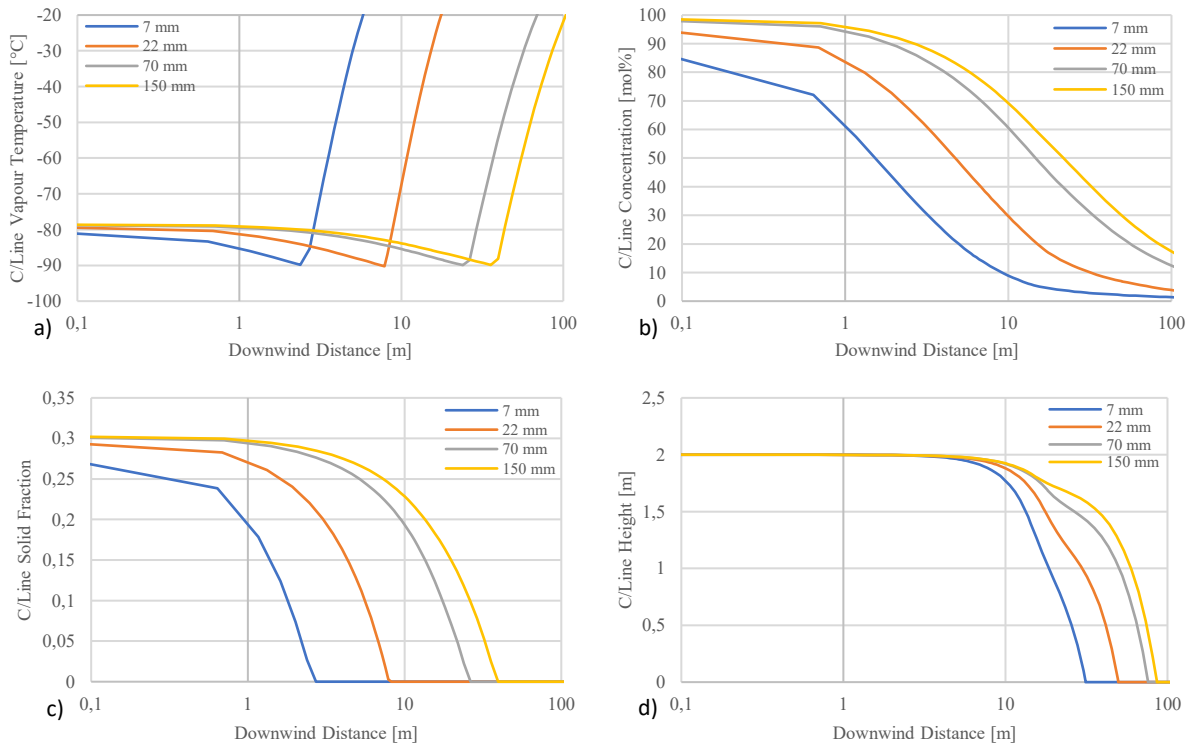


Figure 35. Dispersion predictions with hole size variation.

From these graphs it can be deduced that as the hole size increases, the release rate obviously also increases, and instead for all the holes the solid fraction remains constant. This results in a greater quantity of solid particles which sublimate less quickly and with a consequent greater cooling of the cloud. In fact, the low temperatures for the 150 mm hole reach greater distances than in the other cases. In addition, as the hole increases (release rate), the centre/line peak concentration also increases.

From the graphs of the solid fraction vs distance (Figure 35,c) and centreline height vs distance (Figure 35,d), it can also be observed that for all the holes, the distance at which all the particles sublimate (solid fraction equal to zero) is upwind with respect to the distance at which the centre/line height touches the ground. This means that Phast's limit of not considering rain-out cases, for this study, does not imply a conservative assumption leading to an over-prediction.

From the previous considerations, the 150 mm hole was then chosen to make a comparison between the components in Table 24, with the different solid fraction values. The trends of the cloud centreline parameters were obtained from the Phast report section, with the addition of the C/Line Cloud Density.

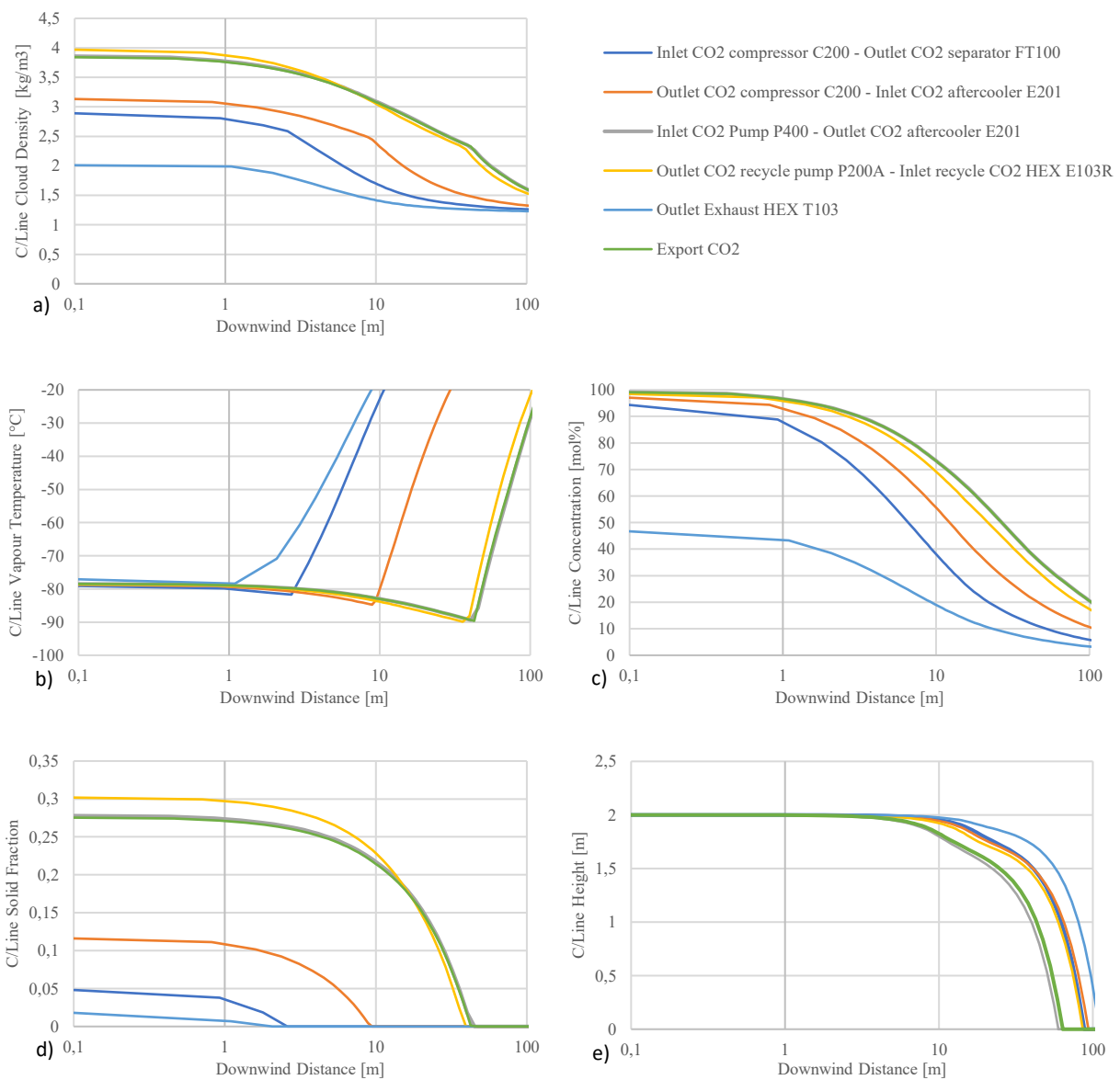


Figure 36. Dispersion prediction with the variation of thermodynamic conditions.

From Figure 36 it can be noted that with the increase of the solid fraction there is a corresponding increase in the distances reached by low temperatures, with a CO<sub>2</sub> cloud that reaches greater distances downwind, due to the effects of buoyancy. In fact, the density of the cloud is greater for the components that have a greater solid fraction on the equilibrium plane, and it can also be seen that the cloud reaches the ground earlier than in the other cases as it is heavier.

In all the cases reported, even for the components with the largest solid fraction, the CO<sub>2</sub> solid fraction seems that sublimates at a distance downwind less than the distance in which the centreline of the cloud reaches the ground. So, also here, seems to justify the assumption of no solid CO<sub>2</sub> deposition on the ground.

It should be noted that CO<sub>2</sub> export and inlet CO<sub>2</sub> pump P400/outlet CO<sub>2</sub> aftercooler E201 have similar starting thermodynamic conditions, different from outlet CO<sub>2</sub> recycle pump P200A, therefore the trends of their properties are superimposed.

### 9.4.2 Determination of damage areas between cold temperatures and toxic CO<sub>2</sub>

During the release of CO<sub>2</sub> into the atmosphere, with certain thermodynamic conditions of stagnation, very low temperatures can be reached during expansion up to the ambient pressure, reaching -78.5 °C and even beyond. To compare the phenomenon of people's exposure to these cold temperatures, with exposure to the toxic concentration of CO<sub>2</sub>, the data relating to the C/Line Cloud Vapour Temperature and the C/Line Cloud Concentration were extracted for all scenarios and for the components with thermodynamic conditions such as to reach these low temperatures. In the other cases, the temperatures reached after expansion at ambient pressure were higher than 0 °C, as they have a much higher stagnation temperature than the critical one.

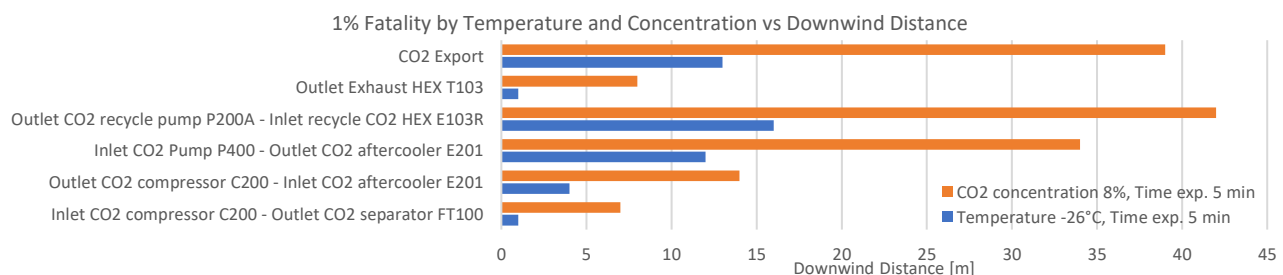
The comparison between these two phenomena was obtained considering the 1 % and 50 % of fatality for the concentrations, temperatures and time exposures reported in the table below.

	1 % fatality		50 % fatality	
Concentration of CO <sub>2</sub>	8 %	10 %	11 %	
Temperature [°C]	-26	-34	-40	
Duration of exposure [min]	5	10	5	

Table 25. Comparison between concentration and temperature thresholds.

The respective safety distances simulated for these values have been obtained from the report section of Phast, so it must be considered that they are before Along Wind Diffusion.

In general, it was observed that the damage area given by the concentration of CO<sub>2</sub> is always higher than that given by the temperature, for the same fatality percentage, for all scenarios. Below there is a sample identification with a 22 mm hole and weather conditions F2.



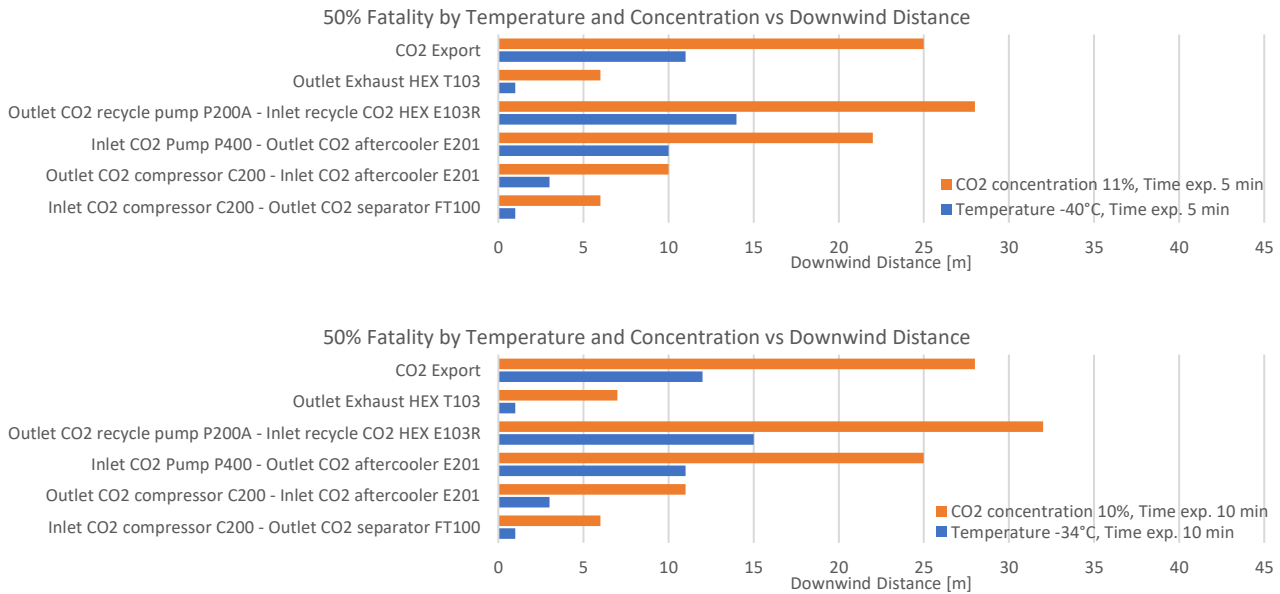


Figure 37. Safety distances comparison between cold exposure and CO<sub>2</sub> concentration, pre-AWD results.

### 9.4.3 Determination of the most critical component

The objective of this analysis was to identify the area of greatest damage associated with certain thermodynamic conditions of entry/exit from the components of the Allam cycle system. As already mentioned, the damage areas have been calculated taking into consideration the IDLH with 4% concentration for 30 minutes, 1% fatality given by a concentration equal to 8 % for 5 minutes and 50% fatality considering 11% concentration for 5 minutes. The simulations were carried out for all scenarios, i.e., considering all the thermodynamic conditions of entry/exit from the components, all the holes, both horizontal and horizontal with impingement release direction and both meteorological classes F2 and D5.

In a risk assessment study, in addition to identifying the area of greatest damage, it is also necessary to consider the frequency of occurrence of the accidental scenario. Therefore, in order to identify the most critical component, it is also necessary to take into account the corresponding leak frequencies, which increase as the hole decreases. For these reasons, the 22 mm hole was chosen as an intermediate scenario for determining the most critical conditions regarding the maximum safety distances reached with a release of CO<sub>2</sub>.

The distances reached by the cloud at the concentrations of interest, therefore equal to 4%, 8%, and 11%, were obtained from the graph of the maximum footprint concentration on the centre/line, at the height of interest equal to that of the release (2 m). It should be noted that these data instead are post Along Wind Diffusion, therefore more accurate than those tabulated in the reports.

Analyzing the results of the simulations for each component, in the scenario with a 22 mm hole and all the possible combinations of release directions and meteorological classes, it was found that the maximum distances reached by the cloud occurred with the scenario having “Horizontal Impingement” as release direction and the weather class “F2”, for all concentrations of interest. The results obtained are shown in the table below, where the leak frequencies are also reported for each component.

Component name	IDHL Concentration 4% Exp. Time 30 min	1% Fatality Concentration 8 % Exp. Time 5 min	50% Fatality Concentration 11% Exp. Time 5 min	Leak Frequency
Inlet CO <sub>2</sub> compressor C200	14	8	6	7.2E-04
Outlet CO <sub>2</sub> separator FT100	14	8	6	1.4E-04
Outlet CO <sub>2</sub> compressor C200	25	13	11	7.2E-04
Inlet CO <sub>2</sub> aftercooler E201	25	13	11	1.8E-04
Inlet CO <sub>2</sub> Pump P400	37	18	16	3.0E-04
Outlet CO <sub>2</sub> aftercooler E201	37	18	16	1.8E-04
<b>Outlet CO<sub>2</sub> recycle pump 200A</b>	<b>62</b>	<b>33</b>	<b>27</b>	<b>3.0E-04</b>
<b>CO<sub>2</sub> recycle HEX E103R</b>	<b>62</b>	<b>33</b>	<b>27</b>	<b>1.8E-04</b>
CO <sub>2</sub> recycle HEX E101C	18	9	7	1.8E-04
Inlet CO <sub>2</sub> combustor CGT100	18	9	7	7.9E-04
CO <sub>2</sub> turbocoolstream HEX E102R	26	12	10	1.8E-04
CO <sub>2</sub> turbocoolstr CGT100	26	12	10	7.9E-04
Inlet Oxidant combustor GT100	15	7	6	7.9E-04
Outlet Exhaust combustor CGT100	9	4	3	7.9E-04
Outlet Exhaust turbine CGT100	4	2	1	7.9E-04
Inlet Exhaust HEX T102	4	2	1	3.0E-04
Outlet Exhaust HEX T103	8	4	3	3.0E-04
CO <sub>2</sub> Export	47	22	19	1.4E-04

Table 26. Components safety distances for IDLH, 1% and 50% fatality, with relative Leak Frequency.

From the results, it was noted that the maximum distances are reached for CO<sub>2</sub> at the outlet of the Pump 200A and at the inlet of the E103R Heat Exchanger, at supercritical temperature and pressure conditions of 52 °C and 305 bar.

The assessment of the most critical component was therefore carried out considering the component with the highest leak frequency, namely the Pump 200A. The Cloud Max Footprint, for these thermodynamic conditions, is shown below.

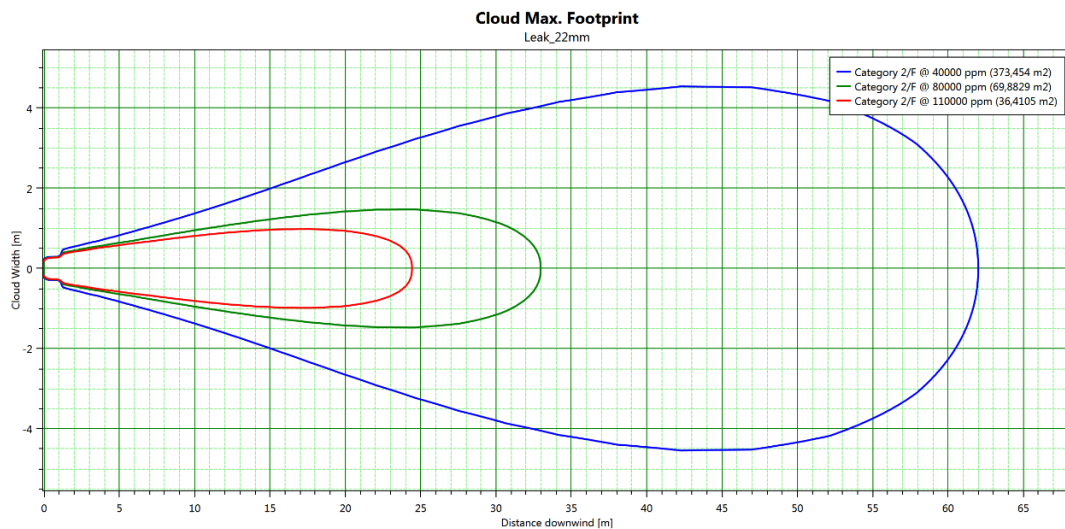


Figure 38. Cloud Maximum Footprint for Outlet CO<sub>2</sub> recycle pump 200A.

From this analysis, it can also be seen that the shortest distances reached are those associated with the Oxidant (O<sub>2</sub> and CO<sub>2</sub>) and Exhaust (CO<sub>2</sub> and H<sub>2</sub>O) flows, especially for the exhaust flow, having a lower percentage of CO<sub>2</sub> (50%) than the oxidant one. This is related to the fact that they are not fluids composed of pure CO<sub>2</sub> but mixed with other substances (H<sub>2</sub>O or O<sub>2</sub>). A comparison can be done by comparing the flow of CO<sub>2</sub> and the flow of Oxidant entering the combustor GCT100, which are under the same thermodynamic conditions (720 °C and 303 bar).

Component name	IDHL Concentration 4% Exp. Time 30 min	1% Fatality Concentration 8 % Exp. Time 5 min	50% Fatality Concentration 11% Exp. Time 5 min	Leak Frequency [y <sup>-1</sup> ]
Inlet CO <sub>2</sub> combustor CGT100	18	9	7	7.9E-04
Inlet Oxidant combustor GT100	15	7	6	7.9E-04

Table 27. Safety distances comparison between pure CO<sub>2</sub> and Oxidant.

Below there is the Side View graph showing the shape of the contours for up to these three concentrations (40000, 80000, 110000 ppm) inside the cloud, measured at the final release time using an averaging time of 600s.

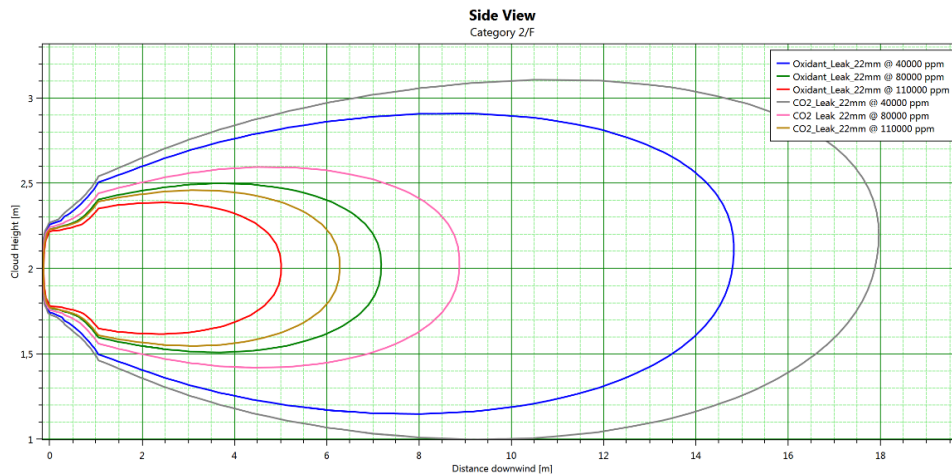


Figure 39. Side View comparison between CO<sub>2</sub> and Oxidant.

Even in this case, the greatest distances are reached by the CO<sub>2</sub> flow for all concentrations considered, as already observed by the distances obtained from the Max Footprint graph.

#### 9.4.4 Comparison of damage areas between CO<sub>2</sub> and CH<sub>4</sub>

Considering the comparison between CO<sub>2</sub> and CH<sub>4</sub>, it is necessary to highlight the difference in terms of both physical properties and implications for human health. Methane is lighter than air and highly flammable, so any leak from a pipeline is likely to ignite, causing gas burn injuries or fatalities. While CO<sub>2</sub> has different properties, being heavier than air and not flammable, thus has different safety considerations. Human exposure to CO<sub>2</sub> can increase blood acidity, triggering adverse effects on the respiratory, cardiovascular and central nervous system causing intoxication.

In this study, starting from the most critical component identified within the Allam-cycle as the one with the highest consequence distances reached, the areas of damage related to 50% fatality, produced by the release of the toxic CO<sub>2</sub> substance at the outlet of the P200A pump, at thermodynamic conditions of 52 °C and 305 bar, were compared with those produced by a possible release of CH<sub>4</sub> at the outlet of compressor C001, at the thermodynamic conditions of 128 °C and 303 bar.

The release of CH<sub>4</sub> can cause Jet Fire Heat radiation if the ignition is immediate and the flame is diffusive, or Fireball Heat radiation, in case of a vessel catastrophic rupture with immediate ignition and diffusive flame. The damage areas obtained from these phenomena have been associated with the resulting thermal radiation equal to 4 kW/m<sup>2</sup> for an exposure time of 4 minutes, to which a 50 % fatality probability is associated. These values of thermal radiation and exposure time were chosen in order to compare them with the 50 % fatality due to exposure of 5 min and 11% concentration to a CO<sub>2</sub> cloud.

The following graphs compare the three phenomena mentioned above, in all weather and release directions.

As the diameter of the hole varies, the Fireball phenomenon damage area remains constant, since it is due to a catastrophic rupture, therefore it is reported only for comparison of the safety distances reached.

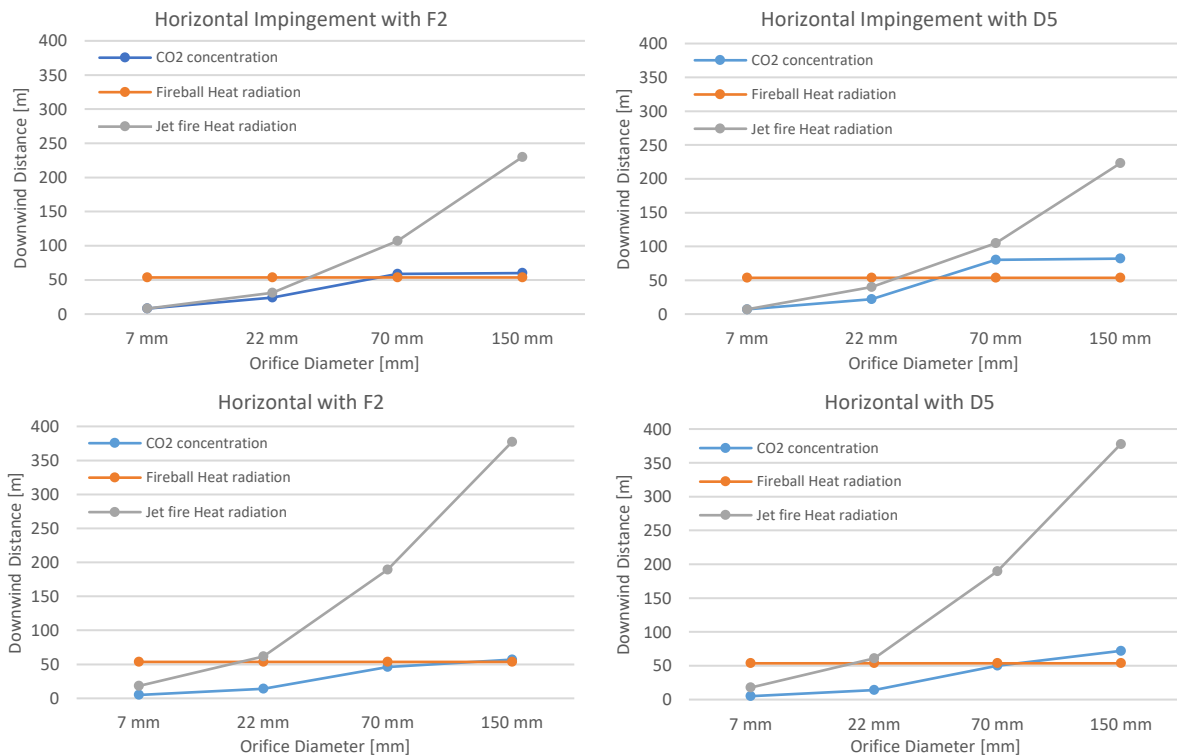


Figure 40. Comparison between the safety distances for Jet Fire and Fireball Radiation for CH<sub>4</sub> with the concentration of CO<sub>2</sub>.

Considering the damage areas produced by Jet Fire and the CO<sub>2</sub> cloud, the first one is always higher, for all hole diameters and for all scenarios considered, with a difference that grows as the hole diameter increases.

A further evaluation was made by observing that the area of damage due to the dispersion of CO<sub>2</sub> for holes greater than 70 mm in diameter becomes higher than that generated by a Fireball. The greatest difference between the two is noted for the Horizontal Impingement scenario with weather condition D5, as reported in the GIS View of the figure below that displays the consequence results in terms of geographical location on the plant, where the maximum concentration of CO<sub>2</sub> has been plotted with the “effect zone only” option, i.e., considering the entire damage area depending on the direction of release without the shape of the cloud.

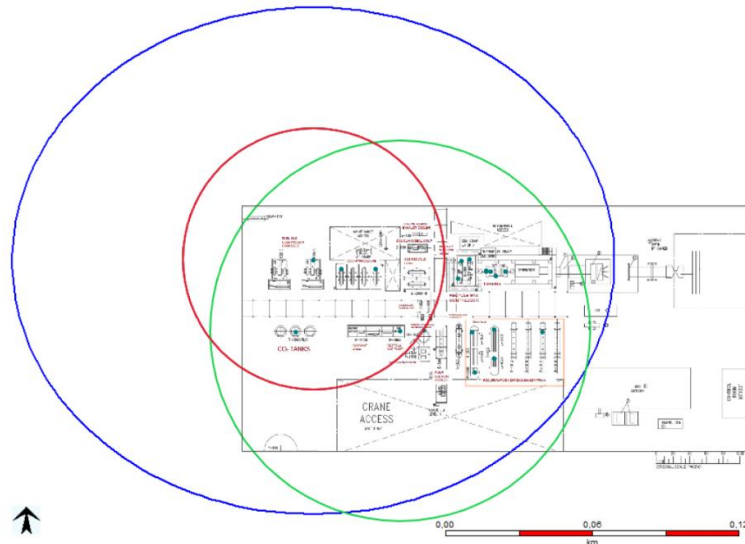


Figure 41. Damage areas comparison between CO<sub>2</sub> concentration (green), Jet Fire radiation (blue) and Fireball radiation (red), with Horizontal impingement, D5 and 70 mm hole.

## 9.5 Case-study conclusions

The analysis of the consequences and the determination of the respective areas of damage were carried out on the Allam cycle system through the use of Phast version 8.23 software. With this software, it was possible to model the stationary releases, through the DISC model at the inlet and outlet of the various components present in the cycle, the expansion of the jet at ambient pressure through the ATEX model, and the subsequent atmospheric dispersion through the model UDM-THRM. It was able to model CO<sub>2</sub> releases into the atmosphere for an assessment of the risk associated with CCS plants, both in terms of production and related transport, considering the solid particles of CO<sub>2</sub> in the jet and in the cloud and also their consequent sublimation. From this analysis the following conclusions were obtained:

- For all the scenarios considered with the presence of the solid fraction, the possible rainout phenomenon was never observed, therefore the Phast limit in not modelling the phenomenon of dry ice bank formation did not lead to a conservative estimate of the results obtained.
- The damage area generated by the cold CO<sub>2</sub> cloud is always smaller than the damage area due to its toxicity, considering however that to obtain these results all the tabulated data present in the reports have been taken, which refer to the calculation of the dispersion Before Along Wind Diffusion.
- From the comparison of the safety distances obtained from all the thermodynamic conditions entering and exiting the various components, the direction of release and the meteorological condition that determine the maximum distance reached by the downwind cloud, were obtained, considering as scenario a release hole of 22 mm, obtaining as critical conditions the Horizontal Impingement direction and F2. By this result, the thermodynamic condition of the most critical component was determined, i.e., the one with the highest safety distance and leak frequency. It has been obtained that the greatest risk is in the case of a loss of CO<sub>2</sub> from the P200A pump at conditions of 52 °C and 305 bar.
- The comparison between the damage areas generated by a CH<sub>4</sub> and a CO<sub>2</sub> leakage, assigned the greater risk to the loss of CH<sub>4</sub>, comparing the thermal radiation deriving from jet fire and the concentration of CO<sub>2</sub>. On the other hand, in comparison with the fireball (whose thermal radiation is obviously

independent of the hole taken into consideration), the damage area produced by CO<sub>2</sub> is larger for holes greater than 70 mm.

## ***10 Thesis conclusions***

Starting from the bibliographic analysis, the software for modelling the release and dispersion of CO<sub>2</sub> in the atmosphere were analyzed and compared, focusing on integral and CFD models.

Among the integral models, the PHAST software, from version 6.6 onwards, is the most widely used and validated, which, in addition to the EFFECTS software, is able to consider the solid particles in the release jet and therefore also their consequent sublimation modifying the dispersion. Among the most validated models there is also the FRED software, produced by Shell, but which on the contrary does not yet include the ability to consider solid particles in the release, but in general the results show a good agreement both with the concentrations and temperature trends if compared with the experimental tests. Integral models are suggested when the topography does not present significant complexity and to represent a dispersion under non zero wind conditions. In the other cases, the CFD models are more suitable, and the most used for the simulation of CO<sub>2</sub> releases are FLUENT, CFX and FLACS.

For the release scenarios analyzed, depending on whether this occurs by emergency, planned or accidental, the various release conditions have been identified on the basis of controlled and non-controlled depressurization and then distinguishing between release above and below the ground. It has also focused on the characterization of the crater that forms with a release from an underground pipeline and on any overpressure effects that can derive from a release of CO<sub>2</sub> with a rapid phase transition. For the latter, some experimental tests have been reported, but in general, there will be necessary more research and validation of the phenomenon for modelling software, since there are few studies in which this consequence has been considered.

To describe the phenomenon, the source-term and the consequent dispersion of CO<sub>2</sub> have been characterized, producing an indicative prospect of the appropriate calculation models to be used and of the main parameters to consider in modelling the CO<sub>2</sub> releases, specifically the depressurization models for long pipeline and models for the consequent dispersion. In addition, a validation analysis of the programs for the dispersion of CO<sub>2</sub> as a dense gas was carried out.

One of the main aspects of this study was the understanding of the particular behaviour of CO<sub>2</sub> during release, i.e., the formation of solid particles, and the possible formation of a dry ice bank. The latter in general was not modelled by the analyzed software, especially in the case of vertical and horizontal release, assuming as a conservative hypothesis that the solid particles remain in the jet and are subjected to total sublimation.

Starting from the knowledge gained on the modelling of CO<sub>2</sub> releases, it was possible to carry out a study through the PHAST software, version 8.23, of the analysis of the consequences associated with certain vulnerability thresholds, applied to the Allam cycle, a system capable to produce electricity and capture CO<sub>2</sub> through oxy-fuel combustion.

Specifically, it was possible to set the simulation environment and confirm the program's ability to carry out this modelling, by calculating the solid fraction present on the equilibrium plane and through the THRM model, also modelling its complete sublimation. It was also observed that the Phast limit of not considering a possible rain-out of the solid particles on the ground was not a conservative assumption, as the distances at which all the particles sublimate (solid fraction equal to zero) are upwind with respect to the distances at which the centre/line height touches the ground, for all the considered scenarios.

Through this software, it was analyzed the trend of the low temperatures reached in the release, due to the presence of the solid fraction during expansion up to -78.5 °C and the heat removed from the surrounding air for sublimation. However, it must be specified that for the temperature trend the software can only consider pre-AWD data, less accurate than post-AWD data.

Instead, to carry out the analysis of safety distances relating to exposure to high concentrations of CO<sub>2</sub>, vulnerability thresholds equal to IDLH, 1% and 50% fatality with the respective concentrations and exposure times were considered. The data obtained from all the simulations were extracted from the Max Footprint graph on the centre/line, which are post-AWD.

From all the results collected it was, therefore, possible to analyze the various consequences deriving from a release of CO<sub>2</sub> and from the mixtures that contain it, to compare them considering the different thermodynamic conditions present within the cycle, and to make a comparison in terms of damage area also with a release of CH<sub>4</sub>.

With Phast, an aspect that could not be analyzed was the possible overpressure generated by the rapid phase transition of CO<sub>2</sub> during release, since it is unable to consider CO<sub>2</sub> as a material that can cause a physical explosion.

In conclusion, the programs available to analysts are adequate to simulate the phenomena of CO<sub>2</sub> release. However, among the integral models, the Phast and EFFECTS software are the only ones that consider the formation of solid particles during the release and their consequent sublimation, on the contrary, all the others consider the phenomenon as a liquid/vapour release. For future developments, the phenomenon of the snow-out of solid particles on the ground and the consequent formation of the dry ice bank could be considered. Furthermore, DEGADIS, SLAB, GASTAR, EFFECTS, SAFER/TRACE, ALOHA, HEGADAS models require greater validation if compared with the validation campaigns carried out for the Phast software, which is the most used integral software for analysis of the consequences in the CO<sub>2</sub> field. On the other hand, CFD models have in general been validated through experimental campaigns, but at the same time require more computational time, so it is recommended to use them, in a quantitative analysis, only in the case of very complex terrain in the near-field.

## References

- [1] IPCC. IPCC Special Report on Carbon Dioxide Capture and Storage. Prepared by Working Group III of the IPCC. Cambridge University Press, Cambridge, UK, (2005).  
<https://repository.ubn.ru.nl/bitstream/handle/2066/230961/230961.pdf?sequence=1>
- [2] Paolo Mocellin. Modellazione del rilascio e della ricaduta al suolo di CO<sub>2</sub> da pipeline per carbon capture and storage, (2013) [ONLINE].  
[http://tesi.cab.unipd.it/44509/1/Paolo\\_Mocellin\\_Modellazione\\_del\\_rilascio\\_e\\_della\\_ricaduta\\_al\\_suolo\\_di\\_CO2\\_da\\_pipeline\\_CCS.pdf](http://tesi.cab.unipd.it/44509/1/Paolo_Mocellin_Modellazione_del_rilascio_e_della_ricaduta_al_suolo_di_CO2_da_pipeline_CCS.pdf)
- [3] DNV GL, CO2RISKMAN, Guidance on CCS CO<sub>2</sub> Safety and Environment Major Accident Hazard Risk Management, (2013, reissued in 2020).
- [4] Eni. Emanuele Domingo, Luca Decarli, Laura Presotto. Safety and environment for Carbon Capture & Storage (CCS) Projects, (2020).
- [5] Loi Hoang, Huy Phuoc Pham, Risza Rusli. A review of experimental and modelling methods for accidental release behaviour of high-pressurized CO<sub>2</sub> pipelines at atmospheric environment. *Process Safety and Environmental Protection*, **104**, pp. 48-84, (2016).  
<https://www.sciencedirect.com/science/article/pii/S0957582016301665>
- [6] Noothout P., Wiersma F., Hurtado O., Macdonald D., Kemper J., van Alphen K. CO<sub>2</sub> pipeline infrastructure-lessons learnt. *Energy Procedia*, **63**, pp. 2481-2492.  
<https://www.sciencedirect.com/science/article/pii/S1876610214020864?via%3Dihub>
- [7] IEA GHG. CO<sub>2</sub> storage in depleted gas fields, report number 2009/01. *International Energy Agency R&D programme*, (2009).
- [8] Alberto Mazzoldi, Tim Hill, Jeremy J. Colls. Assessing the risk for CO<sub>2</sub> transportation CCS projects, CFD modelling. *Internal Journal of Greenhouse Gas Control*, **5**, pp. 816-825, (2011).  
<https://www.sciencedirect.com/science/article/pii/S1750583611000028>
- [9] Energy Institute. Technical guidance on hazard analysis for onshore carbon capture installations and onshore pipelines. 1<sup>st</sup> edition, (2010).
- [10] Energy Institute. Hazard analysis for offshore carbon capture platforms and offshore pipelines. 1<sup>st</sup> edition, (2013).
- [11] Vendrig M., Spouge J., Bird A., Daycock J., Johnsen O., Crown Ed. Risk Analysis of the Geological Sequestration of Carbon Dioxide. *Department of Trade and Industry's Cleaner Coal Technology Transfer Programme*, (2003).
- [12] DNV. Mapping of potential HSE issues related to large-scale capture, transport and storage of CO<sub>2</sub>. DNV report, (2009).
- [13] PHMSA. The State of the National Pipeline Infrastructure. *U.S. Department of Transportation*, (2010).

- [14] Duncan I.J., Wang H. Estimating the likelihood of pipeline failure in CO<sub>2</sub> transmission pipelines: new insights on risks of carbon capture and storage. *Int. J. Greenh. Gas Control* **21**, pp. 49-60, (2014). <http://dx.doi.org/10.1016/j.ijggc.2013.11.005>.
- [15] Sherpa Consulting. Dispersion modelling techniques for carbon dioxide pipelines in Australia, (2015).
- [16] Vianello C., Mocellin P., Macchietto S., Maschio G. Risk assessment in a hypothetical network pipeline in UK transporting carbon dioxide. *Journal of Loss Prevention in the Process Industries* **44**, pp. 515-527, (2016).
- [17] Clausen S., Oosterkamp A., Strøm KL. Depressurization of a 50 km long 24 inches CO<sub>2</sub> pipeline. *Energy Procedia*, **23**, pp. 256-265, (2012).
- [18] Vitali M., Zuliani C., Corvaro F., Marchetti B., Terenzi A., Tallone F. Risks and Safety of CO<sub>2</sub> Transport via Pipeline: A Review of Risk Analysis and Modelling Approaches for Accidental Releases. *Energies*, **14**, 4601 (2021).
- [19] Allason D., Armstrong K., Barnett J., Cleaver P., Halford A. Behaviour of releases of carbon dioxide from pipelines and vents. *American Society of Mechanical Engineers*, (2014).
- [20] Hanna S.R., Chang J.C. Use of the Kit Fox field data to analyze dense gas dispersion modelling issues, pp. 2231-2242, (2001b).
- [21] Hanna S.R., Drivas P., Chang J.C. Guidelines for Use of Vapour Cloud Dispersion Models. New York, (1996).
- [22] Chow FK., Granvold PW., Oldenburg CM. Modelling the effects of topography and wind on atmospheric dispersion of CO<sub>2</sub> surface leakages at geologic carbon sequestration sites. *Energy Procedia*, **1**, pp. 1925-1932, (2009).
- [23] Lake JA., Steven MD., Smith K., Lomax BH. Environmental impact of a hypothetical catastrophic leakage of CO<sub>2</sub> onto the ground surface. *Journal of Pipeline Engineering*, **11**, pp. 239-248, (2012).
- [24] Pursell, M. Experimental investigation of high-pressure liquid CO<sub>2</sub> release behaviour. *Hazards Symp. Ser.*, **158**, pp. 164-171, (2012).
- [25] Allason D., Armstrong K., Cleaver P., Halford A., Barnett J. Experimental studies of the behaviour of pressurized release of carbon dioxide. *ICHEME Symposium Series*, **158**, pp. 42-52, (2012).
- [26] TNO. Yellow Book: Methods for Calculation of Physical Effects due to the releases of hazardous materials (liquids and gases), (2005d).
- [27] Hansen, P.M., Gaathaug, A.V., Bjerketvedt, D., Vaagsaether, K. Shock Waves. Blast from pressurized carbon dioxide released into a vented atmospheric chamber, (2018).
- [28] Molag M., Raben I.M.E. Externe veiligheid onderzoek CO<sub>2</sub> buisleiding bij Zoetermeer, TNO, AperiDoorn, pp. 46, (2006).

- [29] Fan X., Wang Y., Zhou Y., Chen J., Huang Y., Wang J. Experimental study of supercritical CO<sub>2</sub> leakage behaviour from pressurized vessels. *Energy*, **150**, pp. 342-350, (2018).
- [30] Guo X., Yan, X., Zheng Y., Yu J., Zhang Y., Chen S., Chen L., Mahgerefteh H., Martynov S., Collard A. et al. Under-expanded jets and dispersion in high pressure CO<sub>2</sub> releases from an industrial scale pipeline. *Energy*, **119**, pp. 53-66, (2017).
- [31] Guo X., Yan, X., Yu, J., Zhang Y., Chen S., Mahgerefteh H., Martynov S., Collard A., Proust C. Under-expanded jets and dispersion in supercritical CO<sub>2</sub> releases from a large-scale pipeline. *Appl. Energy*, **183**, pp. 1279-1291, (2016).
- [32] Elshahomi A., Lu C., Michal G., Liu X., Godbole A., Venton P. Decompression wave speed in CO<sub>2</sub> mixtures: CFD modelling with the GERG-2008 equation of state. *Appl. Energy*, **140**, pp. 20-32, (2015).  
<http://dx.doi.org/10.1016/j.apenergy.2014.11.054>.
- [33] Mazzoldi A., Hill T., Colls J. J. CO<sub>2</sub> transportation for carbon capture and storage: sublimation of carbon dioxide from a dry ice bank. *International journal of greenhouse gas control* **2**, pp. 210-218, (2008).  
<https://www.sciencedirect.com/science/article/pii/S1750583607001181>
- [34] Vianello C., Mocellin P., Maschio G. Study of Formation, Sublimation and Deposition of Dry Ice from Carbon Capture and Storage Pipelines, *Chemical engineering transactions*, **36**, (2014).
- [35] Mazzoldi A., Hill T., Colls J. J. CFD and Gaussian atmospheric dispersion models: A comparison for leak from carbon dioxide transportation and storage facilities. *Atmospheric environment* **42**, pp. 8046-8054, (2008).  
<https://www.sciencedirect.com/science/article/pii/S1352231008006080>
- [36] McGillivray A., Wilday J. Comparison of risks from carbon dioxide and natural gas pipelines. Health and Safety Laboratory, Research report **749**, (2009).
- [37] Engebø A., Ahmed N., Garstad JJ., Holt H. Risk assessment and management for CO<sub>2</sub> capture and transport facilities. *Energy Procedia*, **37**, pp. 2783-2793, (2013).
- [38] Wareing CJ., Fairweather M., Falle SAEG., Woolley RM. Modelling ruptures of buried high pressure dense phase CO<sub>2</sub> pipelines in carbon capture and storage applications - Part II. A full-scale rupture. *International Journal of Greenhouse Gas Control*, **42**, pp. 712-728, (2015).
- [39] Wareing CJ., Fairweather M., Falle SAEG., Woolley RM. Modelling punctures of buried high pressure dense phase CO<sub>2</sub> pipelines in carbon capture and storage applications. *International Journal of Greenhouse Gas Control*, **29**, pp. 231-247, (2014).
- [40] Martynov S., Brown S., Mahgerefteh H., Sundara V., Chen S., Zhang Y. Modelling three-phase releases of carbon dioxide from high-pressure pipelines. *Process Safety and Environmental Protection*, **92**, pp. 36-46, (2014).

- [41] Ahmad M., Lowesmith B., De Koeijer G., Nilsen S., Tonda H., Spinelli C., Cooper R., Clausen S., Mendes R., Florisson O. COSHER joint industry project: large scale pipeline rupture tests to study CO<sub>2</sub> release and dispersion. *International Journal of Greenhouse Gas Control*, **37**, pp. 340-353, (2015).
- [42] Witlox HWM., Stene J., Harper M., Nilsen SH. Modelling of discharge and atmospheric dispersion for carbon dioxide releases including sensitivity analysis for wide range of scenarios. *Energy Procedia*, **4**, pp. 2253-2260, (2011).
- [43] Esfahanizadeh L., Dabir B. Source terms calculation and atmospheric dispersion for a dynamic release from a CO<sub>2</sub> pipeline containing methane and water as impurities. *Greenhouse Gases: Science and Technology*, **3**, pp. 291-302, (2013).
- [44] Mazzoldi A., Hill T., Colls J. Assessing the risk for CO<sub>2</sub> transportation within CCS projects, CFD modelling, (2011).
- [45] Mazzoldi A., Oldenburg Curtis M. 4th Quarter FY2011 Milestone: Report on pipeline CO<sub>2</sub> leakage risk assessment. Berkeley, CA, (2013).
- [46] Koornneef J., Spruijt M., Molag M., Ramirez A., Turkenburg W., Faaij. Quantitative risk assessment of CO<sub>2</sub> transport by pipeline-A review of uncertainties and their impacts. *Journal of Hazardous Materials*, **177**, pp. 12-27, (2010).
- [47] TetraTech, Final Risk Assessment Report for the FutureGen Project Environmental Impact Statement, CA, USA, (2007).
- [48] Dixon C.M., Gant S.E., Obiorah C., Bilio M. Validation of dispersion models for high pressure carbon dioxide releases, (2012).
- [49] Gant S.E., Narasimhamurthy V.D., Skjold T., Jamois D., Proust C. Evaluation of multi-phase atmospheric dispersion models for application to Carbon Capture and Storage. *Journal of Loss Prevention in the Process Industries*, **32**, pp. 286-298, (2014).
- [50] Knoope M.M.J., Raben I.M.E, Ramirez A. Spruijt M.P.N, Faaij A.P.C. The influence of risk mitigation measures on the risks, costs and routing of CO<sub>2</sub>. *International Journal of Greenhouse Gas Control*, **24**, pp. 104-124, (2014).
- [51] Wentian Zheng. Numerical modelling of the rapid depressurization and outflow of high pressure containments in the framework of Carbon Capture and Sequestration, (2018).
- [52] Liu B., Liu X., Lu C., Godbole A., Michal G., Tieu A.K. Computational fluid dynamics simulation of carbon dioxide dispersion in a complex environment. *J. Loss Prev. Process. Ind.* **40**, pp. 419-432, (2016).
- [53] Woolley R., Fairweather M., Wareing C., Proust C., Hebrard J., Jamois D., Narasimhamurthy V., Storvik I., Skjold T., Brown S. et al. An integrated multi-scale modelling approach for the simulation of multiphase dispersion from accidental CO<sub>2</sub> pipeline release in realistic terrain. *International Journal of Greenhouse Gas Control*, **27**, pp. 221-238, (2014).
- [54] Britter R., McQuaid J. Workbook on the dispersion of dense gases. HSE, Sheffield, UK (1988).

- [55] Xiong Liu, Ajit Godbole, Cheng Lu, Guillaume Michal, Valerie Linton. Investigation of the consequences of high-pressure CO<sub>2</sub> pipeline failure through experimental and numerical studies. **250**, pp. 32-47, (2019).  
<https://www.sciencedirect.com/science/article/pii/S0306261919308669>
- [56] IOGP. Consequence modelling. *International association of Oil & Gas Producers*, (2010).
- [57] Mahgerefteh H., Zhang P., Brown S. Modelling brittle fracture propagation in gas and dense-phase CO<sub>2</sub> transportation pipelines.
- [58] Preeti Joshi, Prem Bikkina, Qingsheng Wang. Consequence analysis of accidental release of supercritical carbon dioxide from high pressure pipelines. *International Journal of Greenhouse Gas Control*, **55**, pp. 166-176, (2016).
- [59] Mocellin P., Maschio G., Vianello C. Carbon Capture and Storage Hazard Investigation: numerical analysis of hazards related to dry ice bank simulation following accidental carbon dioxide releases. *Chemical Engineering Transactions*, (2015).
- [60] Mocellin P., Maschio G., Vianello C. Hazard investigation of dry-ice bank induced risks related to rapid depressurization of CCS pipelines. Analysis of different numerical modelling approaches. *International Journal of Greenhouse Gas Control*, **55**, pp. 82-96, (2015).
- [61] Xiong Liu, Ajit Godbole, Cheng Lu, Guillaume Michal, Philip Venton. Study of the consequences of CO<sub>2</sub> released from high-pressure pipelines. *Atmospheric Environment*, **116**, pp. 51-64, (2015).  
<https://www.sciencedirect.com/science/article/pii/S1352231015301618>
- [62] Eni. Marika Francesconi. Modelling of the risk associated with CCS technology, (2020).
- [63] Jennifer X. W., Pierre L. F., Hongen J., Vendra C. M. R. Further development and validation of CO<sub>2</sub>FOAM for atmospheric dispersion of accidental releases from carbon dioxide pipelines. *International Journal of Greenhouse Gas Control*, **52**, pp. 293-304, (2016).
- [64] HSE. Overview of carbon capture and storage (CCS) projects at HSE's Buxton Laboratory, (2017).
- [65] Eni. Quantitative Risk Assessment (QRA) Methodology, Attachment 4.
- [66] Henk W.M. Witlox, Mike Harper, Adeyemi Oke, Jan Stene. Phast validation of discharge and atmospheric dispersion for pressurized carbon dioxide releases. *Journal of Loss Prevention in the Process Industries*, **30**, pp. 243-255, (2014).
- [67] Eni. Oxy & Pre-combustion technologies: Allam cycle. Process description.
- [68] Fernandes D., Wang S., Xu Q., Buss R., Chen D. Process and Carbon Footprint Analyses of the Allam Cycle Power Plant Integrated with an Air Separation Unit. *Clean technologies*, (2019).

- [69] Process Release Frequencies. Risk Assessment Data Directory. IOGP.  
<https://www.iogp.org/bookstore/product/risk-assessment-data-directory-process-release-frequencies/>
- [70] Rachael Rettner. How does a person freeze to death? *LiveScience*, (2019).  
<https://www.livescience.com/6008-person-freeze-death.html>
- [71] Health And Safety Executive (HSE). Indicative human vulnerability to the hazardous agents present offshore for application in risk assessment of major accidents, (2008).
- [72] DNV-GL. Release Notes, PHAST. Taking hazard and risk analysis one step further, (2017).



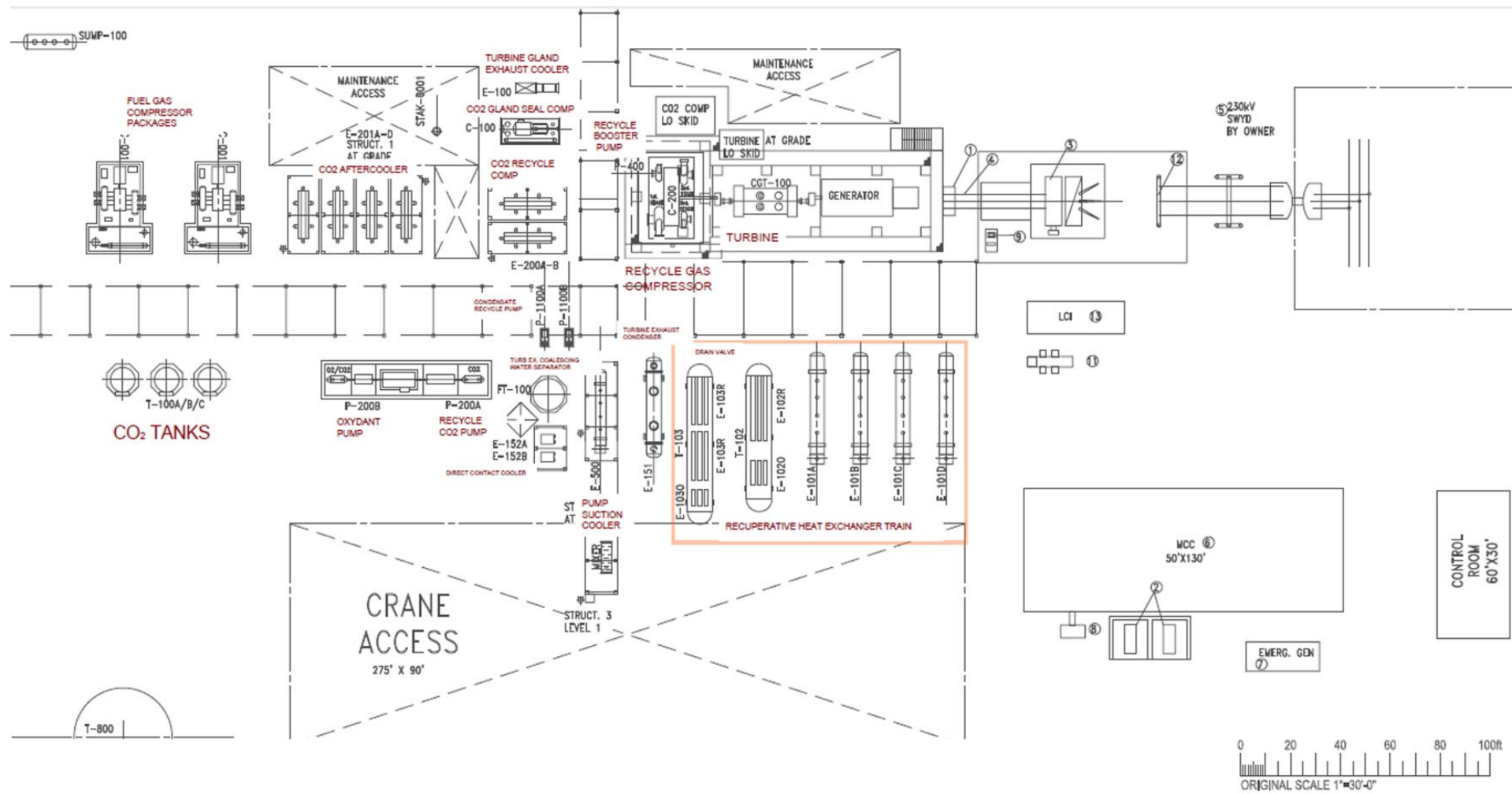


Figure 43. Attachment B.